Reinhold Kainhofer
reinhold@kainhofer.com

Exploration of different confinement and hyperfine interactions in a constituent quark model for baryons

Diplomarbeit
zur Erlangung des akademischen Grades eines
Magisters
an der Naturwissenschaftlichen Fakultät der
Karl-Franzens-Universität Graz

durchgeführt bei

Ao.Univ.Prof. Dr. Willibald Plessas
Institut für Theoretische Physik

Graz, Jänner 2003

Abstract

In this work we investigate the spectra of light and strange baryons for different effective interactions between constituent quarks. In particular we examine the influence of an additional Coulomb term on top of a linear confinement and variants of the hyperfine interactions derived from Goldstone-boson-exchange (GBE) dynamics; the latter include specifically pseudoscalar, vector and scalar exchanges. We present our own parametrization of an extended GBE constituent quark model (CQM) with all but spin-orbit forces included. The resulting spectra produce most states to a high accuracy, and the correct level orderings in the nucleon, Λ and Σ spectra can be obtained. The only remaining problems are the states $N(1680)$ and $N(1675)$, which cannot be described in accordance with their almost degeneracy observed in experiment, and the $\Lambda(1405)$, which is obviously much influenced by the nearby KN threshold and can probably not be explained by a constituent quark model relying on $\{QQQ\}$ configurations only.

The version of the extended GBE CQM constructed here is mainly intended to serve as a basis for the inclusion of the missing spin-orbit terms of the meson-exchange potentials, which is the central subject matter in a parallel diploma work.

Contents

Chapter 1

Introduction

Quantum chromodynamics (QCD) is generally accepted as the fundamental theory of strong interactions. It can be solved reliably in the limit of high energies by perturbative methods. The corresponding predictions are well confirmed by experiments. In the range of low-energies, however, perturbative methods are no longer applicable. Here one has to resort to alternative approaches. For years one has tried to solve QCD directly by discretization on a lattice. While a number of valuable results have been gained in this way, one has not yet reached a quantitative description of the wealth of hadron phenomena at low and intermediate energies. Another way consists in developing effective theories or models for non-perturbative QCD.

The properties of QCD are drastically changed when proceeding from high to low energies. While such phenomena like confinement (in contrast to asymptotic freedom) and the spontaneous breaking of chiral symmetry (SBχS) have become quite evident by now, one is still far away from understanding their mechanisms. This makes it difficult to deduce an effective theory from the original QCD. Rather one tries to include the consequences of the above features in the construction of effective approaches. In fact, it appears mandatory to take into account the established properties of QCD at low energies in any effective model.

The picture of low-energy hadrons consisting (primarily) of confined constituent quarks has recently become more and more supported by results from lattice QCD [A$^+$99]. One may assume that the transmutation of current quarks (as the original QCD degrees of freedom) to constituent quarks (as quasi-particles of low-energy QCD) happens in parallel with SBχS and/or is a consequence thereof. The assumption of constituent quarks as building blocks of low-energy hadrons should thus be accompanied by the generation of Goldstone bosons due to the spontaneous breaking of the symmetry $SU(3)_L \otimes SU(3)_R \to SU(3)_V$ (here we deal only with three flavors). In other words, constituent quarks and Goldstone bosons should represent the essential QCD degrees of freedom at low energies.

As a consequence, it also appears reasonable to construct constituent quark models (CQM) for the description of mesons and baryons. In fact, this approach already has a long tradition, and it has also lead to several useful insights into the physics of

low-energy hadrons. CQMs have appeared in a variety of different frameworks. Earlier years have seen non-relativistic CQMs, but one has soon learned that constituent quarks confined inside the volume of hadrons are essentially relativistic particles. Also the (effective) interaction between constituent quarks has been assumed due to various dynamical concepts.

In the early times of CQMs the confinement was assumed in a simple harmonic-oscillator form. Nowadays a linear confinement as suggested by QCD is preferred, at least in the peripheral range.

For the hyperfine interaction, one has originally adopted the idea of one-gluon exchange (OGE) [RGG75]. Subsequently, modifications of the corresponding color-magnetic interaction were applied and other types of interactions were added in so-called hybrid CQMs. A few years ago the suggestion of a Goldstone-boson-exchange (GBE) interaction was put forward [GR96]. It was motivated as a consequence of SBχS.

In this work we will be essentially concerned with a CQM based on this latter idea of GBE. So far, a first version of a CQM constructed with a restricted interaction deriving from GBE (namely, a pseudoscalar boson exchange with only the spin-spin part taken into account) has been rather successful in describing the light and strange baryon spectra. It is the aim of our work to complete the GBE CQM by including further parts of the interactions that can be mediated by the exchange of bosons. Upon attempting to construct an extended version of the GBE CQM we also study the influences of different force components in some detail.

Chapter 2

Motivation of the GBE constituent quark model

Contents

In this chapter, we will consider the physical motivations for the idea of a Q-Q hyperfine interaction mediated by the exchange of Goldstone bosons. We will discuss the Hamiltonian that serves as the base for our parametrization of the extended GBE CQM presented in this diploma thesis. The early models, advocating GBE dynamics as published e.g. by Glozman, Papp, Plessas, Varga, and Wagenbrunn ([GPP96] and [GPVW98]), were already able to describe the spectra of light and strange baryons to an astonishing degree, although only a very small number of parameters was needed to fit to the experimental spectra.

The GBE CQMs presented in chapters 1 to 3 were developed by other authors, and nothing new will be presented until chapter 6, where I present my own parametrization of the extended GBE CQM.

The previous models have already been described in several works (e.g. in Robert Wagenbrunn's doctoral thesis [Wag98] or in K. Berger's [Ber02] or K. Glantschnig's [Gla02] diploma theses). In my discussion I will essentially follow these sources, so I will not explicitly cite them any more, except where I want to point out something particular. Wherever I find it worthwhile, I will try to explain things in more detail and show general connections.

2.1 The general form of the Hamiltonian

In the GBE constituent quark model, the baryons are viewed as particles made of three constituent quarks (which are different from the current quarks of original QCD and should be understood as quasi-particles with a dynamical mass heavier than the current quark mass). Together with the constituent quarks there arise Goldstone bosons as effective degrees of freedom of low-energy QCD. They are suggested by the spontaneous breaking of chiral symmetry. As a result the interaction between confined constituent quarks can be attributed to Goldstone-boson exchange, even though it is not strictly derived within QCD.

In general, the Hamiltonian of the Q-Q interaction consists of a confinement part and a hyperfine interaction:

$$H = H_0 + \sum_{i<j} \left[V_{\mathrm{hf}}(\vec{r}_{ij}) + V_{\mathrm{conf}}(\vec{r}_{ij}) \right] . \tag{2.1}$$

Here H_0 is the kinetic energy of the three-quark system. In the early model of Glozman, Papp, and Plessas [GPP96] it was taken in the non-relativistic form [Wag98]

$$H_0 = \sum_{i=1}^{3} \left(m_i + \frac{\vec{p}_i^{\,2}}{2m_i} \right) \tag{2.2}$$

with m_i being the masses of the three constituent quarks, and $\vec{p}_i$ their individual three-momenta.

This non-relativistic kinetic approach has the fundamental flaw that the magnitude of the expectation value of the kinetic-energy operator generally implies $\frac{v}{c} > 1$, i.e. the mean velocity of a constituent quark is larger than the speed of light. From this observation one learns that the kinetic energy must not be treated non-relativistically. Rather one has to use a relativistic kinetic-energy operator to avoid such problems from the beginning. Later models used a semi-relativistic approach, where the kinetic-energy operator is taken in relativistic form. We will discuss them in the next chapter.

In the Hamiltonian (2.1) above, the term $V_{\mathrm{hf}}(\vec{r}_{ij})$ describes the hyperfine interaction between the two constituent quarks i and j, and it is subject to discussions. Its specific form in case of GBE will be motivated in the next few sections.

2.2 Confinement

In equation (2.1), $V_{\mathrm{conf}}(r_{ij})$ is the confinement potential for constituent quarks. It is taken as a mutual interaction. In principle, for a three-quark system, one would also have a Y-like confinement as proposed e.g. in [CKP83]. In this context each quark is the source of a flux tube and the three flux tubes meet at a single point generating the regular star configuration so that the static energy is minimized.

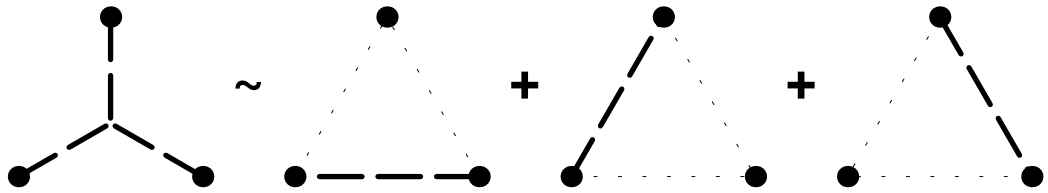

Figure 2.1: *The Y-like three-quark confinement can be approximated as sum over all two-quark confinements (Δ-like confinement)*

Such a Y-like confinement can well be approximated by a Δ-like configuration, which relies only on two-body confining forces (see figure 2.1). The string tension in that case has to be taken as half of the string tension of the quark-antiquark confinement [DM76] (usually $C \approx 2.5$ fm^{-2} resulting from theoretical considerations, and $C \approx 2 - 2.4$ fm^{-2} in the semi-relativistic GBE CQMs).

Originally, Glozman and Riska [GR96] used a harmonic confinement potential

$$V_{\text{conf}}(\vec{r}_{ij}) = V_0 + \frac{1}{6} m\omega^2 (\vec{r}_i - \vec{r}_j)^2 \tag{2.3}$$

Glozman, Papp, and Plessas [GPP96] already employed a linear confinement of the form

$$V_{\text{conf}}(\vec{r}_{ij}) = V_0 + C r_{ij} \,. \tag{2.4}$$

In subsequent models by the Graz group (e.g. [GPP$^+$97], [GPVW98], [GPP$^+$98], [WGPV00b]) the same form was used, but with different numerical values for the string tension C and the constant V_0.

In [SSRT00], Stassart, Richard, Stancu, and Theussl presented indications that a concave potential is favorable for the level ordering. Inspired by these findings, in works by Wagenbrunn, Glozman, Plessas, and Varga [WGPV00a, PGVW99] a slightly modified confinement potential

$$V_{\text{conf}}(r_{ij}) = V_0 + C r_0 \left(1 - e^{\frac{-r_{ij}}{r_0}}\right) \approx \begin{cases} V_0 + C r_{ij} & \text{for } r_{ij} << r_0 \\ V_0 + C r_0 = \text{ const.} & r_{ij} >> r_0 \,. \end{cases}$$

was considered. Here the parameters take valued of $r_0 = 7$ fm and $C = 2.53$ fm^{-2}. This form is more or less linear below r_0, and becomes flat beyond. The constant V_0 is needed to shift the nucleon ground state to the desired value of 939 MeV, but it is not explicitly needed in the calculations. Instead, since the effect of V_0 is just an overall shift of the whole spectrum after the calculations are done, all the energies are shifted by the same amount such that the nucleon ground state $N(939)$ assumes the value of 939 MeV.

Other possible forms of confinement can also include a Coulomb term $\frac{1}{r}$, like the confinement potential derived from lattice QCD calculations and described in section 7.2. There we will also give numerical results for a fit with such a potential including a Coulomb term

$$V(\vec{r}) = V_0 + \sigma r - \frac{c}{r} \,. \tag{2.5}$$

2.3 Spontaneously broken chiral Symmetry

The QCD Lagrangian of the light baryons (consisting only of u and d quarks) displays an almost exact chiral symmetry $SU(3)_L \times SU(3)_R$ (since the masses of the current quarks are rather small, $m^0_{u,d} \lesssim 10$ MeV). For strange baryons (which also include s quarks) this symmetry is only approximate due to the considerable mass of the s quark ($m^0_s \simeq 150$ MeV). This (approximate) chiral symmetry is broken by the QCD vacuum to $SU(3)_V$ in the low-energy regime, and the symmetry is realized in the hidden Nambu-Goldstone mode. As a consequence of this spontaneous breaking of the chiral symmetry (SBχS in short), an octet of pseudoscalar mesons ($\pi, K, \bar{K}, \eta$) of low mass appears as approximate Goldstone bosons, and the valence quarks acquire a dynamical mass (e.g. $m_{u,d} \simeq 300$ MeV), which is much larger than the current quark mass.

The masses of these pseudoscalar mesons are connected to the quark condensate of QCD by the Gell-Mann-Oakes-Renner relations [GMOR68], which for the π read

$$m^2_{\pi^0} = -\frac{1}{f^2_\pi}\left(m^0_u\langle\bar{u}u\rangle + m^0_d\langle\bar{d}d\rangle\right) + O({m^0_{u,d}}^2) \tag{2.6a}$$

$$m^2_{\pi^{+,-}} = -\frac{1}{f^2_\pi}\frac{m^0_u + m^0_d}{2}\left(\langle\bar{u}u\rangle + \langle\bar{d}d\rangle\right) + O({m^0_{u,d}}^2)\,. \tag{2.6b}$$

Similar relations exist for the K and η mesons.

In the chiral limit (where the current-quark masses tend to zero), these pseudoscalar mesons would have zero mass (cf. equations (2.6a)). Additionally, there exists a flavor singlet η' which decouples form the original octet due to the axial $U(1)$ anomaly [Wei75, tH76]. Although the η' cannot be considered as a Goldstone boson due to its large mass, in the large N_C limit (where N_C denotes the number of colors) the SBχ S appears as $U(3)_R \times U(3)_L \to U(3)_V$ implying a nonet of pseudoscalar Goldstone bosons, including the η'. For the real-world case of $N_C = 3$, the η' still gives non-negligible contributions to the GBE exchange and needs to be included in the corresponding CQM.

Manohar and Georgi suggested two different scales for a QCD with three flavors: The first, $\Lambda_{SB\chi S} \simeq 4\pi f_\pi \simeq 1$ GeV, is the scale of the spontaneous breaking of chiral symmetry, and the other, $\Lambda_{\mathrm{QCD}} \simeq 100 - 300$ MeV, corresponds to confinement. Between these two scales, the effective degrees of freedom in baryons should be assumed as constituent quarks as well as gluons and Goldstone bosons mediating the forces between them.

Glozman and Riska [GR96] suggested that beyond the scale of SBχS baryons should be described as systems of three constituent quarks, with the Q-Q hyperfine interaction deriving from Goldstone-boson exchange, i.e. the exchange of the nonet of pseudoscalar mesons between the constituent quarks.

2.4 GBE between constituent quarks

Both the instanton liquid model of the QCD vacuum [Shu93, NRZ] as well as explicit QCD lattice calculation suggest a point-like interaction between the constituent quarks forming the baryon. For a realistic description of the hyperfine interaction, this interaction has to be iterated in the t-channel to overcome the restriction to flavor-antisymmetric quark pairs.

According to Glozman and Varga [GV00] this leads to a meson-exchange interaction between the constituent quarks, where the pseudoscalar coupling corresponds to the exchange of Goldstone bosons. In the resulting interaction the long-range term describes the pion exchange between the constituent quarks, whereas the short-range term has the most influence on the spectra of the light and strange baryons. As it turned out, this GBE interaction displays a spin-flavor symmetry which is particularly well-suited to achieve a correct level splitting in the excitation spectra of the N, Δ, Λ and Σ baryons. Glozman and Riska [GR96] as well as Varga [GPP$^+$98] were able to show such a dynamical concept to be reasonable and working.

Although the exchange of single mesons (One-Meson-Exchange, OME) already describes the spectra of the light and strange baryons quite well, it still suffers from some problems. In particular, the tensor force component implied by the exchange of single pseudoscalar mesons causes a spin-orbit splitting in the low-lying negative-parity multiplets ($N\left(\frac{1}{2}^-\right) - N\left(\frac{3}{2}^-\right)$, $\Delta\left(\frac{1}{2}^-\right) - \Delta\left(\frac{1}{2}^-\right)$,...), which is too large as compared to the measured spectra. One attempt to cure this shortcoming is to also include the exchange of multiple Goldstone bosons into the interaction. In an effective description, the exchange of two Goldstone bosons can be approximated by the exchange of a ρ, σ or K^* meson, whereas a triple Goldstone-boson exchange can effectively be described as the exchange of one ω or ϕ meson (see Figure 2.2).

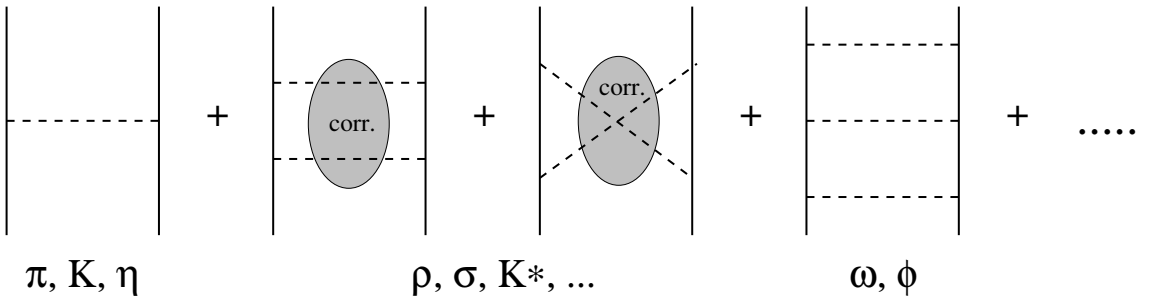

Figure 2.2: *Multiple pion exchange, described by pseudoscalar and vector meson exchange*

2.4.1 The Q-Q potential in configuration-space representation

Using the pseudoscalar Goldstone bosons as exchange particles for the inter-quark forces (in the $SU(3)_F$ symmetric approximation) leads to an interaction Lagrangian

of the form

$$ig\bar{\Psi}\gamma_5\vec{\lambda}^F\cdot\vec{\Phi}\Psi\,. \tag{2.7}$$

Here, Ψ denotes the fermion field of the constituent quarks, $\vec{\Phi}$ is the boson field of the octet of Goldstone boson, g is the coupling constant, and $\vec{\lambda}^F$ denote the $SU(3)_F$ Gell-Mann matrices. It is not feasible to treat this interaction in its full form in a (relativistic) CQM. Rather one resorted to non-relativistic reduction (thus the model is called semi-relativistic, since the kinetic term is taken in its relativistic form) for the constituent quark spinors. This results in a hyperfine potential between the constituent quarks i and j, which to lowest order includes a spin-spin component $(\vec{\sigma}_i\cdot\vec{\sigma}_j)$ as well as a tensor component $(\hat{S}_{ij})$:

$$V_\chi^{\text{octet}}(\vec{r}_{ij}) = \vec{\lambda}_i^F\cdot\vec{\lambda}_j^F\left(V^{\text{ss}}(r_{ij})\vec{\sigma}_i\cdot\vec{\sigma}_j + V^{\text{tensor}}(r_{ij})\hat{S}_{ij}\right)\,. \tag{2.8}$$

Here, the $\vec{\sigma}_i$ denote the spin matrices for the constituent quark i, and $\hat{S}_{ij}$ the tensor operator

$$\hat{S}_{ij} = 3\,(\hat{r}_{ij}\cdot\vec{\sigma}_i)\,(\hat{r}_{ij}\cdot\vec{\sigma}_i) - \vec{\sigma}_i\cdot\vec{\sigma}_j\,. \tag{2.9}$$

This reduction is too simplified and does not take into account the different quark masses $m_u = m_d \neq m_s$ and different meson masses $\mu_\pi \neq \mu_K \neq \mu_\eta$ (the u and d masses as well as the the masses of the π and K multiplets are not exactly equal, but the small discrepancies are neglected, as one always assumes isospin symmetry). Due to these different masses, the π, K and η exchange will not be exactly the same anymore, although each of them still has the same form. The interaction (2.8) then has to be generalized to

$$\begin{aligned} V_\chi^{\text{octet}}(\vec{r}_{ij}) = &\left(\sum_{a=1}^{3} V_\pi^S(\vec{r}_{ij})\lambda_i^a\lambda_j^a + \sum_{a=4}^{7} V_K^S(\vec{r}_{ij})\lambda_i^a\lambda_j^a + V_\eta^S(\vec{r}_{ij})\lambda_i^8\lambda_j^8\right)\vec{\sigma}_i\cdot\vec{\sigma}_j \\ &+\left(\sum_{a=1}^{3} V_\pi^T(\vec{r}_{ij})\lambda_i^a\lambda_j^a + \sum_{a=4}^{7} V_K^T(\vec{r}_{ij})\lambda_i^a\lambda_j^a + V_\eta^T(\vec{r}_{ij})\lambda_i^8\lambda_j^8\right)\hat{S}_{ij}\,. \end{aligned} \tag{2.10}$$

While V_π and V_K are flavor-independent (π and K exchanges only happen for quark pairs of equal masses), the η exchange (which can happen for all light and strange pairs) is flavor dependent.

The potential (2.10) of the inter-quark hyperfine interaction includes all Goldstone bosons of the pseudoscalar octet $\left(\pi^-,\pi^0,\pi^+,K^0,K^+,K^-,\bar{K}^0,\eta\right)$. However, as motivated in the previous chapter, although the η' cannot be exactly seen as a Goldstone boson, it still needs to be included in the potential, as it would become the ninth Goldstone boson in the large N_C-limit. The pseudoscalar flavor-singlet potential caused by η'-exchange has a form similar to the octet potential:

$$V_\chi^{\text{singlet}}(\vec{r}_{ij}) = \vec{\lambda}_i^0\cdot\vec{\lambda}_j^0\left(V_{\eta'}^{\text{ss}}(r_{ij})\vec{\sigma}_i\cdot\vec{\sigma}_j + V_{\eta'}^{\text{tensor}}(r_{ij})\hat{S}_{ij}\right)\,. \tag{2.11}$$

The λ_i^0 take the explicit form

$$\lambda^0 = \sqrt{\frac{2}{3}} \begin{pmatrix} 1 & 0 & 0 \\ 0 & 1 & 0 \\ 0 & 0 & 1 \end{pmatrix},$$

and $\lambda^0/2$ represents the ninth generator of $U(3)$, in addition to the eight generators of $SU(3)$. Thus, the term $\lambda_i^0 \lambda_j^0$ simplifies to a factor $\frac{2}{3}$.

To complete the potential, one has to define the radial dependences $V_\gamma^{S,T}(\vec{r}_{ij})$ for $\gamma = \pi, K, \eta, \eta'$. If one assumes that the boson fields fulfill a linear Klein-Gordon equation, and that both the bosons and the constituent quarks can be treated as point-like particles, the radial dependence in non-relativistic derivation is found to be

$$V_\gamma^S(\vec{r}_{ij}) = \frac{g_\gamma^2}{4\pi} \frac{1}{12 m_i m_j} \left(\mu_\gamma^2 \frac{e^{-\mu_\gamma r_{ij}}}{r_{ij}} - 4\pi\delta(\vec{r}_{ij}) \right) \tag{2.12}$$

$$V_\gamma^T(\vec{r}_{ij}) = \frac{g_\gamma^2}{4\pi} \frac{1}{12 m_i m_j} \mu_\gamma^2 \left(\frac{3}{(\mu_\gamma r_{ij})^2} + \frac{3}{\mu_\gamma r_{ij}} + 1 \right) \frac{e^{-\mu_\gamma r_{ij}}}{r_{ij}} \,. \tag{2.13}$$

Once again, these assumptions are not fulfilled in reality. In particular, all particles involved have a certain structure, and the fields fulfill a linear equation only for large radii. Consequently, the radial dependence has to be modified from (2.12) and (2.13) to reflect this different short-range behavior. This can be achieved by smearing out the contact interaction, represented by the δ-function in the spin-spin part of the potential, for example like:

$$4\pi\delta(\vec{r}_{ij}) \approx \Lambda_\gamma^2 \frac{e^{-\Lambda_\gamma r_{ij}}}{r_{ij}} \,. \tag{2.14}$$

In this Yukawa-type smearing, the Λ_γ represent the individual extensions of the exchanged mesons and should be expected to be somehow related to the mass of the exchange particles. Even without the physical motivations mentioned, the δ-function would have to be regularized, as an attractive δ-function interaction inevitably leads to a three-particle spectrum which is not bounded from below.

2.4.2 The momentum space representation and its consequences

The momentum space representation

$$V_\gamma(\vec{q}) \approx (\vec{\sigma}_i \cdot \vec{q})(\vec{\sigma}_j \cdot \vec{q})(\vec{\lambda}_i^F \cdot \vec{\lambda}_j^F) D_\gamma(q^2) F_\gamma^2(q^2) \tag{2.15}$$

of the potential can give us an even better understanding of its specific form. In this representation, $D_\gamma(q^2)$ is the dressed Green's function for the chiral field, including fermion loops as well as nonlinear terms of the chiral Lagrangian, and $F_\gamma^2(q^2)$ denotes a meson-quark form factor describing the internal structure and the extension of the

quasi-particles. For large distances and thus small momenta (i.e. in the limit $\vec{q} \to 0$), the potential $V_\gamma(\vec{q})$ tends toward zero, because both $D_\gamma(q^2)$ and $F_\gamma^2(q^2)$ stay finite:

$$D_\gamma(q^2) \xrightarrow{q\to 0} -\frac{1}{q^2+\mu_\gamma^2}$$
$$F_\gamma^2(q^2) \xrightarrow{q\to 0} 1\,.$$

This relation $V_\gamma(\vec{q}=0)=0$ in momentum space corresponds to the volume integral in configuration space, which is the Laplace transform of $V_\gamma(\vec{q})$ (and vice versa):

$$V_\gamma(\vec{q}) = \mathcal{L}_r[V_\gamma(\vec{r})](\vec{q}) = \int_{\mathbb{R}^3} d^3r e^{-\vec{r}\vec{q}} V_\gamma(\vec{r})\,.$$

So for $\vec{q}=0$ this has the consequence that for the pseudoscalar meson exchange the volume integral has to vanish

$$\int_{\mathbb{R}^3} d^3r V_\gamma(\vec{r}) = 0\,. \tag{2.16}$$

The tensor part $\vec{\lambda}_i^F \cdot \vec{\lambda}_j^F V^{\text{tensor}}(r_{ij})\hat{S}_{ij}$ of the pseudoscalar potential (2.8) automatically fulfills this relation due to the angular dependence of the tensor operator, which essentially behaves like an anti-symmetric function under the integral.

In the spin-spin part (2.12) of the potential the Yukawa term $\mu_\gamma^2 \frac{e^{-\mu_\gamma r_{ij}}}{r_{ij}}$ and the δ-function $4\pi\delta(\vec{r}_{ij})$ (or its smeared out equivalent) have opposite signs and the same volume integral of 1. Consequently they cancel each other and the volume integral condition (2.16) is also fulfilled by the spin-spin part. At large distances, the Yukawa term dominates over the smeared out δ-function, but for small values of r the latter has to contribute a very strong short-range term to compensate for the heavy Yukawa tail. It is this short-range potential that is most important for the baryon spectra, and therefore the type of smearing has to be chosen very carefully. In all GBE constituent quark models, the smearing will be realized by Yukawa-type forms, which in the momentum-space representation correspond to meson-constituent quark form factors

$$F_\gamma(q^2) = \left(\frac{\Lambda_\gamma^2 - \mu_\gamma^2}{\Lambda_\gamma^2 + \vec{q}^2}\right)^v\,,$$

where the exponent v is either $\frac{1}{2}$ or 1. This exponent in some sense measures the regularity of the potential at small distances, as the form factor tends to zero for large $\vec{q}$ (and thus small $\vec{r}$) like $\vec{q}^{-v}$. The specific choice of the smearing parameters Λ_γ is up to the model, and may vary from a linear dependence on the meson masses to a completely free fit of the value to the experimental spectrum.

One also has to notice the $\frac{1}{r_{ij}^3}$ singularity at $r=0$ in the tensor term (2.13) of the pseudoscalar Goldstone-boson-exchange potential. This singularity can be weakened, and even regularized if one takes into account the finite extension of the constituent quarks and the exchange mesons. However, even then the use of only

pseudoscalar Goldstone-boson exchange, in particular the tensor part of the meson-exchange potential, causes too large spin-orbit splittings in the low-lying negative-parity multiplets.

2.4.3 Level orderings of the excited baryon states

As a final physical motivation, before we present the first parameterizations of GBE constituent quark models, we now take a look at the implications by pseudoscalar Goldstone-boson exchange for the baryon spectra, and in particular for the level orderings of the first excitations in the light and strange baryons. Traditionally, CQMs like the One-Gluon-Exchange (OGE) model were unable to obtain a N excitation spectrum where the first positive-parity excitation lies below the first negative-parity excitation as it is observed in experiment. E.g., the lowest positive-parity excitation $N(1440)$ should be below the lowest negative-parity excitations $N(1535) - N(1520)$, the $\Delta(1600)$ should be below the $\Delta(1620)$.

As we will see in this section, the specific choice of the potential in the GBE model is finally able to produce spectra which display the correct level orderings in the baryon excitations. It will become clear that the $(\vec{\sigma}_i \cdot \vec{\sigma}_j)\left(\vec{\lambda}_i^F \cdot \vec{\lambda}_j^F\right)$ structure together with the sign of the short-range part in the spin-spin term of the GBE potential is most appropriate to describe the correct level ordering and thus produce adequate spectra for all light and strange baryons. To show this, we have to evaluate the spin-flavor matrix elements of the pseudoscalar meson-exchange interaction, and there only the matrix elements of the spin-spin component of the pseudoscalar octet exchange potential at small distances, where the Yukawa term prevails over all other contributions.

A pair (i, j) of constituent quarks can either be symmetric in its spin-components ($[2]_S$ in Young pattern notation) or antisymmetric ($[11]_S$). Likewise, for the flavor component one can construct symmetric ($[2]_F$) or antisymmetric ($[11]_F$) states. Thus, one has a combined number of four different spin-flavor symmetry states. If we now also consider the $SU(3)_F$-symmetric limit, where all contributions of the various exchange particles are equal in the spin-spin part of the potential ($V_\pi^S = V_K^S = V_\eta^S = V^S$)[1], the spin-flavor matrix elements of the spin-spin part of the pseudoscalar octet potential for these four possible states become

$$+\frac{4}{3}V^S(\vec{r}_{ij}) \qquad \text{for } [2]_F[2]_S, \tag{2.17a}$$

$$+8V^S(\vec{r}_{ij}) \qquad \text{for } [11]_F[11]_S, \tag{2.17b}$$

$$-4V^S(\vec{r}_{ij}) \qquad \text{for } [2]_F[11]_S, \tag{2.17c}$$

$$-\frac{8}{3}V^S(\vec{r}_{ij}) \qquad \text{for } [11]_F[2]_S\,. \tag{2.17d}$$

[1] As we have argued before, the contributions are certainly *not* equal. However, here we only use hand-waiving arguments for our "proof" where small deviations from this assumption are not important. Therefore we might safely assume this equality here to make our point clearer.

One has to notice the opposite sign of the matrix element for the two totally symmetric states and the two totally antisymmetric states, so at short distances, where the contact interaction dominates, the attracting configurations are the two flavor-spin symmetric states $[2]_F[2]_S$ and $[11]_F[11]_S$, while the two flavor-spin antisymmetric states $[11]_F[2]_S$ and $[2]_F[11]_S$ are repulsive at short distances. Another thing to notice is that the absolute value of the matrix element is much larger for the two spin-antisymmetric states. One may now ask how this different behavior influences the spectra, and in how far one can adjust the level ordering by tweaking the parameters of the potential.

It turns out that in the nucleon ground state $N(939)$ and its first positive-parity excitation $N(1440)$ the two attractive configurations ($[2]_S[2]_F$ and $[11]_S[11]_F$) dominate because these nucleon states are mainly totally spin-flavor symmetric. In contrast, the first negative-parity excitations $N(1535) - N(1520)$ are mainly in a flavor-spin mixed symmetric state and thus the repulsive configurations $[2]_F[11]_S$ and $[11]_F[2]_S$ prevail. By choosing appropriate parameter values for the effective potential, one might thus be able to shift the first two positive-parity states $N(939)$ and $N(1440)$ below the first negative parity states and so achieve the experimentally observed level ordering in the nucleon spectrum.

For similar reasons it should be possible to adjust the level ordering in the Δ spectrum, too: The ground state $\Delta(1232)$ and the first positive-parity excitation $\Delta(1600)$ are predominantly in a totally symmetric flavor-spin state, and thus again the two attractive states $[2]_F[2]_S$ and $[11]_F[11]_S$ occur, shifting the states to lower energies. In turn, the lowest negative-parity state $\Delta(1620)$ is dominated by flavor-spin mixed-symmetric states, so the two antisymmetric and thus repulsive configurations $[11]_F[2]_S$ and $[2]_F[11]_S$ appear, shifting the state to higher energies. Again, it might be possible to use this phenomenon to create the correct level ordering in the Δ-spectrum in accordance with the phenomenological spectrum. While for the nucleon this can be achieved in the GBE constituent quark model, in our fits we were not able to produce the correct level ordering in the Δ spectrum, although our theoretical results are still within the experimental error bounds for the observed states.

The level ordering of the Λ baryon is more involved, as the lowest negative-parity excitation $\Lambda(1405)$ does not only include octet states, but also flavor-singlet states, which are influenced differently from the octet states by a flavor-dependent interaction. This has the pleasant effect that the first positive-parity excitation $\Lambda(1600)$ is not shifted below the lowest negative-parity states $\Lambda(1405)$ and $\Lambda(1520)$. Already the first GBE constituent quark models could produce the correct level ordering for the Λ baryon.

For a more more detailed discussion of this level shifting due to symmetry considerations, see section 6 of the article of Glozman and Riska [GR96].

Chapter 3

Goldstone-boson-exchange CQMs

Contents

In this section, I will review the past development of the GBE constituent quark models. First I will briefly describe the non-relativistic model of Glozman, Papp, and Plessas published in [GPP96], which used only four free parameters, but had several other shortcomings besides adhering to a non-relativistic form of the kinetic-energy operator. Later on it was modified to a first semi-relativistic model by Glozman, Papp, Plessas, Varga, and Wagenbrunn in [GPP$^+$98] and [GPVW98], including only the spin-spin components of the pseudoscalar Goldstone-boson-exchange potential. The tensor-force components were subsequently included in [WPGV99a], and also multiple Goldstone-boson exchange in the form of scalar and vector mesons was investigated at about the same time [WPGV99b]. Finally, I will describe the extended GBE constituent quark model, which was published in a preliminary version in [WGPV00b] and [WGPV00a]. Therein almost all possible force components of the pseudoscalar, vector and scalar meson exchanges were considered, only spin-orbit forces and the central components of the octet vector-meson exchanges were left out.

It also provides the basis for the investigations in this work. The addition of spin-orbit force components was the aim of the diploma thesis by K. Glantschnig [Gla02], and will not be further considered here.

3.1 The non-relativistic model of Glozman, Papp, and Plessas (GPP)

The first model providing a parametrization of GBE dynamics was published by Glozman, Papp, and Plessas [GPP96]. It was constructed essentially in a non-relativistic framework. The Hamiltonian was taken in the general form as given in equations (2.1) and (2.2), however, one neglected all tensor components in the octet and singlet exchange potentials (2.10) and (2.11). This was justified by the small fine-structure splittings observed in the LS-multiplets. Due to that one assumed that the tensor components could only play a minor role in the description of the light and strange baryon spectra.

The smearing of the δ-function in the short-range term of the spatial parts of the meson-exchange potentials (2.12) was chosen in the form of a Gaussian with a width α and a shift r_0 from the origin:

$$4\pi\delta(\vec{r}_{ij}) \mapsto \frac{4}{\sqrt{\pi}}\alpha^3 e^{-\alpha^2(r-r_0)^2} \,. \tag{3.1}$$

The Yukawa part of the GBE was cut off for distances $r < r_0$. Since r_0 can be related to the size of the exchanged mesons and the size of the constituent quarks, this cut-off simply means that below the size of the particles involved in the exchange, there is no chiral boson-exchange interaction and the QCD degrees of freedom prevailing in the domain are not considered. Different from what Glozman and Riska had used in [GR96], the confinement was taken as a linear potential with the strength C as a free parameter:

$$V_{\text{conf}}(\vec{r}_{ij}) = C r_{ij} \,. \tag{3.2}$$

This parametrization involves a set of parameters, many of which can be taken as their phenomenological values. For the meson masses in the radial parts (2.12) and (2.13) of the potential the corresponding physical masses $\mu_\pi = 139$ MeV, $\mu_K = 494$ MeV, $\mu_\eta = 547$ MeV and $\mu_{\eta'} = 958$ MeV were assumed. Similarly the values for the constituent quark masses $m_{u,d} = 340$ MeV and $m_s = 440$ MeV were chosen as suggested. In the work by Glozman, Papp, and Plessas, only the light baryons (which do not include strange constituent quarks) were considered, so there are no K exchanges. The meson-quark coupling constant g_8^2 of the octet was taken as $\frac{g_8^2}{4\pi} = 0.67$ like the phenomenological pion-nucleon coupling suggests. For the coupling constant g_0^2 of the flavor-singlet η' no such phenomenological value exists, so it had to be taken as a free parameter. All in all, the model had four free parameters which were fitted

to the N and Δ spectra:

$$r_0 = 0.43 \text{ fm}, \quad \alpha = 2.91 \text{ fm}^{-1}, \quad (g_0/g_8)^2 = 1.8, \quad C = 0.474 \text{ fm}^{-2}\,.$$

The approach of replacing the δ-function in the contact interaction by a Gaussian of the form as in equation (3.1) has the disadvantage that the volume integral condition (2.16) is not fulfilled by the exchange potential.

This deficiency was cured in [GPP+97], where one used the same force components but adhered to a different type of smearing, namely a Yukawa-like smearing with Λ_γ being a cut-off parameter depending on the type of exchange particle. In a sense it describes the extension of the meson-quark interaction vertex:

$$4\pi\delta(\vec{r}_{ij}) \mapsto \Lambda_\gamma^2 \frac{e^{-\Lambda_\gamma r_{ij}}}{r_{ij}}\,. \tag{3.3}$$

The dependence of the cut-off parameters Λ_γ on the mesons masses was chosen as a linear scaling

$$\Lambda_\gamma = \Lambda_0 + \kappa\mu_\gamma\,. \tag{3.4}$$

In effect two free parameters Λ_0 and κ were introduced instead of the cut-off r_0 and the width α in the smearing (3.1) above. In this model also strange baryons were considered and the meson-quark coupling strengths were all regarded as free parameters. So in addition to the seven a-priori fixed parameters, the model has five free parameters (a sixth parameter is the constant V_0 in the confinement potential which is only used to shift the whole spectrum so that the nucleon ground state becomes 939 MeV):

Fixed parameters (physical or phenomenological values)		
$m_u = m_d = 340$ MeV	$\mu_\pi = 139$ MeV	$\mu_K = 494$ MeV
$m_s = 500$ MeV	$\mu_\eta = 547$ MeV	$\mu_{\eta'} = 958$ MeV
Free parameters (fitted to the experimental spectra)		
$\frac{g_8^2}{4\pi} = 1.24$	$\left(\frac{g_0}{g_8}\right)^2 = 2.23$	$C = 0.77$ fm^{-2}
$\Lambda_0 = 5.82$ fm^{-1}	$\kappa = 1.34$	$V_0 = -112$ MeV

Although the model could already produce the baryon spectra rather well - especially, it was able to show the correct level ordering in the lowest positive- and negative-parity states of the nucleon and the Δ as well as in the Λ baryon, it still suffered from several problems, mainly the non-relativistic treatment of the kinetic energy.

3.2 The semi-relativistic GBE constituent quark model

Although the non-relativistic GBE CQM was able to cure some long-standing problems in the effective description of baryon spectra, the shortcomings mentioned

above motivated Glozman, Papp, Plessas, Varga and Wagenbrunn ([GPP+98] and [GPVW98]) to propose a semi-relativistic version of the GBE constituent quark model. Its Hamiltonian has the form

$$H = \sum_{i=1}^{3} \sqrt{\vec{p}_i^{\,2} + m_i^2} + \sum_{i<j=1}^{3} \left(V_0 + C r_{ij} + V_\chi(\vec{r}_{ij}) \right), \tag{3.5}$$

where now the relativistic form of the kinetic-energy operator is used. The assumption of a relativistic kinetic energy, however, is only part of a fully relativistic treatment. Since the Q-Q interaction is still non-relativistic the model was called semi-relativistic. Like in the non-relativistic case, the tensor-components are left out, and only the spin-spin components of the radial terms $V_\chi(\vec{r}_{ij})$ are included. The δ-functions in the contact interaction terms are also replaced by a Yukawa-type smearing as given in equation (3.3) with the same linear dependence (3.4) of the cut-off parameters on the meson masses. The employed form factor is of the form

$$F_\gamma(q^2) = \sqrt{\frac{\Lambda_\gamma^2 - \mu_\gamma^2}{\Lambda_\gamma^2 + \vec{q}^{\,2}}},$$

so the complete radial dependence of the spin-spin component reads

$$V_\gamma(\vec{r}_{ij}) = \frac{g_\gamma^2}{4\pi} \frac{1}{12 m_i m_j} \left(\mu_\gamma^2 \frac{e^{-\mu_\gamma r_{ij}}}{r_{ij}} - \Lambda_\gamma^2 \frac{e^{-\Lambda_\gamma r_{ij}}}{r_{ij}} \right) . \tag{3.6}$$

This model needs 4 free fit parameters (and the over-all shift V_0 as a fifth parameter) and several a-priori fixed parameters like the meson and quark masses as well as the octet coupling constant:

Fixed parameters (physical or phenomenological values)		
$m_u = m_d = 340$ MeV	$\mu_\pi = 139$ MeV	$\mu_K = 494$ MeV
$m_s = 500$ MeV	$\mu_\eta = 547$ MeV	$\mu_{\eta'} = 958$ MeV
$g_8^2/4\pi = 0.67$		

Free parameters (fitted to the experimental spectra)		
$\left(\frac{g_0}{g_8}\right)^2 = 1.34$	$\Lambda_0 = 2.87$ fm^{-1}	$\kappa = 0.81$
$V_0 = -416$ MeV	$C = 2.33$ fm^{-2}	

This type of GBE CQM was able to produce the baryon spectra to a satisfying degree (see figure 3.1 for the predicted spectrum), e.g. the correct level orderings in the N, Λ and Σ spectra were obtained in contrast to other models[1]; also the Δ, Σ^* and Ξ^* ground states practically fall inside their very tight experimental error bounds. The $\frac{1}{2}^+$ Roper resonance $N(1440)$ is shifted well below the two degenerate

[1]See [GPP+98] for a comparison of the GBE model with the model proposed by Valcarce, González, Fernández, and Vento and the model proposed by Dziembowski, Fabre and Miller.

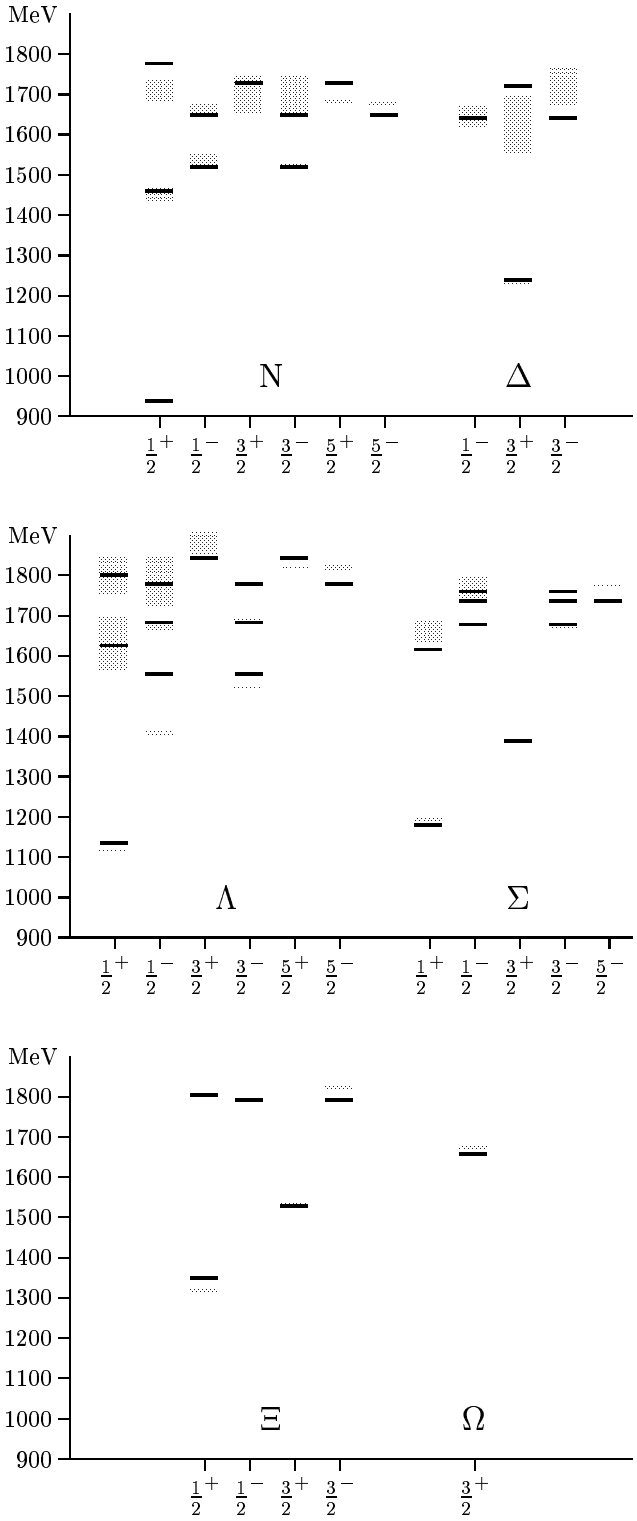

Figure 3.1: *The predicted spectrum in the first semi-relativistic version of the GBE CQM [GPP+98, GPVW98] matches the experimental data quite well. In particular, the correct level ordering in the nucleon, Λ, Σ and Ξ spectra is reproduced, and most of the ground states fall within the experimental error bounds*

negative-parity $\frac{1}{2}^-$ and $\frac{3}{2}^-$ states $N(1535)$ and $N(1520)$ which form an LS-doublet, and the correct level ordering can also be observed in the Λ and Σ spectra. In the Λ spectrum, the two negative-parity $\frac{1}{2}^-$ and $\frac{3}{2}^-$ states, correctly remain the lowest excitations in the spectrum. In their papers [GPP+98] and [GPVW98] the authors showed that in this case no level crossing appears with increasing coupling strength $\frac{g_8^2}{4\pi}$. On the other hand, from the level crossings occurring in the N spectrum one learns that the correct choice of this coupling constant is of vital importance for the description of the right level orderings.

However, the flavor singlet $\Lambda(1405)$, which is the first negative-parity state in the Lambda spectrum, could not be reproduced to a satisfying degree. Very probably Fock components higher than the QQQ components play a major role in this state and they are not yet included in the model. This represents a persisting problem, which is common to all constituent models.

The semi-relativistic GBE CQM also faces the problem that in the Δ spectrum the level structure as suggested by experimental data is not reproduced. In particular, the lowest positive-parity $\frac{3}{2}^+$ excitation $\Delta(1600)$ lies above the $\frac{1}{2}^-$ and $\frac{3}{2}^-$ states $\Delta(1620)$ and $\Delta(1700)$ and thus also above the experimental data.

One has to notice that the choice of parameters given above is not unique. For instance, if one changes some of the fixed parameters slightly, the free parameters can be re-adjusted so as to produce a spectrum that matches the experimental data in a similar manner. Even if one of the free parameters is taken as fixed to a certain value, in many cases the remaining free parameters can be chosen so that the spectrum looks like the one shown in figure 3.1. This clearly indicates that the baryon spectra alone simply do not determine the effective Goldstone-boson-exchange potential uniquely.

3.3 The extended GBE CQM model

The models presented so far, have neglected all tensor components in the GBE potentials (2.10) and (2.11). These tensor-force components are responsible for the hyperfine splitting of the LS-multiplets in the baryon spectra, which were degenerate in the results above. Since these splittings are quite small, it was argued that the tensor components give only small contributions to the whole baryon spectrum.

Studies of the Pavia group suggested [BDRW99] that forces other than the spin-spin components of the pseudoscalar exchange needed to be included to fully describe contributions also from two-body electromagnetic current operators. Subsequently, the tensor-force component has been included into the calculations in [WPGV99a], where it became clear that the tensor force of the pseudoscalar meson-exchange potential is much too strong to yield an acceptable spectrum for the baryons. It turned out that one has to consider also multiple Goldstone-boson exchange to cure this problem. The exchange of two Goldstone bosons can effectively be described as the exchange of a ρ, σ, or K^* meson, and a three Goldstone-boson exchange can be modeled as the exchange of an ω or ϕ. So to extend the GBE model, in addition

to the pseudoscalar exchange mesons (π, K, η, η'), one also has to include the exchange of vector mesons $(\rho, \omega, K^*, \phi)$ and scalar mesons $(\sigma, \kappa, a_0, f_0)$. One then finds that the effects of these additional exchanges almost cancel the tensor-force components of the pseudoscalar meson exchange, and the hyperfine level splitting goes back to an acceptable magnitude, where for example the $N(1535) - N(1520)$ and the $N(1650) - N(1700) - N(1675)$ are almost degenerate.

A preliminary parametrization of this extended GBE constituent quark model, including all possible force-components (except the spin-orbit forces and the central components of the octet vector-meson exchanges) of the pseudoscalar, vector, and scalar meson exchange, was given in [WGPV00a] and [WGPV00b] by Wagenbrunn, Glozman, Plessas, and Varga. The neglected spin-orbit forces would only contribute very little to the spectrum, as the effects coming from the different types of exchanges practically cancel each other. This is also supported by a work of Riska and Brown [RB99] studying the two-pion exchange between constituent quarks. Nevertheless, the inclusion of the spin-orbit forces will be done among the items of the diploma thesis of K. Glantschnig [Gla02].

The extended GBE of [WGPV00a] model is based on a semi-relativistic Hamiltonian of the form

$$H = \sum_{i=1}^{3} \sqrt{\vec{p}_i^{\,2} + m_i^2} + \sum_{i<j} \left(V_\chi(\vec{r}_{ij}) + V_{\text{conf}}(\vec{r}_{ij}) \right) \ . \tag{3.7}$$

Instead of a linear confinement a different type was used, which behaves linearly below a certain threshold r_0 and is constant above:

$$V_{\text{conf}}(\vec{r}_{ij}) = V_0 + Cr_0(1 - e^{-r_{ij}/r_0}) \approx \begin{cases} V_0 + Cr_{ij} & r_{ij} \ll r_0 \,, \\ V_0 + Cr_0 = \text{const.} & r_{ij} \gg r_0 \,. \end{cases} \tag{3.8}$$

For the smearing of the δ-function in the meson-exchange potential the following Yukawa form was employed

$$4\pi\delta(\vec{r}_{ij}) \to \mu_\gamma^2 + \frac{\Lambda_\gamma(\Lambda_\gamma^2 - \mu_\gamma^2)r}{2} \frac{e^{-\Lambda_\gamma r_{ij}}}{r_{ij}} \ , \qquad \gamma = \pi, K, \eta, \eta', \rho, \sigma, K^*, \omega, \phi \,, \tag{3.9}$$

which corresponds to vertex form factors of the type

$$F(\vec{q}^{\,2}) = \frac{\Lambda_\gamma^2 - \mu_\gamma^2}{\Lambda_\gamma^2 + q^2} \ . \tag{3.10}$$

The cut-off parameters Λ_γ had to be taken differently for the pseudoscalar and for the vector and scalar mesons. The dependences on the meson masses are still linear, but a different starting point was used for the two kinds of exchange mesons:

$$\Lambda_\gamma^{\text{ps}} = \Lambda_\pi + \kappa\,(\mu_\gamma - \mu_\pi) \ , \tag{3.11a}$$

$$\Lambda_\gamma^{\text{vect,scal}} = \Lambda_\rho + \kappa\,(\mu_\gamma - \mu_\rho) \ . \tag{3.11b}$$

Fixed parameters (physical values)		
$m_u = m_d = 340$ MeV	$m_s = 500$ MeV	$C = 2.53$ fm^{-2}
$\mu_\pi = 139$ MeV	$\mu_K = 494$ MeV	$\mu_\eta = 547$ MeV
$\mu_{\eta'} = 958$ MeV	$\mu_\rho = 770$ MeV	$\mu_{K^*} = 892$ MeV
$\mu_{\omega_8} = 869$ MeV	$\mu_{\omega_0} = 947$ MeV	$\mu_\sigma = 680$ MeV
$g_8^2/4\pi = 0.67$	$\left(\frac{g_0}{g_8}\right)^2 = 1$	$g_\sigma^2/4\pi = 0.67$
$\left(g_8^{\mathrm{V}}\right)^2/4\pi = 0.026$	$\left(g_8^{\mathrm{T}}\right)^2/4\pi = 0.97$	
$\left(g_0^{\mathrm{V}}\right)^2/4\pi = 2.14$	$\left(g_0^{\mathrm{T}}\right)^2/4\pi = 0.11$	

Free parameters (fitted to the spectrum)		
$\Lambda_\pi = 700$ MeV	$\Lambda_\rho = 1200$ MeV	$\kappa = 1.2$
$V_0 = -419$ MeV	$r_0 = 7$ fm	

Table 3.1: *Parameters of the extended GBE CQM as published in [WGPV00a] and [WGPV00b]*

In order to take into account that all the exchange particles have different masses and maybe also different flavor-dependent coupling constants, the complete chiral interaction constructed from ps + v + s exchange has to be expressed in the form

$$\begin{aligned} V_\chi(\vec{r}_{ij}) =& V^{ps}(\vec{r}_{ij}) + V^{v}(\vec{r}_{ij}) + V^{s}(\vec{r}_{ij}) = \\ =& \sum_{a=1}^{3} \left(V_\pi(\vec{r}_{ij}) + V_\rho(\vec{r}_{ij})\right) \lambda_i^a \lambda_j^a + \sum_{a=4}^{7} \left(V_K(\vec{r}_{ij}) + V_{K^*}(\vec{r}_{ij})\right) \lambda_i^a \lambda_j^a + \\ &+ \left(V_\eta(\vec{r}_{ij}) + V_{\omega_8}(\vec{r}_{ij})\right) \lambda_i^8 \lambda_j^8 + \frac{2}{3} \left(V_{\eta'}(\vec{r}_{ij}) + V_{\omega_0}(\vec{r}_{ij})\right) + V_\sigma(\vec{r}_{ij}) \end{aligned} \tag{3.12}$$

where each of the V_γ for $\gamma = \pi, \rho, K, K^*, \eta, \omega_8, \eta', \omega_0, \sigma, \kappa, a_0, f_0$ can contain central, spin-spin, tensor as well as spin-orbit forces.

Before giving the exact forms of the potential terms, let us take a quick look at the results of the parametrization published in [WGPV00a] and [WGPV00b]. All constituent quark masses as well as all exchange meson masses were taken as their corresponding physical or phenomenological values. The coupling constants were also derived from phenomenology[2], and the confinement strength C was fixed to the value $C = 2.53$ fm^{-2} in accordance with lattice results for the string tension in the quark-antiquark potential. Thus there are only five free parameters left: three (Λ_π, Λ_ρ and κ) for the linear scaling of the cut-off parameters of the contact interaction, the cut-off r_0 of the confinement, and the over-all shift V_0. Their values were determined by a fit to the experimental spectra as given in table 3.1.

The corresponding predicted spectra of the light and strange baryons are shown in figure 3.2. If one compares this with the results from the semi-relativistic model

[2]See, e.g., section 3.2.6 of [Gla02] for the derivation of the coupling constants

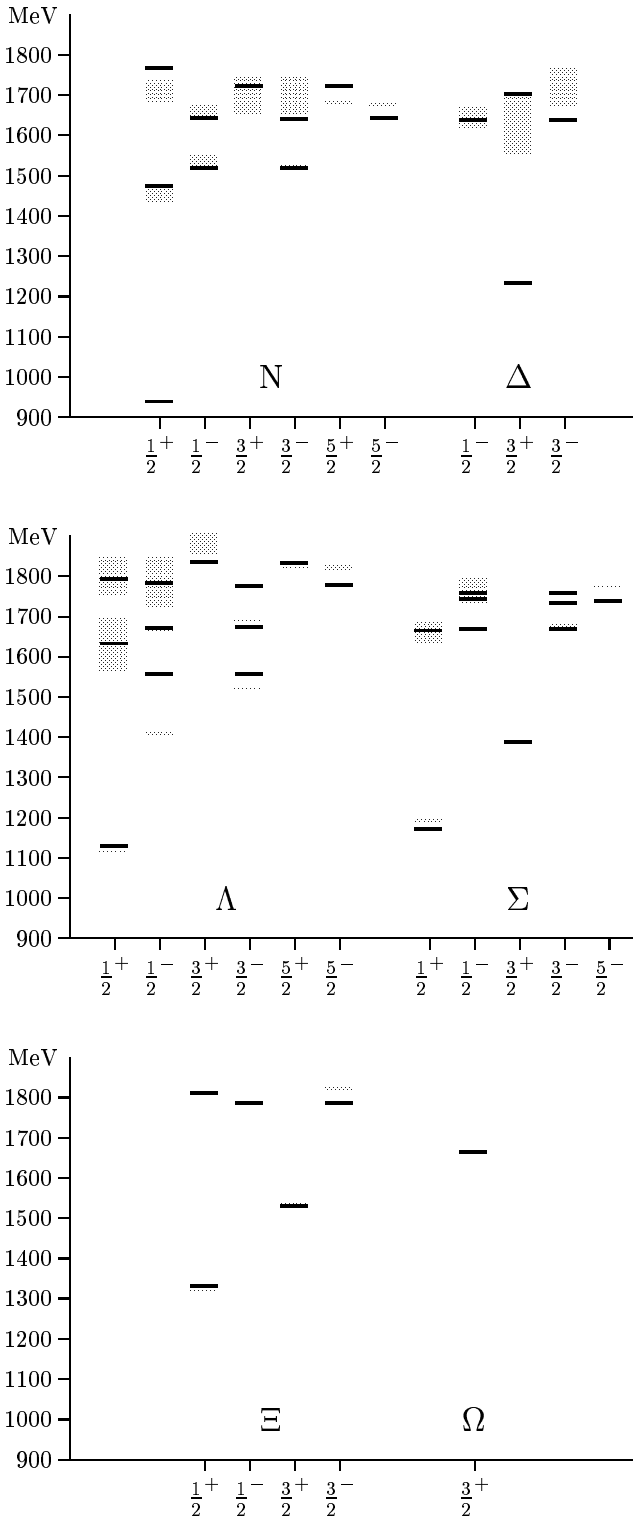

Figure 3.2: *The predicted spectrum of the preliminary extended GBE model as published in [WGPV00a]. The correct level ordering of the lowest states is preserved even with the inclusion of all tensor force components and the addition of vector and scalar meson exchanges. The gray boxes represent the observed values of the baryon states with their uncertainties as given in [H+02].*

(figure 3.1, which neglects all tensor-components and all tensor- and scalar-meson exchanges, one has to notice that the inclusion of all components present in the GBE exchange preserves all the features of the previous (pseudoscalar) model, especially the correct level ordering of the lowest positive- and negative-parity states.

The structure of the pseudoscalar, vector, and scalar components of the Goldstone-boson-exchange potential is exactly the same as for the extended GBE constituent quark model we shall work on in the present thesis. It will be further elaborated in the next section. Thus we refrain from a thorough discussion of the components here and leave that for the next section.

The main aims of our work will be to improve this result by investigating other possible confinement strategies, a different set of free parameters, and to investigate the particular effects of certain parameters (especially the cut-off parameters in the smearing of the δ-function).

3.4 The extended GBE CQM used in our calculations

In this work, we shall consider a similar extended GBE constituent model, which includes all possible components of the pseudoscalar, vector, and scalar exchange, except the spin-orbit components, and the central component of the octet vector mesons. The corresponding (semi-relativistic) Hamiltonian thus has the same form as given in equation (3.7).

The hyperfine interaction $V_\gamma(r_{ij})$ in the dynamic part of the Hamiltonian consists of contributions from each of the three exchange-particle families:

- The pseudoscalar meson nonet ($\gamma = \pi,\ K,\ \eta,\ \eta'$) causes spin-spin and tensor components.
- The vector meson nonet ($\gamma = \rho,\ K^*,\ \omega_8,\ \omega_0$) has contributions from all forces (i.e. central, spin-spin, tensor and spin-orbit forces)
- The scalar meson singlet σ comes only with central and spin-orbit forces.

The expressions for the corresponding potential terms can be found in [PGVW99].

3.4.1 The confinement

The confinement potential we use is again a linear confinement (which is different from the preliminary model of the last section, where the confinement was taken as constant outside a certain range determined by r_0) of the form

$$V_{\text{conf}}(\vec{r}_{ij}) = V_0 + C r_{ij} \tag{3.13}$$

with a string tension C and the over-all shift V_0 as free parameters to adjust th ground state of the spectrum.

3.4.2 Multiple GBE

Let us first take a closer look at multiple-GBE and the appearance of vector and scalar exchange mesons.

Although the first Goldstone-boson-exchange constituent quark models, which included only the spin-spin component of the pseudoscalar (π, K, η, η') mesons, clearly showed that these components are by far the most important terms to get the structure of the baryon spectra and already produce the correct level orderings, the tensor-force components cannot be left out. Unfortunately, their inclusion leads to a level splitting at variance with the experimental data. The pseudoscalar GBE constituent quark model thus does not appear to be a complete description of the GBE dynamics in the light and strange baryons. Very probably it misses further important dynamical ingredients. In its derivation one assumes the exchange of single Goldstone bosons (independently from each other and only one exchange at a time). This assumption appears too restrictive and one is tempted to include multiple Goldstone boson exchanges.

In models of the NN-interaction, the same problem has been solved effectively [Mac89] by the inclusion of vector and scalar meson exchanges to account for the simultaneous (and possible correlated) exchange of two or more mesons. It seems to be quite natural to include also vector and scalar meson exchange in the GBE constituent quark model to describe multiple GBE.

In the 2 π exchange, for example, the two simultaneously exchanged pions can either interact during the exchange or not. If they interact and the 2π pair can be in a P-wave state. Such an exchange receives the main contribution from the P-wave resonance and it can be modeled as a ρ-exchange. If in turn, the two correlated π's are in an S-wave state, Durso et al. [DJV80] showed that one can approximate them by the exchange of a scalar σ meson. Similarly, the correlated 3π exchange can be approximated by the exchange of one ω meson, and the multiple exchange of the remaining Goldstone bosons can be treated in an analogous fashion (see figure 2.2). Thus, the GBE model has to be extended from the exchange of pseudoscalar mesons to the additional exchange of the vector meson nonet (ρ, K^*, ω_8, ω_0) and the exchange of the scalar mesons (a_0, κ, f_0, σ)[3]. Although the scalar σ meson is important for NN dynamics at a medium range, in the description of the baryons it plays only a minor role. Since the σ meson exchange contains only a small spin-orbit component (which is neglected in this work anyway) and an attractive central potential, it might be effectively included into the confinement potential between the constituent quarks.

The exchange of the vector mesons, however, is of crucial importance to counterbalance the effect of the large spin-orbit splitting introduced by the tensor-component of the pseudoscalar exchange potential. As we will see, the spin-spin component of the vector exchange has the same sign as the spin-spin component of the pseudoscalar

[3]Of the scalar mesons we shall only include the σ meson in our calculations, as the other ones are only needed for the spin-orbit terms.

exchange, whereas the tensor components are of opposite signs, so they practically cancel each other. Thus, the inclusion of the vector meson exchange decreases the large spin-orbit splitting caused by the tensor-component of the pseudoscalar exchange. The coupling of the constituent quarks to the octet vector meson fields $\vec{v}^{\mu}$ has the form [Glo98][4]

$$L^{v} = -g^{v}\bar{\psi}\gamma_{\mu}\vec{\lambda}^{F}\cdot\psi\vec{v}^{\mu} + \frac{g^{t}}{2m}\bar{\psi}\sigma_{\mu\nu}\vec{\lambda}^{F}\cdot\psi\partial^{\nu}\vec{v}^{\mu}\ , \tag{3.14}$$

with g^{v} and g^{t} being the vector and tensor coupling constants. If, like in the pseudoscalar exchange, one performs a non-relativistic reduction to lowest order, the vector-meson exchange includes spin-spin, tensor, spin-orbit as well as central force components between the constituent quarks.

As outlined in [Gla02] and other sources, the pseudoscalar meson-quark vertex with its $\vec{\sigma}\cdot\vec{\nabla}$ structure leads to spin-spin and tensor components for the pseudoscalar exchange of the structure

$$\left(\vec{\sigma}_i\cdot\vec{\nabla}\right)\left(\vec{\sigma}_j\cdot\vec{\nabla}\right) = \frac{1}{3}\left(\vec{\sigma}_i\cdot\vec{\sigma}_j\right)\nabla^2 + \frac{1}{3}\left(3\left(\vec{\sigma}_i\cdot\vec{\nabla}\right)\left(\vec{\sigma}_j\cdot\vec{\nabla}\right) - \left(\vec{\sigma}_i\cdot\vec{\sigma}_j\right)\nabla^2\right)\ .$$

In contrast, the vector-meson exchange has a structure $\vec{\sigma}\times\vec{\nabla}$ at the vertex, which leads to spin-spin and tensor components for the vector-meson exchange of the form

$$\left(\vec{\sigma}_i\cdot\vec{\nabla}\right)\left(\vec{\sigma}_j\cdot\vec{\nabla}\right) = \frac{2}{3}\left(\vec{\sigma}_i\cdot\vec{\sigma}_j\right)\nabla^2 - \frac{1}{3}\left(3\left(\vec{\sigma}_i\cdot\vec{\nabla}\right)\left(\vec{\sigma}_j\cdot\vec{\nabla}\right) - \left(\vec{\sigma}_i\cdot\vec{\sigma}_j\right)\nabla^2\right)\ .$$

In the pseudoscalar and the vector-meson exchange, the two spin-spin components thus have the same sign and the spin-spin part of the vector-meson exchange is twice as large as the one of the pseudoscalar exchange. On the other hand, the tensor-components are exactly the same and have opposite sign, so they act against each other, and the tensor-force contribution to the spectra is small in total. Note, however, that this is only valid in lowest order. In higher order different contributions from tensor forces can occur which need not cancel each other. Nevertheless their net effect should have no great influence on the baryon spectra. Like in the pseudoscalar case, the same volume integral condition like equation (2.16) can be deduced for the vector-meson exchange, so the short-range part of the spin-spin component of the vector meson exchange can be expected to be similar to the pseudoscalar meson exchange.

Summarizing, these hand-waving arguments on the effects of the vector meson exchange, one can expect that the pseudoscalar and vector-meson exchanges produce similar spin-spin components, while their tensor components more or less cancel, so the spin-orbit splitting is decreased and this problem of the pseudoscalar model can be solved by the inclusion of vector exchange mesons.

[4]Like in the pseudoscalar coupling case given in equation (2.7) we will only use a $SU(3)_F$-symmetric approximation.

The vector meson exchange also leads to a spin-orbit force in its exchange potential, but this will be neglected in this work.

3.4.3 The pseudoscalar meson exchange

Although we have already discussed the exchange potential of the pseudoscalar mesons in great detail in chapter 2, we will quickly repeat the most important facts and equations here to allow an easier comparison to the potentials introduced by the vector and scalar meson exchange.

The octet of pseudoscalar Goldstone bosons (π, K, η) leads to spin-spin and tensor components as discussed in section 2.4.1. The η' cannot exactly be considered a Goldstone boson, which it becomes only beyond the scale of the spontaneously broken symmetry $SU(3)_R \times SU(3)_L$ to $SU(3)_V$. Still, we will include it in our considerations of the pseudoscalar GBE, and so work with the nonet $\gamma \in (\pi, K, \eta, \eta')$ of pseudoscalar exchange mesons.

The structure of the pseudoscalar exchange potential is

$$V_\gamma(\vec{r}_{ij}) = V_\gamma^{SS}(\vec{r}_{ij})\vec{\sigma}_i \cdot \vec{\sigma}_j + V_\gamma^{T}(\vec{r}_{ij}) \left[3\left(\hat{r}_{ij} \cdot \vec{\sigma}_i\right)\left(\hat{r}_{ij} \cdot \vec{\sigma}_j\right) - \vec{\sigma}_i \cdot \vec{\sigma}_j\right] . \tag{3.15}$$

where V_γ^{SS} contains the radial dependence of the spin-spin part, and V_γ^{T} describes the radial dependence of the tensor-component. These radial dependences can be written in the form of equations (2.12) and (2.13), if one assumes that the boson fields fulfill a linear Klein-Gordon equation and the involved particles are pointlike. This assumption cannot be maintained in reality, so the finite extension has to be accounted for by the inclusion of a form factor for the meson-quark interaction vertex. We take a monopole-type parametrization of the meson-quark vertex as in equation (3.10). The cut-off parameters therein will be different for different particles, although for all pseudoscalar mesons we employed a linear scaling as given in (3.11). Such a linear scaling can be justified insofar, as a larger mass of the exchanged mesons should also lead to a larger cut-off. Otherwise the potential might change sign and become attractive or repulsive where it should not be so. This type of form factor leads to a Yukawa-type smearing of the δ-function in the spin-spin part.

Using this form factor and the Yukawa-smearing in the spin-spin part, we obtain the following spatial parts for the pseudoscalar meson-exchange potential:

Spin-spin component:

$$V_\gamma^{SS}(\vec{r}) = \frac{g_\gamma^2}{4\pi} \frac{1}{12 m_i m_j} \left[\mu_\gamma^2 \frac{e^{-\mu_\gamma r}}{r} - \left(\mu_\gamma^2 + \frac{\Lambda_\gamma(\Lambda_\gamma^2 - \mu_\gamma^2) r}{2}\right) \frac{e^{-\Lambda_\gamma r}}{r}\right] \tag{3.16}$$

Tensor-force component:

$$V_\gamma^T(\vec{r}) = \frac{g_\gamma^2}{4\pi}\frac{1}{12 m_i m_j}\left[\mu_\gamma^2\left(1+\frac{3}{\mu_\gamma r}+\frac{3}{\mu_\gamma^2 r^2}\right)\frac{e^{-\mu_\gamma r}}{r} - \right. \\ - \Lambda_\gamma^2\left(1+\frac{3}{\Lambda_\gamma r}+\frac{3}{\Lambda_\gamma^2 r^2}\right)\frac{e^{-\Lambda_\gamma r}}{r} - \\ \left. - \frac{(\Lambda_\gamma^2-\mu_\gamma^2)(1+\Lambda_\gamma r)}{2}\frac{e^{-\Lambda_\gamma r}}{r}\right]. \tag{3.17}$$

The coupling constants $\frac{g_\gamma^2}{4\pi}$ can be fixed to values deriving from phenomenology (see section 3.2.6 of [Gla02] for a derivation of the values for the coupling constants). Of course, one might also take the coupling constants as free parameters, but that would lead to a model with too many free parameters. So we decided to take well-motivated fixed values for them and to fit only the cut-off parameters Λ_γ and the confinement parameters.

3.4.4 The vector mesons

As we have already elaborated above, multiple GBE can be modeled by the exchange of a meson from the vector nonet $\gamma \in (\rho, K^*, \omega_8, \omega_0)$. The specific coupling of the vector mesons to the constituent quarks gives rise to all possible force types: spin-spin forces, tensor forces, spin-orbit forces and central forces. Thus the structure of the vector exchange potential is

$$V_\gamma(\vec{r}_{ij}) = V_\gamma^C(\vec{r}_{ij}) + V_\gamma^{SS}(\vec{r}_{ij})\vec{\sigma}_i\cdot\vec{\sigma}_j + \\ + V_\gamma^T(\vec{r}_{ij})\left[3\left(\hat{r}_{ij}\cdot\vec{\sigma}_i\right)\left(\hat{r}_{ij}\cdot\vec{\sigma}_j\right) - \vec{\sigma}_i\cdot\vec{\sigma}_j\right] + \\ + V_\gamma^{LS}(\vec{r}_{ij})\vec{L}_{ij}\cdot\vec{S}_{ij}\,. \tag{3.18}$$

The radial dependence for the components can be obtained similarly to the pseudoscalar case, with the same form factor and the same type of smearing used.

The central component then has the spatial dependence

$$V_\gamma^C(\vec{r}) = \frac{(g_\gamma^V)^2}{4\pi}\left[\frac{e^{-\mu_\gamma r}}{r} - \left(1+\frac{(\Lambda_\gamma^2-\mu_\gamma^2)r}{2\Lambda_\gamma}\right)\frac{e^{-\Lambda_\gamma r}}{r}\right], \tag{3.19}$$

while the spin-spin and the tensor components have the same structure as the pseudoscalar mesons. However, different coupling constants need to be chosen, including both tensor and vector coupling:

$$\text{Spin-spin potential:} \quad \frac{g_\gamma^2}{4\pi} \to 2\frac{(g_\gamma^V+g_\gamma^T)^2}{4\pi}, \\ \text{Tensor potential:} \quad \frac{g_\gamma^2}{4\pi} \to -\frac{(g_\gamma^V+g_\gamma^T)^2}{4\pi}.$$

Thus the spin-spin and the vector components of the vector exchange potential becomes

$$V_\gamma^{SS}(\vec{r}) = 2\frac{(g_\gamma^V + g_\gamma^T)^2}{4\pi}\frac{1}{12m_i m_j}\left[\mu_\gamma^2\frac{e^{-\mu_\gamma r}}{r} - \left(\mu_\gamma^2 + \frac{\Lambda_\gamma(\Lambda_\gamma^2-\mu_\gamma^2)r}{2}\right)\frac{e^{-\Lambda_\gamma r}}{r}\right] \tag{3.20}$$

$$\begin{aligned} V_\gamma^T(\vec{r}) = -\frac{(g_\gamma^V + g_\gamma^T)^2}{4\pi}\frac{1}{12m_i m_j}\Bigg[&\mu_\gamma^2\left(1+\frac{3}{\mu_\gamma r}+\frac{3}{\mu_\gamma^2 r^2}\right)\frac{e^{-\mu_\gamma r}}{r} - \\ &-\Lambda_\gamma^2\left(1+\frac{3}{\Lambda_\gamma r}+\frac{3}{\Lambda_\gamma^2 r^2}\right)\frac{e^{-\Lambda_\gamma r}}{r} - \\ &-\frac{(\Lambda_\gamma^2-\mu_\gamma^2)(1+\Lambda_\gamma r)}{2}\frac{e^{-\Lambda_\gamma r}}{r}\Bigg]. \end{aligned} \tag{3.21}$$

Finally, the spin-orbit spatial component of the vector meson potential has the form

$$\begin{aligned} V_\gamma^{LS}(\vec{r}) = -\frac{(g_\gamma^V)^2}{4\pi}\left(3+4\frac{g_\gamma^T}{g_\gamma^V}\right)\frac{1}{2m_i m_j}\Bigg[&\mu_\gamma^3\left(\frac{1}{\mu_\gamma^2 r^2}+\frac{1}{\mu_\gamma^3 t^3}\right)\frac{e^{-\mu_\gamma r}}{r} - \\ &-\Lambda_\gamma^3\left(\frac{1}{\Lambda_\gamma^2 r^2}+\frac{1}{\Lambda_\gamma^3 r^3}\right)\frac{e^{-\Lambda_\gamma r}}{r} - \frac{\Lambda_\gamma^2-\mu_\gamma^2}{2r}\frac{e^{-\Lambda_\gamma r}}{r}\Bigg]. \end{aligned} \tag{3.22}$$

Although this spin-orbit force appears in this derivation, we will neglect it due to its small contributions.

3.4.5 The scalar mesons

The scalar σ, κ, a_0 and f_0 mesons induce only central and spin-orbit forces, both of which have the same form as with vector meson exchange.

$$V_\gamma(\vec{r}_{ij}) = V_\gamma^C(\vec{r}_{ij}) + V_\gamma^{LS}(\vec{r}_{ij})\vec{L}_{ij}\cdot\vec{S}_{ij} \tag{3.23}$$

$$V_\gamma^C(\vec{r}) = -\frac{g_\sigma^2}{4\pi}\left[\frac{e^{-\mu_\gamma r}}{r} - \left(1+\frac{(\Lambda_\gamma^2-\mu_\gamma^2)r}{2\Lambda_\gamma}\right)\frac{e^{-\Lambda_\gamma r}}{r}\right], \tag{3.24}$$

$$\begin{aligned} V_\gamma^{LS}(\vec{r}) = -\frac{g_\sigma^2}{4\pi}\frac{1}{2m_i m_j}\Bigg[&\mu_\gamma^3\left(\frac{1}{\mu_\gamma^2 r^2}+\frac{1}{\mu_\gamma^3 t^3}\right)\frac{e^{-\mu_\gamma r}}{r} - \\ &-\Lambda_\gamma^3\left(\frac{1}{\Lambda_\gamma^2 r^2}+\frac{1}{\Lambda_\gamma^3 r^3}\right)\frac{e^{-\Lambda_\gamma r}}{r} - \frac{\Lambda_\gamma^2-\mu_\gamma^2}{2r}\frac{e^{-\Lambda_\gamma r}}{r}\Bigg]. \end{aligned} \tag{3.25}$$

For the scalar mesons the coupling constants in equations (3.19) and (3.22) have to be replaced by :

$$\begin{aligned} \text{Central force:} \quad & \frac{(g_\gamma^V)^2}{4\pi} \to -\frac{g_\sigma^2}{4\pi} \\ \text{Spin-orbit force:} \quad & \frac{(g_\gamma^V)^2}{4\pi}\left(3+4\frac{g_\gamma^T}{g_\gamma^V}\right) \to \frac{g_\sigma^2}{4\pi} \end{aligned}$$

Again, we will neglect the spin-orbit forces, and only include the central-force component, which might even effectively be included in the confinement, and one could work without scalar-meson exchange altogether.

Chapter 4

Stochastic variation

Contents

4.1 Introduction to the stochastic variation

In our calculations of the quantum-mechanical energy eigenstates of the GBE CQM discussed in the previous chapters, we will employ a variational method, which is based on the famous Ritz theorem:

Theorem 4.1 (Ritz Theorem). *For an arbitrary function Ψ of a Hilbert space $\mathcal{H}$ (the state space) the expectation value $E(\Psi)$ of a Hamilton operator H in the state Ψ is such that*

$$E(\Psi) = \frac{\langle \Psi | H | \Psi \rangle}{\langle \Psi | \Psi \rangle} \geq E_0 \ ,$$

where equality holds iff Ψ is an eigenstate of H with eigenvalue E_0. The constant E_0 in this inequality denotes the energy of the ground state of the Hamiltonian H.

In other words, this theorem states that whatever wave function we use to calculate the energy (eigenvalue of the Hamiltonian), we will always stay above the ground state energy. Thus, we can take any arbitrary function, calculate the expectation value and so get an upper bound for the ground state energy, no matter how diligent or careless we choose our parameters and basis functions. Of course, the better the wave function (i.e. the better it approximates the ground state eigenfunction of the Hamiltonian), the better our bound will be.

Since we are working in a Hilbert space, any function Ψ can be written as a linear combination of basis functions

$$\Psi = \sum c_i \psi_i \; . \tag{4.1}$$

Unfortunately, we are dealing with infinite-dimensional Hilbert spaces, so we need to choose the most important basis functions beforehand and approximate the function Ψ, represented by a coefficient set $A = \{c_i, i = 1, \ldots N\}$, by a linear combination of these basis functions $\Psi(A) = \sum_{i=1}^{N} c_i \psi_{\alpha_i}$. We are now searching for the the best parameter set $\tilde{A}$, i.e. the parameter set A for which the expectation value $E_{K,1} = \langle \Psi(\tilde{A}) \, | H | \, \Psi(\tilde{A}) \rangle$ is minimized.

4.2 Motivation and basics

Naïvely looking at our ansatz for the wave function, one would expect that the parameters for the basis functions ψ_i are chosen prior to the calculation and then the coefficients c_i are determined in a way to minimize the total energy. Once the basis functions are chosen by some arbitrary selection algorithm (probably not even depending on the Hamiltonian), the best, i.e. lowest, upper bound for the energy is the lowest eigenvalue E_0^N of the eigenvalue problem

$$\sum_{j=1}^{N} \langle \psi_i | H | \psi_j \rangle c_j = E_N \sum_{j=1}^{N} \langle \psi_i | \psi_j \rangle \; . \tag{4.2}$$

One cannot expect to calculate the exact ground state, because by taking only a finite number of basis functions, this optimization is done only in a subspace of our Hilbert space $\mathcal{H}$.

To be more concise, I will use the following notation in the sequel:

$$H_{ij} = \langle \psi_i | H | \psi_j \rangle \, , \qquad\qquad B_{ij} = \langle \psi_i | \psi_j \rangle \, .$$

The matrices $\mathbf{H}_{ij}$ and $\mathbf{B}_{ij}$ are both $N \times N$ matrices and can be computed once the basis functions are selected. The best estimate for the energy, and the coefficients c_i can now be calculated as the eigenvalues and eigenfunctions of the generalized eigenvalue problem:

$$\sum_{j=1}^{N} H_{ij} c_j = E_N \sum_{j=1}^{N} B_{ij} c_j \quad \text{or} \quad \mathbf{H} \cdot \mathbf{c} = E_N \, \mathbf{B} \cdot \mathbf{c} \; . \tag{4.3}$$

By using an orthogonal set of basis functions, the eigenvalue problem simplifies to a standard eigenvalue problem, since $B_{ij} = \delta_{ij}$, and can be treated with linear algebra methods to find an accurate numerical solution. In our programs, the diagonalization itself is done by the numerical functions provided by the NAG library.

For the ground state energy we would only need the lowest eigenvalue, but we can also use the higher eigenvalues as bounds for the higher excitations in the spectrum.

This second theorem on which we base our work, generally known as the "Mini-Max Theorem", makes a statement for the higher eigenvalues of our Hamiltonian H similar to what the Ritz-theorem says about the ground state energy:

Theorem 4.2 (Mini-Max Theorem). *Let H be an Hermitian operator with discrete eigenvalues $E_1 \leq E_2 \leq \ldots$. Let $\varepsilon_1 \leq \varepsilon_2 \leq \cdots \leq \varepsilon_K$ be the eigenvalues of H restricted to the subspace $\mathcal{V}_K$ of a linearly independent set of K functions $\Psi(\alpha_1), \ldots, \Psi(\alpha_K)$. Then*

$$E_1 \leq \varepsilon_1,\ E_2 \leq \varepsilon_2,\ \ldots\ E_K \leq \varepsilon_K\ .$$

This theorem simply says that if we do our optimization only in a space with a finite number of basis states (i.e. the wave functions are only a linear combination of a finite number of preselected basis functions), the i-th eigenvalue of this finite eigenvalue problem is an upper bound for the exact i-th eigenvalue. So if we do a complete diagonalization of the eigenvalue problem, we automatically get upper estimates for the higher excitations of the baryons.

Again, intuitively it should be clear that the more basis functions we use, the better our bounds will be. This is also the statement of a further theorem that quantifies the change in the energy eigenvalues by adding more basis functions to our system. It states that by adding an additional linearly independent (if the new basis function is linearly dependent on the ones already included, of course, we cannot gain anything) basis function $\Psi(\alpha_{K+1})$, all eigenvalues improve and keep their order:

$$\varepsilon'_1 \leq \varepsilon_1 \leq \varepsilon'_2 \leq \varepsilon_2 \leq \cdots \leq \varepsilon'_K \leq \varepsilon_K \leq \varepsilon'_{K+1}\ , \tag{4.4}$$

where the ε_i are the eigenvalues with K basis functions and the ε'_i denote the eigenvalues with $K+1$ basis functions (where the first K basis functions coincide).

The eigenvalue problem (4.3) can be further simplified, if one notices that for eigenstates of operators that commute with the Hamiltonian, the matrix elements H_{ij} of the Hamilton operator between states with different quantum numbers (eigenvalues of the commuting operators) vanish, just like the overlaps B_{ij} between such states do. This causes a block structure to appear in the matrices $\mathbf{H}$ and $\mathbf{B}$, so the problem decomposes into an eigenvalue subproblem for each set of quantum numbers. Consequently, the problem can be solved for each set of different quantum (e.g. the states $N(\frac{1}{2}^-)$, $N(\frac{1}{2}^+)$, $N(\frac{3}{2}^-)$, etc.) numbers separately.

Combining all these motivations, the lowest eigenvalue of (4.2) is a bound for the ground state energy, and the remaining $(N-1)$ eigenvalues can be used as upper bounds (and if one takes enough basis functions, even as estimates with a small positive bias) for the energies of the lowest $(N-1)$ excited states of the Hamiltonian. Consequently, the variational wave functions for the ground and the $N-1$ lowest excited states can be written as

$$\Psi_n = \sum_{i=1}^{N} c_{n,i}\psi_i, \quad (n = 1, \ldots, N) \tag{4.5}$$

using the eigenvectors $(c_{n,1}, \ldots, c_{n,N})$ of equation (4.2), which are normalized with respect to the kernel B_{ij}:

$$\sum_{i,j=1}^{N} c_{n,i} B_{ij} c_{n,j} = 1 \ . \tag{4.6}$$

One has to notice that we minimize the energy in this problem, and as a by-product get the wave functions for the ground and excited states of the baryons. The quality of these wave functions, however, might not be optimal, since the errors are quadratic in the wave functions, but only linear in the energies.

If one solves the eigenvalue problem for a fixed set of basis functions, and then wants to improve the result, one can always add as many additional basis function as necessary to obtain a required accuracy. The time to solve the eigenvalue problem using an extended set of states from a complete set of basis functions in a Hilbert space, however, grows dramatically, and furthermore numerical instabilities arise, what poses limitations in practice.

4.3 The stochastic variational method

As one might imagine, fixing the basis functions in advance and independent of the specific problem is inferior to the use of basis functions that are chosen specifically for a particular Hamiltonian. However, the problem of finding for a fixed N the optimal set of basis functions from the Hilbert space $\mathcal{H}$ is certainly not a trivial task, and does not even have a unique solution. Thus, we will apply a variational method, which adds one (more or less optimal) basis function at a time, and so builds a well-optimized set of basis functions. This approach turned out to avoid even the problem of being trapped in one of the possibly many local minima of the potential.

The so-called "stochastic variational method" (SVM) we will use here was introduced by Kukulin and Krasnopolsky [KK77] and further elaborated by Suzuki and Varga and is described in great detail in their book [SV98]. Thus I just want to give a brief outline of this method here.

Instead of fixing a number of basis functions beforehand, one tries to keep the set of basis functions (each characterized by a certain parameter set α_i as described in the next chapter) as small as possible, and instead optimizes the choice of the parameter sets of the basis functions

$$\psi_i = \psi_{\alpha_i} \ . \tag{4.7}$$

By this approach, one extends the problem of minimizing the energies from finding optimal values for the linear parameters $(c_1, \ldots, c_N)$ to the problem of optimizing the set A of linear parameters as well as the parameters of the basis functions

$$A = \{(c_i, \alpha_i), i = 1, \ldots, N\} \ . \tag{4.8}$$

Depending on the exact structure of the basis functions (in our case generalized Gaussians and spherical harmonics for the spatial part and spinors and flavor wave functions for the remaining part, as we will elaborate in chapter 5), the parameters α_i will probably not enter the problem in a linear manner, so we call them the non-linear parameters of the optimization problem. This additional choice of the parameter sets glows up the whole problem to a point where conventional exact optimization methods can no longer be applied (e.g. if one takes only 30 basis function – a number which is certainly too low to get an acceptable result – one has to do a non-linear optimization over 420 variables, because the wave functions contain 11 non-linear parameters as elaborated in the next chapter. Due to the high computational effort for each evaluation, this is simply not treatable with conventional methods.). Also, the parameter sets α_i will contain discrete parameters like quantum numbers of subsystems of few-body systems.

A feasible approach to this problem is to choose the parameter sets of the basis functions randomly, and use the best basis functions one can find this way. This is the basic point of the SVM.

We should mention, that it is not only the stochastic variational method, but also the special choice of correlated Gaussians for the wave functions that account for the good performance of this method. They seem to be particularly suited for the description of the correlations of the particles of few-body problems, and additionally carry the advantage that the matrix elements can be calculated exactly for most cases. This further increases accuracy and reduces calculation time on the computer. We will discuss the exact forms of the wave functions in the next chapter 5.

The random selection of the basis states is now implemented stepwise, meaning that we add one linearly independent basis function at a time to the existing preliminary basis, that minimizes the energy most. We must start off from a basis containing at least one basis function, which we create in a straightforward manner: We generate randomly a number of possible parameter sets α_i^{try} for a basis function, and for each of them calculate the Matrix element $E_i^0 = \left\langle \psi(\alpha_i^{\text{try}}) \left| H \right| \psi(\alpha_i^{\text{try}}) \right\rangle$ of the Hamiltonian for the corresponding normalized basis functions. As we have to minimize this energy, we select the parameter set which gives the lowest energy, i.e. fulfills

$$\langle \psi(\alpha_0) \left| H \right| \psi(\alpha_0) \rangle = \min_i \left\langle \psi(\alpha_i^{\text{try}}) \left| H \right| \psi(\alpha_i^{\text{try}}) \right\rangle \ , \tag{4.9}$$

as the first basis function $\psi(\alpha_0)$.

Starting from this set of one basis function, we perform the following steps to add one additional basis function after the other, until our result reaches the desired accuracy:

1. In every step k (i.e. our existing basis has already k selected basis states), one generates a random set of N parameter sets α_i^{try}.

2. For each of these parameter sets, one adds the corresponding basis function to the k existing basis functions and calculates the energy by first calculating the matrix elements with this new function (the matrix elements that involve only the k already existing basis functions are stored and need not be recalculated) and then diagonalizing this matrix as described below. This procedure yields eigenvalues[1] $E_{k+1,n}(\alpha_i^{\mathrm{try}})$ for $n = 1, \ldots, k+1$ for each trial set of parameters α_i^{try}.

3. From this set of new parameters, one chooses that parameter set and adds it as the $(k+1)$-st basis function which maximizes the improvement in a certain sense. When one is interested mainly in the ground state energy, it is best to consider just the improvement gained for the ground state, i.e. to select as new basis state ψ_{α_j} the one with

$$E_{k+1,1}(\alpha_j) = \min_i E_{k+1,1}(\alpha_i^{\mathrm{try}}) \ .$$

4. The previous two steps are repeated until the improvement of the latest m added wave functions falls below a certain threshold. m should be chosen not too small, otherwise statistical fluctuations can cause the algorithm to stop before the lowest possible state is actually reached.

The algorithm described above minimizes only the ground state energy, but not necessarily the higher excitations. According to the theorems given above, the higher excitations will not get worse by the selection method used in step 3, but nothing guarantees that the basis functions are chosen such that the upper bounds to the higher excitation energies are really tight bounds.

So, if also the excited states are of importance, it is better to modify the selection step above to use the parameter set which maximizes a linear combination of the improvements including the n lowest eigenvalues

$$\sum_{l=1}^{n} w_k \left(E_{k,l} - E_{k+1,l}(\alpha_j) \right) \ ,$$

where the weights w_k represent the importance one puts on the k-th eigenvalue. Note also, that the last theorem mentioned above ensures that each term in the selection strategies above is positive and so in every step all the energies are improved. The selection method just determines which ones are improved most, the simplest approaches being $w_0 = 1, w_i = 0$ for $i > 0$ (this is just the ground state energy) or $w_i = 1$ for $i = 0, 1, \ldots$, which means that all excitations are taken as equally important. In reality, one will weight the ground state as most important, and

[1] $E_{k+1,n}(\alpha_i^{\mathrm{try}})$ denotes the n-th eigenvalue of the Hamiltonian using $(k+1)$ basis functions, where the last basis function is determined by the parameter set α_i^{try}.

assign lower weights to the first few excitation, while the higher excitation are not so important[2] and can be left out from the consideration.

As a stopping criterion, one might choose a fixed size of the basis, but in that case it is not a-priori clear that the energies have already converged to the exact value. Thus, it is better to leave the number of basis functions free, and choose as a stopping criterion the improvement ΔE of the ground state energy (or a linear combination of the improvements of the first few excitations). If the improvement

$$\delta_m E_n^\nu := \sum_{k=1}^{\nu} (E_{N-m,k} - E_{N,k}) \tag{4.10}$$

of m consecutive steps does no longer exceed the threshold ΔE, one may assume that the investigated energy levels have converged, and the variational search can be stopped. If, however, ΔE is chosen too big, there is a chance that the energy levels have not completely converged and would still decrease by a considerable amount, so ΔE should be chosen rather small. Additionally, it is advisable to choose $m \gg 1$, because otherwise the method might stop prematurely due to statistical fluctuations (i.e. there is a non-zero chance that one variational step does not improve the energies considerably, although the next few steps would still lead to a certain improvement).

4.4 Optimizations of the SVM

When adding a basis function ψ_{k+1}, one does not have to diagonalize the whole matrix again, which would require an n^3 effort, but one can use the results from the previous diagonalization with k basis functions as described in [VS95].

In the $(k+1)$-st repetition of the selection algorithm (where we already have calculated the diagonalization with k basis states), the generalized eigenvalue problem with $k+1$ basis functions looks like

$$\begin{pmatrix} E_1 & 0 & \dots & 0 & \langle\psi_1|H|\psi_{k+1}\rangle \\ 0 & & & & \\ \vdots & & & \vdots & \vdots \\ 0 & & \dots & E_k & \langle\psi_k|H|\psi_{k+1}\rangle \\ \langle\psi_{k+1}|H|\psi_1\rangle & & \dots & \langle\psi_{k+1}|H|\psi_k\rangle & \langle\psi_{k+1}|H|\psi_{k+1}\rangle \end{pmatrix} \begin{pmatrix} c_1 \\ \vdots \\ \vdots \\ c_k \\ c_{k+1} \end{pmatrix} =$$

$$\begin{pmatrix} 1 & 0 & \dots & 0 & \langle\psi_1|\psi_{k+1}\rangle \\ 0 & & & & \\ \vdots & & & \vdots & \vdots \\ 0 & & \dots & 1 & \langle\psi_k|\psi_{k+1}\rangle \\ \langle\psi_{k+1}|\psi_1\rangle & & \dots & \langle\psi_{k+1}|\psi_k\rangle & \langle\psi_{k+1}|\psi_{k+1}\rangle \end{pmatrix} \begin{pmatrix} c_1 \\ \vdots \\ \vdots \\ c_k \\ c_{k+1} \end{pmatrix} . \tag{4.11}$$

[2] In the context of baryon spectroscopy, higher excitations are affected with increasing uncertainties or are not found at all.

By a Gram-Schmidt orthogonalization of ψ_{k+1} with respect to the existing basis functions $\psi_1, \ldots, \psi_k$, yielding the orthonormal function $\bar{\psi}_{k+1}$, this matrix equation can be further simplified to an ordinary eigenvalue problem

$$\begin{pmatrix} E_1 & 0 & \ldots & 0 & \langle\psi_1|H|\bar{\psi}_{k+1}\rangle \\ 0 & & & & \\ \vdots & & & \vdots & \vdots \\ 0 & & \ldots & E_k & \langle\psi_k|H|\bar{\psi}_{k+1}\rangle \\ \langle\bar{\psi}_{k+1}|H|\psi_1\rangle & & \ldots & \langle\bar{\psi}_{k+1}|H|\psi_k\rangle & \langle\bar{\psi}_{k+1}|H|\bar{\psi}_{k+1}\rangle \end{pmatrix} \begin{pmatrix} c_1 \\ \vdots \\ \vdots \\ c_k \\ c_{k+1} \end{pmatrix} = E \begin{pmatrix} c_1 \\ \vdots \\ \vdots \\ c_k \\ c_{k+1} \end{pmatrix} .$$

However, this simplification can only be done at the expense of the additionally needed Gram-Schmidt orthogonalization. The eigenvalues of this ordinary eigenvalue problem can be calculated as the roots of the secular equations, which – due to the special form of the matrices in the eigenvalue problem – can be explicitly written as

$$\lambda(E) = \prod_{i=1}^{k}(E_{k,i} - E)\left((\langle\bar{\psi}_{k+1}|H|\bar{\psi}_{k+1}\rangle - E) - \sum_{j=1}^{k}\frac{\langle\bar{\psi}_{k+1}|H|\psi_i\rangle^2}{E_{k,j} - E}\right) = 0 .$$

As one can see, the secular equation has poles at the eigenvalues $E = E_{k,j}$ of the previous step, and the left limit at this poles is $-\infty$, while in the right limit $\lambda(E)$ tends to ∞. Since the secular equation is continuous between the poles, there has to be a zero between each two previous eigenvalues, and these zeros are the new eigenvalues. As $\lambda(E) \xrightarrow{E\to-\infty} \infty$ and $\lambda(E) \xrightarrow{E\to\infty} -\infty$, the values $E = \pm\infty$ can be seen as the remaining two poles, so there has to be one zero below the previous ground state (the new ground state), and one zero above the previous highest excitation. These arguments can also be seen as an informal proof of equation (4.4). This knowledge can be exploited to further reduce the calculation effort in the trial step 3 of the SVM algorithm given above, because only the lowest few eigenvalues need to be calculated in order to be able to select or reject a trial parameter set. Only after the best parameter set has been selected, a full diagonalization needs to be performed in each variational step.

Although this process chooses the k-th single basis function optimally (when the $k-1$ previous functions are regarded as fixed), by adding the k-th function, the best choice of all k basis functions might not be ensured. As an example, let us take a look at $k = 1$. We choose the function $\psi(\alpha_2)$ that improves the energy most with the fixed first basis function and is optimal in that sense. However, one might find two other basis functions, that in combination improve the energy more, even though each single one of them is not optimal.

Thus, after adding several new basis functions, it is generally a good idea to implement an additional optimization run. This time, however, no additional basis function is added to the existing set of basis functions, but the existing basis itself is improved stochastically, while its dimension is kept fixed. Again, a set of random

parameter values is generated, but instead of adding them as new basis functions, we randomly select one of the existing basis functions and replace it with the new parameter set. If this new basis yields a better value for the energies, it is accepted instead of the old basis, otherwise this optimization run is done again (until it has been performed a certain number of times). In this optimization run, it might happen that although the energies of the ground state (and maybe even of the lowest excitations) decrease, the higher excitations actually go up[3]. Thus, one might adapt a slightly modified selection strategy for this optimization run. The new basis with one replaced state is only accepted, if

(a) the ground state energy in the new set of basis functions goes down, and

(b) in case one includes bounds of excited states, a thoroughly chosen convex combination of the shifts of the (bounds for the) lowest k excited states is still positive, ensuring that each of these states does not go up too much.

The advantage of this additional optimization is that it does not enlarge the number of basis states, which would lead to higher computational costs for the following stochastic variational steps, and still can lead to an improvement.

Concluding, one can say that in practice the SVM can calculate the spectra to any required accuracy in a fraction of time and by much less computational effort than other optimization methods need (see [VS95, SV98] for a more detailed comparison with other methods). Additionally, our experience shows that the eigenvalues quickly converge using the SVM, so after 30 basis states the ground state energy is usually correct within several MeV, and hardly ever more than 100 or 120 basis states are needed to describe the first three excitations very accurately. This happens independently of the chosen random paths, which is important to avoid being trapped in local minima of the potential.

[3]The theorems we gave above only assured the improvement in all excitations if one adds a new basis function, but not if one of the basis functions is removed and a new one employed instead.

Chapter 5

Wave functions and matrix elements

Contents

5.1 The wave functions

The wave functions describing the baryons as a system of three constituent quarks are built as linear combinations of basis functions with 11 parameters [Wag98], which will be described in detail in the sequel. In general, the wave function Ψ_{XSFC} will depend on the spatial coordinates, spin, flavor and color degrees of freedom and needs to be totally antisymmetric. The latter property is required by the Pauli principle since the considered particles (the constituent quarks) fulfill Fermi statistics.

Another consequence of the QCD properties of the investigated baryons is that we can factor the color part out of the wave function. This is the case because every baryon has to form a color-singlet (i.e. is has to be color-neutral, so that baryons have to consist of three quarks, each with a different color quantum number), and there exists only one $SU(3)$ color-singlet. Additionally, this color part of the wave function is antisymmetric with respect to the exchange of either two of the constituent quarks,

so the remaining space-spin-flavor wave function Ψ_{XSF} has to be symmetric to fulfill Pauli's principle.

This factorization

$$\Psi^{\text{as}}_{XSFC} = \Psi_C^{\text{singlet, as}} \cdot \Psi^{\text{symm}}_{XSF} \tag{5.1}$$

of the wave function also leads to a factorization of each operator $\mathcal{O}$, as the contribution of Ψ_C to the matrix elements will always be the same factor O_C independent of the remaining wave function Ψ_{XSF}. Thus any operator can also be factorized[1] by

$$\mathcal{O} = \mathcal{O}_C \mathcal{O}_{XSF}$$

into a space-spin-flavor part $\mathcal{O}_{XSF}$ (which acts only on the subspace $\mathcal{H}'$ of $\mathcal{H}$ containing the space, spin and flavor coordinates) and a color part $\mathcal{O}_C$. The operator $\mathcal{O}_C$ always contributes the same factor O_C to the matrix element. For this reason, the color part of the wave function can be left out[2], and in the sequel when we speak of the wave function, we only mean the symmetric space-spin-flavor part Ψ_{XSF}.

5.1.1 Requirements for the wave functions

Like for any variational method, also for the stochastic variational method to be efficient and to give good results, the choice of the basis and the optimization functions is of crucial importance. On the one hand, the trial functions have to be flexible enough to be able to describe all possible relevant correlations between the particles of the system under consideration, while on the other hand they need to be simple enough to guarantee an efficient calculation of the corresponding matrix elements. This idea suggests the use of so-called correlated Gaussians as trial functions, like discussed by Suzuki and Varga in their monograph [SV98].

Another requirement for the basis functions comes from the condition that the final wave function (except for the color part) has to be symmetric. As we construct the totally symmetric wave functions as a linear combination

$$\Psi^S_{XSF} = \sum_{i=1}^{n} c_i \psi_{\alpha_i}$$

of several basis functions ψ_{α_i}, these basis functions must have the same total symmetry with respect to the exchange of any two constituent quarks. Constructing such basis functions in one step is not so simple, but one can create them in two steps:

[1] Actually, it can only be factorized into $\mathcal{O} = \sum_i \mathcal{O}_{i,C}\mathcal{O}_{i,XSF}$, but for each of the summands the argumentation remains valid, and the calculation will be reduced to the calculation of such summands, anyway.

[2] Actually this is not strictly correct. The $\mathcal{O}_C$ cannot be left out in general since the operator $\mathcal{O}$ can only be written as a sum of factorized operators. Therefore one cannot take out a common factor from the whole sum. However, the way to resolve this problem and get rid of the color-dependence is to absorb the O_C as a constant factor into the space-spin-flavor part $\mathcal{O}_{XSF}$ and continue the calculations with this modified operator.

First we create basis functions $\psi_{\alpha_i}^{(k,pq)}$, which are symmetric only with respect to the two particles p and q

$$\psi_{\alpha_i}^{(k,pq)} = \psi_{\alpha_i}^{(k,qp)} ,$$

where the triple (k,p,q) is any single permutation of $(1,2,3)$. We use the index of the third (non-symmetrized) constituent quark k as an identifier for this special symmetry, and call the wave function $\psi_{\alpha_i}^{(k,pq)}$ a basis function for configuration k. As $(\tilde{k})$ identifies this basis function uniquely, we will henceforth write $\psi_{\alpha_i}^{(\tilde{k})}$ instead of $\psi_{\alpha_i}^{(k,pq)}$ for the basis function in configuration $(\tilde{k})$.

Using these semi-symmetrized functions, one can now construct a totally symmetric basis function as

$$\psi_{\alpha_i} = \psi_{\alpha_i}^{(1,23)} + \psi_{\alpha_i}^{(2,13)} + \psi_{\alpha_i}^{(3,12)} . \tag{5.2}$$

5.1.2 Coordinate systems

In all potentials and matrix element calculations so far, the coordinates $\vec{r}_{ij}$ represented the absolute coordinates of the constituent quarks i and j. As one of them is redundant and can be calculated from the remaining coordinates (and the center of mass), it would be more convenient to introduce a simpler coordinate system [SV98], like taking the center of mass as coordinate origin, or the heavy-particle center coordinate system, where one of the involved particles is taken as the center, or the so-called Jacobi-coordinate system, where the j-th relative coordinate is measured between the j-th particle and the center of mass of the particles $1,\ldots,j-1$. These Jacobi-coordinates turn out to be particularly well-suited for our calculations, so we will use the Jacobi-coordinate system to specify the relative coordinates of the constituent quarks in our baryon.

In a three-particle system k,p,q with mass m_k, m_p, and m_q one has 3 coordinates $\vec{x}_k$, $\vec{x}_p$, and $\vec{x}_q$. By separating out the center of mass motion, one is left with the internal motion which is most easily described by Jacobi coordinates $(\vec{\xi}_k, \vec{\eta}_k)$. The first coordinate measures the relative coordinate of the specifically chosen quarks p and q, while the second coordinate measures the relative coordinate of the remaining quark k to the center of mass of the first two quarks p and q (see figure 5.1). Again, we have three possible choices for this partition[3], so we again use the special index k as a label for this partition. The three graphics in figure 5.1 visualize the three possible Jacobi coordinate systems for a three-quark system.

So, the index of the partition $(\tilde{k})$ specifies which relative coordinate system we use, while the index k of the configuration just represents a specific symmetry property of the wave function.

For constructing the fully symmetric wave function as given in equation (5.2), we first need to agree on a certain coordinate system defined by the partition k, and

[3]We disregard the possibilities of exchanging the particles p and q, as this affects only the sign of the Jacobi coordinate $\vec{\xi}_k$, which will be irrelevant for our further calculations.

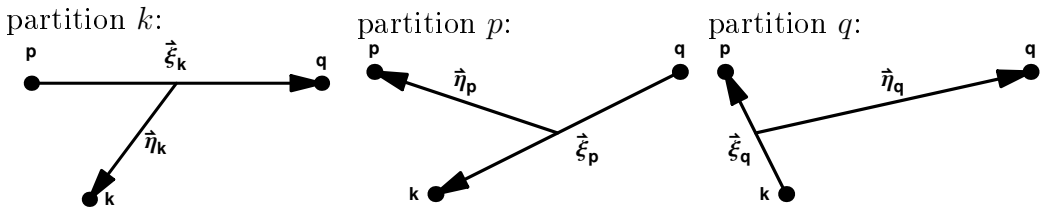

Figure 5.1: *Jacobi coordinates in partitions k, p and q. The first coordinate $\vec{\xi}_k$ in partition k is the relative distance between the particles p and q, while the second Jacobi coordinate $\vec{\eta}_k$ is the relative distance of the remaining particle to the center of mass of the first two. Note that these are just different coordinate systems, needed for the mathematical representation. The result on the calculation cannot depend on the selected set of Jacobi coordinates.*

then have to use the same Jacobi-coordinates in all summands:

$$\psi_{\alpha_i} = \psi^{(\tilde{k})}_{\alpha_i}(\vec{\xi}_k, \vec{\eta}_k) + \psi^{(\tilde{p})}_{\alpha_i}(\vec{\xi}_k, \vec{\eta}_k) + \psi^{(\tilde{q})}_{\alpha_i}(\vec{\xi}_k, \vec{\eta}_k)\,. \tag{5.3}$$

Although the specific mathematical representation of each of the functions $\psi^{(\tilde{k})}_{\alpha_i}$ will be different in each partition k (given by a transformation between different partitions, as we will discuss in section 5.2), the end result of the calculations cannot depend on our partition choice. In the following few sections we will discuss the problem of constructing a wave function for a specific configuration $(\tilde{k})$ where Jacobi coordinates from the partition with the same index k are used. This simplifies the calculations a lot, and finally we will see that the two remaining semi-symmetric wave functions for configurations $(\tilde{p})$ and $(\tilde{q})$ can be obtained by a certain transformation. In practice, we can apply a partition transformation to the matrix element itself and thus only have to do calculations of matrix elements between basis functions expressed by coordinates of one single partition.

I will first present the three components of the wave function – the spatial part $\phi^{(\tilde{k})}_{(\beta,\gamma,\delta,\nu,n,\lambda,lLM_L)}$ depending on the Jacobi coordinates $(\vec{\xi}_k, \vec{\eta}_k)$ in partition k, the spin part $\chi^{(\tilde{k})}_{k,(s,SM_S)}$ and the flavor part $\phi^{(\tilde{k})}_F$ – from which the complete semi-symmetric wave function $\phi^{(\tilde{k})}_{\alpha_i}$ for partition k can be constructed as a tensor product

$$\psi^{(\tilde{k})}_{\alpha_i} = \left\{\varphi^{(\tilde{k})}_{(\beta,\delta,\nu,n,\lambda,l,L)}\left(\vec{\xi}_k, \vec{\eta}_k\right) \otimes \chi^{(\tilde{k})}_{(s,S)}\right\}_{JM_J} \phi^{(\tilde{k})}_F$$

where the parameter set α_i includes 11 components:

$$\alpha_i = \{\beta, \delta, nu, n, \lambda, l, L, s, S, F, b\}$$

which will be discussed along with the individual parts of the basis wave function.

5.1.3 The spatial part of the basis functions

For the spacial part we will use Jacobi coordinates for a pre-selected partition k, which means that we separate off the center-of-mass motion

$$\vec{R} = \frac{m_1\vec{x}_1 + m_2\vec{x}_2 + m_3\vec{x}_3}{m_1 + m_2 + m_3}$$

and then take the relative coordinate of particles q and p as the first coordinate $\vec{\xi}_k$, while the second coordinate $\vec{\eta}_k$ is the coordinate of the remaining quark k relative to the center of mass of the first two particles (see figure 5.1), i.e.

$$\vec{\xi}_k = \vec{x}_p - \vec{x}_q \tag{5.4}$$

$$\vec{\eta}_k = \vec{x}_k \frac{m_p\vec{x}_p + m_q\vec{x}_q}{m_p + m_q} \,, \tag{5.5}$$

where (k, p, q) is an even permutation of $(1, 2, 3)$.

The spatial part of the semi-symmetric wave function will be constructed as described in [Wag98] from functions formed as a product of a correlated Gaussian with bipolar spherical harmonics:

$$\tilde{\varphi}^{(\tilde{k})}_{(\beta,\gamma,\delta,\nu,n,\lambda,l,LM_L)}(\vec{\xi}_k, \vec{\eta}_k) = \left(\vec{\xi}_k\right)^{2\nu+\lambda} (\vec{\eta}_k)^{2n+l} \exp\left(-\beta\vec{\xi}_k^{\,2} - \delta\vec{\eta}_k^{\,2} + \gamma\vec{\xi}_k \cdot \vec{\eta}_k\right) \mathcal{Y}^{LM_L}_{\lambda l}(\vec{\xi}_k, \vec{\eta}_k) \,. \tag{5.6}$$

The functions of this type depend on 9 parameters $(\beta, \gamma, \delta, \nu, n, \lambda, l, LM_L)$, where β, γ and δ are continuous and might take any positive[4] value (except for γ which can also assume negative values). An additional constraint on their values due to normalization is that they need to fulfill the inequality $\beta\delta > \gamma^2/4$. In addition to these continuous parameters, the function is determined by the remaining 6 parameters, which represent certain quantum numbers and can only be chosen from a discrete set of possible values. λ and l define the angular momentum, and ν and n the behavior at short distances; all need to be non-negative[5]. Table 5.2 explains the meaning of these parameters in some more detail.

The bipolar spherical harmonics $\mathcal{Y}^{LM_L}_{\lambda l}(\hat{\xi}_k, \hat{\eta}_k)$ in equation (5.6) are defined as the tensor product of conventional spherical harmonics Y_{lm} where the angular momenta l and λ according to the Jacobi coordinates $\left(\vec{\xi}_k, \vec{\eta}_k\right)$ are coupled together to total orbital angular momentum L with z-component M_L:

$$\mathcal{Y}^{LM_L}_{\lambda l}(\hat{x}, \hat{y}) = \{Y_\lambda(\hat{x}) \otimes Y_l(\hat{y})\}_{LM_L} = \sum_{\mu,m} \langle \lambda\mu lm | LM\rangle \, Y_{\lambda\mu}(\hat{x}) Y_{lm}(\hat{y}) \,. \tag{5.7}$$

[4] The positivity of the parameters β and γ is needed to ensure that the integral over $\mathbb{R}^2_+$ stays finite and the wave function is normalizable.

[5] We can even set the two parameters ν and n equal to zero in our calculations, since the wave function must only be regular at the origin, and the detailed behavior at very short distances will not be important. In higher excitations than the ones we are interested in, non-vanishing values might be needed. One also has to notice that even if $\nu = n = 0$, in a linear combination of such basis functions the behavior might be similar to the case with non-vanishing ν and n.

Here $\langle \lambda\mu lm|LM\rangle$ denotes the Clebsch-Gordan coefficients corresponding to total orbital angular momentum L.

The choice of these correlated Gaussian functions as basis functions is motivated by the use of the stochastic variational approach, where the basis functions need to fulfill certain criteria to keep the calculations as simple and as fast as possible. Especially they should meet the following requirements [SV98]:

- They can be easily generalized for an N-body system. Actually this is not so important for this work, but in the future, additional degrees of freedom might be added. (Especially for the first $\Lambda\left(\frac{1}{2}^-\right)$ excited state this is of importance, which may not be a simple three-quark state, but probably has sizable $QQQQ\bar{Q}$ configurations.)
- Their matrix elements can be calculated analytically.
- They are easily adaptable to the permutational symmetry of the system.
- They are flexible enough to approximate even rapidly changing functions.

The functions defined in (5.6) themselves do not yet fulfill the required symmetry properties for the spatial part, but as we shall see in a moment, for any configuration $(\tilde{k})$ at most a linear combination of them can be constructed fulfilling the symmetry properties with respect to the exchange of the $(\tilde{p})$ and $(\tilde{q})$ particles.

In these functions, the Jacobi coordinates are taken in partition k, and their representation in partition q or p will look differently with the Jacobi coordinates transformed into a different partition by a unitary transform as discussion in section 5.2. Thus the explicit form of the function depends on the choice of the Jacobi partition k, and we will indicate this by an index k on the arguments of the function.

As we are interested in the symmetry properties of the functions $\tilde{\varphi}_\alpha^{(\tilde{k})}(\vec{\xi}_k, \vec{\eta}_k)$ (for configuration $(\tilde{k})$) let us now look what happens if we exchange the particles $(\tilde{p})$ and $(\tilde{q})$. If we use partition $k = (\tilde{k})$ to describe the spatial part, this exchange has the following effects on the functions (as a quick look at the definition of the Jacobi coordinates shows):

Term in (5.6)	Replacement for $(\tilde{p}) \leftrightarrow (\tilde{q})$
$\vec{\xi}_k$	$-\vec{\xi}_k$
$\vec{\eta}_k$	$\vec{\eta}_k$
$\mathcal{Y}_{\lambda l}^{LM_L}(\hat{\xi}_k, \hat{\eta}_k)$	$(-1)^\lambda \mathcal{Y}_{\lambda l}^{LM_L}(\hat{\xi}_k, \hat{\eta}_k)$
$\exp(\gamma \hat{\xi}_k \cdot \hat{\eta}_k)$	$\exp(-\gamma \hat{\xi}_k \cdot \hat{\eta}_k)$

Combining these symmetry properties and an additional assumption[6] $\gamma = 0$, we find that the functions $\tilde{\varphi}^{(\tilde{k})}_{(\beta,\gamma,\delta,\nu,n,\lambda,l,LM_L)}$ already display the required symmetry with parity $P = (-1)^{\lambda+l}$ for configuration $(\tilde{k})$, if we use the same Jacobi partition $k = (\tilde{k})$:

$$\varphi^{(\tilde{k})}_{\alpha}(\vec{\xi}_k, \vec{\eta}_k) = \tilde{\varphi}^{(\tilde{k})}_{(\beta,\gamma,\delta,\nu,n,\lambda,l,LM_L)}(\vec{\xi}_k, \vec{\eta}_k) \leftrightarrow (-1)^{\lambda} \tilde{\varphi}^{(\tilde{k})}_{(\beta,\gamma,\delta,\nu,n,\lambda,l,LM_L)}(\vec{\xi}_k, \vec{\eta}_k). \tag{5.8}$$

If we use the Jacobi coordinates of partitions q or p in the function (5.6), the exchange of p and q has the following symmetry effects:

Jacobi coordinates of partition p:

Term in (5.6)	Replacement for $p \leftrightarrow q$
$\vec{\xi}_p$	$-\vec{\xi}_q$
$\vec{\eta}_p$	$\vec{\eta}_q$
$\mathcal{Y}^{LM_L}_{\lambda l}(\hat{\xi}_p, \hat{\eta}_p)$	$(-1)^{\lambda}\mathcal{Y}^{LM_L}_{\lambda l}(\hat{\xi}_q, \hat{\eta}_q)$
$\exp(\gamma\hat{\xi}_p \cdot \hat{\eta}_p)$	$\exp(-\gamma\hat{\xi}_q \cdot \hat{\eta}_q)$

Jacobi coordinates of partition q:

Term in (5.6)	Replacement for $p \leftrightarrow q$
$\vec{\xi}_q$	$-\vec{\xi}_p$
$\vec{\eta}_q$	$\vec{\eta}_p$
$\mathcal{Y}^{LM_L}_{\lambda l}(\hat{\xi}_q, \hat{\eta}_q)$	$(-1)^{\lambda}\mathcal{Y}^{LM_L}_{\lambda l}(\hat{\xi}_p, \hat{\eta}_p)$
$\exp(\gamma\hat{\xi}_q \cdot \hat{\eta}_q)$	$\exp(-\gamma\hat{\xi}_p \cdot \hat{\eta}_p)$

As one can see, the wave function of partition p turns into the wave function of partition q and vice versa (modulo a factor $(-1)^{\lambda}$) if one again assumes $\gamma = 0$. Thus, a linear combination

$$\varphi^{(\tilde{k})}_{\alpha} = \tilde{\varphi}^{(\tilde{k})}_{(\beta,\gamma,\delta,\nu,n,\lambda,l,LM_L)}(\vec{\xi}_p, \vec{\eta}_p) + (-1)^{\lambda} \tilde{\varphi}^{(\tilde{k})}_{(\beta,\gamma,\delta,\nu,n,\lambda,l,LM_L)}(\vec{\xi}_q, \vec{\eta}_q) \tag{5.9}$$

of these two functions will be symmetric with respect to the exchange of particles p and q, and the corresponding negative linear combination

$$\varphi^{(\tilde{k})}_{\alpha} = \varphi^{(\tilde{k})}_{(\beta,\gamma,\delta,\nu,n,\lambda,l,LM_L)}(\vec{\xi}_p, \vec{\eta}_p) - (-1)^{\lambda} \tilde{\varphi}^{(\tilde{k})}_{(\beta,\gamma,\delta,\nu,n,\lambda,l,LM_L)}(\vec{\xi}_q, \vec{\eta}_q) \tag{5.10}$$

will be antisymmetric.

5.1.4 The spin part of the basis functions

Like in the spatial part, where we first "coupled" the coordinates of two of the three quarks together by means of the Jacobi coordinate $\vec{\xi}_k$, and then "coupled" the last

[6] Without loss of generality we can safely make this assumption $\gamma = 0$, because our fully symmetric wave function also consists of contributions from the remaining two configurations $(\tilde{p})$ and $(\tilde{q})$. When constructing their wave-functions, we first write them in Jacobi coordinates p and q, respectively, and then need to transform all to the same Jacobi partitions k, i.e. $(\hat{\xi}_p, \hat{\eta}_p) \to (\hat{\xi}_k, \hat{\eta}_k)$ and $(\hat{\xi}_q, \hat{\eta}_q) \to (\hat{\xi}_k, \hat{\eta}_k)$. By this transformation, both new Jacobi coordinates are a linear combination of the old, and thus the square also contains their correlations, effectively leading to $\gamma' \neq 0$.

quark to the system (center of mass) of the first two quarks, for the spin part we will proceed in a similar fashion. For the spin part in configuration $(\tilde{k})$ we will first couple the two spins of the quarks p and q together to a system with spin s and its projection m by a tensor product of the two spinors $\chi_{\frac{1}{2}}(p)$ and $\chi_{\frac{1}{2}}(q)$

$$\chi^{(\tilde{k})}_{sm}(p,q) = \left\{\chi_{\frac{1}{2}}(p) \otimes \chi_{\frac{1}{2}}(q)\right\}_{sm} . \tag{5.11}$$

The spin basis function is then obtained by coupling the spin of the remaining particle k to this system with spin s, yielding a tensor product

$$\chi^{(\tilde{k})}_{s,SM_S}(k) = \left\{\chi^{(\tilde{k})}_{sm}(p,q) \otimes \chi_{\frac{1}{2}}(k)\right\}_{SM_S} . \tag{5.12}$$

for the system with total spin S and its corresponding projection M_S.

These spin functions fulfill a symmetry relation akin to the symmetry of the spatial part. If we use the same configuration and partition $(\tilde{k}) = k$, the spin function is already symmetric when exchanging particles p and q:

$$\chi^{(\tilde{k})}_{s,SM_S}(k) \leftrightarrow (-1)^{s+1}\chi^{(\tilde{k})}_{s,SM_S}(k) . \tag{5.13}$$

However, if we use a different configuration index $(\tilde{k})$ than we take for the partition k, the spin functions in partitions p and q will get exchanged,

$$\chi^{(\tilde{k})}_{s,SM_S}(p) \leftrightarrow (-1)^{s+1}\chi^{(\tilde{k})}_{s,SM_S}(q) \quad \text{in partition } p \tag{5.14}$$

$$\chi^{(\tilde{k})}_{s,SM_S}(q) \leftrightarrow (-1)^{s+1}\chi^{(\tilde{k})}_{s,SM_S}(p) \quad \text{in partition } q, \tag{5.15}$$

and the symmetric spin function can be constructed as $\chi^{(\tilde{k})}_{s,SM_S}(p) - (-1)^s\chi^{(\tilde{k})}_{s,SM_S}(q)$, while the antisymmetric spin basis function is $\chi^{(\tilde{k})}_{s,SM_S}(p) + (-1)^s\chi^{(\tilde{k})}_{s,SM_S}(q)$.

These spin basis functions contain only two parameters for the stochastic variation: The spin s of the (p, q) system and the total spin S, which can only take three possible values $(s, S) = (0, \frac{1}{2})$, $(1, \frac{1}{2})$ or $(0, \frac{3}{2})$.

5.1.5 The flavor part of the basis functions

Although the flavor wave function could be constructed similar to the spin basis function[7], it is much easier to explicitly write down the flavor wave functions

$$\phi^{(\tilde{k})}_F = \sum_{i_1,i_2,i_3 \in \{u,d,s\}} a_F^{(i_1 i_2 i_3)_k} |i_1(k) i_2(p) i_3(q)\rangle. \tag{5.16}$$

where $(i_1, i_2, i_3)_k$ denotes the set $\{i_1, i_2, i_3\}$ shifted to the left[8] by $k-1$. The coefficients $a_F^{(i_1 i_2 i_3)_k}$ assume values that are determined from the construction of the flavor wave function.

[7] T. Thonhauser used such a construction for the flavor wave functions of mesons in [Tho98].

[8] For example $(i_1, i_2, i_3)_2 = (i_2, i_3, i_1)$.

F	Baryon	$\phi_F^{(\tilde{3})}$	Y	T, M_T	P_F
1	p	$\frac{1}{\sqrt{2}}(udu - duu)$	1	$\frac{1}{2}, \frac{1}{2}$	1
2	p	$-\frac{1}{\sqrt{6}}(udu + duu - 2uud)$	1	$\frac{1}{2}, \frac{1}{2}$	0
3	n	$\frac{1}{\sqrt{2}}(udd - dud)$	1	$\frac{1}{2}, -\frac{1}{2}$	1
4	n	$\frac{1}{\sqrt{6}}(udd + dud - 2ddu)$	1	$\frac{1}{2}, -\frac{1}{2}$	0
5	Δ^{++}	uuu	1	$\frac{3}{2}, \frac{3}{2}$	0
6	Δ^{+}	$\frac{1}{\sqrt{3}}(uud + udu + duu)$	1	$\frac{3}{2}, \frac{1}{2}$	0
7	Δ^{0}	$\frac{1}{\sqrt{3}}(udd + dud + ddu)$	1	$\frac{3}{2}, -\frac{1}{2}$	0
8	Δ^{-}	ddd	1	$\frac{3}{2}, -\frac{3}{2}$	0
9	Λ	$\frac{1}{\sqrt{2}}(uds - dus)$	0	$0, 0$	1
10	Σ^{+}	uus	0	$1, 1$	0
11	Σ^{0}	$\frac{1}{\sqrt{2}}(uds + dus)$	0	$1, 0$	0
12	Σ^{-}	dds	0	$1, -1$	0
13	Ξ^{0}	ssu	-1	$\frac{1}{2}, \frac{1}{2}$	0
14	Ξ^{-}	ssd	-1	$\frac{1}{2}, -\frac{1}{2}$	0
15	Ω	sss	-2	$0, 0$	0

Table 5.1: *Flavor basis functions for all 15 light and strange baryons (for the specific configuration $(\tilde{k}) = 3$). The quantum numbers defining the state are the hypercharge Y, isospin T, and its projection M_T. The symmetry of the wave function is given by P_F. To obtain the flavor basis functions for the other two configurations $(\tilde{k}) = 1$ and $(\tilde{k}) = 2$, according to equation (5.16) one has to apply a cyclic permutation on the functions given here.*

Table 5.1 gives the flavor wave functions of all 15 light and strange baryons together with their quantum numbers. Each particle – and so each flavor wave function – is determined by a specific hypercharge Y and a total isospin T with its projection M_T[9]. The symmetry of the flavor basis functions is also given in the table as symmetric ($P_F = 0$) or antisymmetric ($P_F = 1$) with respect to the exchange of particles p and q.

The flavor basis functions for the light baryons N and Δ as well as the strange baryon Ω are states of the irreducible mixed-symmetric and mixed-antisymmetric octet resp. totally symmetric decuplet representations of $SU(3)_F$. These three baryons consist of three constituent quarks of the same mass, so the Jacobi coordinates do not depend on the particular distribution of the flavor on the three quarks.

[9]The multiplets with identical hypercharge and isospin, but different isospin projection (e.g. p and n, or Δ^{++}, Δ^{+}, Δ^{0} and Δ^{-}) are degenerate, so for the spectrum it suffices to calculate only one member of the multiplet. To obtain the wave function, we only have to replace the flavor part by the corresponding new flavor part. E.g., to obtain the wave function for the neutron ($F = 3$ and $F = 4$), one can start from the proton ($F = 1$ and $F = 2$) wave function and just replace $\phi_1^{(\tilde{k})}$ and $\phi_2^{(\tilde{k})}$ with $\phi_3^{(\tilde{k})}$ and $\phi_4^{(\tilde{k})}$, respectively.

For the strange baryons Λ, Σ, and Ξ, where two constituent quarks have a mass different from the third, the Jacobi coordinates in different configurations will be different. To simplify the calculation, we put the specific quark with different mass at the position $(\tilde{k})$, corresponding to the partition k, and construct a basis wave function that is symmetric with respect to the two quarks p and q with equal masses[10]. One thus has to ensure that the correct constituent quark masses are used in the Jacobi coordinates, depending on the current configuration and the baryon of our calculations:

$$\vec{\xi}_k^{(\tilde{k})} = \vec{x}_p - \vec{x}_q \tag{5.17}$$

$$\vec{\eta}_k^{(\tilde{k})} = \vec{x}_k - \frac{m_p^{(\tilde{k})}\vec{x}_p + m_q^{(\tilde{k})}\vec{x}_q}{m_p^{(\tilde{k})} + m_q^{(\tilde{k})}} \,. \tag{5.18}$$

Figure 5.2 shows the difference in the Jacobi coordinate system for each of the three possible configurations.

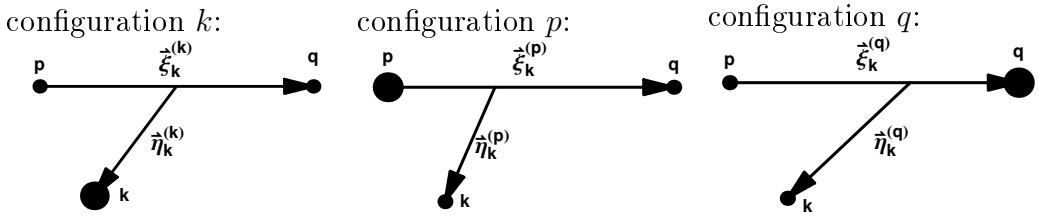

Figure 5.2: *For different configurations we place the different quark at different positions, so the Jacobi coordinates depend on the particular configuration.*

5.1.6 The construction of the complete basis functions ψ_{α_i}

Now that we know the bits and pieces for each of the three parts and their exact symmetry properties, we can construct the full basis wave functions for a configuration $(\tilde{k})$, which then form the completely symmetric basis wave functions according to equation (5.3). First we create intermediate basis functions by coupling a spatial basis function $\tilde{\varphi}^{(\tilde{k})}_{(\beta,\gamma,\delta,\nu,n,\lambda,l,LM_L)}(\vec{\xi}_k, \vec{\eta}_k)$ with total orbital momentum L to a spin basis function $\chi_{s,SM_S}(k)$ with total spin S. Both of the functions have to be created for configuration $(\tilde{k})$ and need to use the same Jacobi coordinates (partition) k. Finally, we combine the resulting space-spin basis function with the flavor basis to yield the 'intermediate' function

$$\psi^{\mathrm{int},(\tilde{k}),k}_{(\beta,\gamma,\delta,\nu,n,\lambda,l,L,s,S,F)JM_J,Y,TM_T} = \left\{ \varphi^{(\tilde{k}),k}_{(\beta,\gamma,\delta,\nu,n,\lambda,l,L)} \otimes \chi^{(\tilde{k}),k}_{(s,S)} \right\}_{JM_J} \phi_F^{(\tilde{k})} \,. \tag{5.19}$$

[10]The resulting full basis wave function will be totally symmetric, as it is the sum of all three possible configurations, and the exchange of two quarks p and q does not change the $(\tilde{k})$ configuration, while the wave functions for configurations $(\tilde{q})$ and $(\tilde{q})$ are turned into each other. Note that we can only make one such assumption on the distribution of the three constituent quarks in each configuration without missing some possible states. Since in the construction of the spatial and spin parts, no such assumptions were made, this is the only one and we do not lose generality.

The parameters J, M_J, Y, T and M_T are inherent properties of the baryonic states we need to calculate, so they are fixed for the calculation of the spectrum of a given baryon with given angular momentum (e.g., $N\left(\frac{1}{2}^-\right)$).

If we choose the configuration $(\tilde{k})$ and the partition k to be equal $(\tilde{k}) = k$, the symmetry considerations of the previous sections show that equation (5.19) already is symmetric or antisymmetric under the exchange of p and q, and thus can be used as full wave function for configuration $(\tilde{k})$:

$$\psi^{(\tilde{k})}_{(\beta,\gamma,\delta,\nu,n,\lambda,l,L,s,S,F)JM_J,Y,TM_T}(\vec{\xi}_k,\vec{\eta}_k) = \psi^{\mathrm{int},(\tilde{k}),k}_{(\beta,\gamma,\delta,\nu,n,\lambda,l,L,s,S,F)JM_J,Y,TM_T}(\vec{\xi}_k,\vec{\eta}_k)\,. \tag{5.20}$$

If we need the basis wave functions in a partition different from the configuration (i.e. $(\tilde{k}) \neq k$), a simple linear combination

$$\psi^{(\tilde{k})}_{(\beta,\gamma,\delta,\nu,n,\lambda,l,L,s,S,F)JM_J,Y,TM_T} = \psi^{\mathrm{int},(\tilde{k}),p}_{(\beta,\gamma,\delta,\nu,n,\lambda,l,L,s,S,F)JM_J,Y,TM_T} \pm \psi^{\mathrm{int},(\tilde{k}),q}_{(\beta,\gamma,\delta,\nu,n,\lambda,l,L,s,S,F)JM_J,Y,TM_T} \tag{5.21}$$

will be symmetric. According to the choice of the sign, we will attribute an additional parameter b to the basis wave function, where $b = -1$ stands for the function using the negative and $b = 1$ using the positive linear combination. A value $b = 0$ indicates the wave function is symmetric for $(\tilde{k}) = k$ (i.e. no linear combination is needed).

All in all, we need a total of eleven parameters

$$\alpha = \{\beta,\gamma,\delta,\nu,n,l,L,s,S,F,b\} \tag{5.22}$$

to completely define a basis function

$$\psi^{(\tilde{k})}_{(\alpha)JM_J,Y,TM_T} \tag{5.23}$$

for configuration $(\tilde{k})$, where the basis function is symmetric only if

$$(-1)^{\lambda+s+1+P_F} = \begin{cases} 1, & \text{for } b = 0 \text{ or } b = 1 \\ -1, & \text{for } b = -1\,. \end{cases} \tag{5.24}$$

From these configurational basis functions the fully symmetric basis wave functions are constructed as

$$\psi_{(\alpha)JM_J,Y,TM_T} = \psi^{(\tilde{k})}_{(\alpha)JM_J,Y,TM_T} + \psi^{(\tilde{p})}_{(\alpha)JM_J,Y,TM_T} + \psi^{(\tilde{q})}_{(\alpha)JM_J,Y,TM_T}\,. \tag{5.25}$$

5.2 Transformation between two partitions

When we calculate the expectation value of an arbitrary operator $\mathcal{O}$ we need to use general baryonic states Ψ, which are formed as a linear combination of the basis wave

β, δ, $\gamma = 0 \ldots$	coefficients of the exponential in the spatial part
λ, $l \ldots$	angular momenta in the spatial part
ν, $n \ldots$	threshold behavior at short distances (set to 0 for most cases)
$L \ldots$	total angular momentum
$S \ldots$	total spin
$s \ldots$	spin quantum number of the (p, q) quark pair
$F \ldots$	flavor index of the particle ($F \in \{1, \ldots, 15\}$)
$b \ldots$	describes the linear combination to construct the basis function, $b = -1, 0, 1$

Table 5.2: *Meaning of the eleven parameters that determine one basis wave function*

functions described above (which in turn are sums over all three possible configurations). Thus we can reduce the calculation to the evaluation of the matrix element of the operator between two arbitrary configurations $(\tilde{k})$ and $(\tilde{q})$:

$$\langle \Psi | \mathcal{O} | \Psi' \rangle = \sum_{i,i'} c_i c'_{i'} \langle \psi_{\alpha_i} | \mathcal{O} | \psi_{\alpha'_{i'}} \rangle = \sum_{i,i'} c_i c'_{i'} \sum_{q,k=1}^{3} \langle \psi_{\alpha_i}^{(\tilde{q})} | \mathcal{O} | \psi_{\alpha'_{i'}}^{(\tilde{k})} \rangle. \tag{5.26}$$

Mathematically, it is clear that all functions have to be expressed in terms of the same coordinate system in order that this sum exists. So we have to transform both the bra $\langle \psi_{\alpha_i}^{(\tilde{q})}|$ and the ket $|\psi_{\alpha'_{i'}}^{(\tilde{k})}\rangle$ to the same partition, which will result just in a linear combination of matrix elements with basis states given in the same partition. In other words, we are able to simplify the calculation to a point where we only need to calculate matrix elements between basis functions given in coordinates of one single partition.

5.2.1 Transformation of the spatial part

In the spatial part, we need to transform the Jacobi coordinates of partition q to the corresponding Jacobi coordinates in partition k. As the flavor part determines the masses of the particles[11], without loss of generality, we will only look at configuration $(\tilde{k})$. The transformation between two sets of Jacobi coordinates is given by a simple linear transformation as elaborated in [SV98]

$$\begin{pmatrix} \vec{\xi}_k \\ \vec{\eta}_k \end{pmatrix} = A_{kq} \begin{pmatrix} \vec{\xi}_q \\ \vec{\eta}_q \end{pmatrix}. \tag{5.27}$$

Here the transformation matrix A_{kq} is given as

$$A_{kq} = \begin{pmatrix} -\frac{\mu_q}{m_p} & -P(kpq) \\ P(kpq)\frac{\mu_k}{M_q} & -\frac{\mu_k}{m_p} \end{pmatrix}. \tag{5.28}$$

[11] Remember the restriction we had to impose, namely that the quark with different mass – if such one occurs – should be located at position $(\tilde{k})$ for configuration $(\tilde{k})$.

The element $P(kpq)$ is defined as the parity of the permutation (kpq) of (123), and μ_k and M_k denote the reduced masses of the system:

$$\begin{aligned} \mu_k &= \frac{m_p m_q}{m_p + m_q}, \\ M_k &= \frac{m_k(m_p + m_q)}{m_k + m_p + m_q}. \end{aligned} \tag{5.29}$$

Naturally, if we (trivially) transform from a partition k to itself, the transformation matrix A_{kk} turns into the 2-dimensional unit matrix.

In the spatial part of the wave function, the Jacobi coordinates appear in the exponent of the Gaussian, as integer powers of their absolute value and as arguments in the bipolar spherical harmonics. In the exponent of the Gaussian, the above transformation only has the effect of changing the numerical values of the parameters β, δ and γ (which only appear there) to new values β_{kq}, δ_{kq}, and γ_{kq}

$$-\beta(\vec{\xi}_k)^2 - \delta(\vec{\eta}_k)^2 + \gamma\vec{\xi}_k \cdot \vec{\eta}_k = -\beta_{kq}(\vec{\xi}_q)^2 - \delta_{kq}(\vec{\eta}_q)^2 + \gamma_{kq}\vec{\xi}_q \cdot \vec{\eta}_q, \tag{5.30}$$

with the explicit form

$$\begin{aligned} \beta_{kq} &= [(A_{kq})_{11}]^2\beta + [(A_{kq})_{21}]^2\delta - (A_{kq})_{11}(A_{kq})_{21}\gamma, \\ \delta_{kq} &= [(A_{kq})_{12}]^2\beta + [(A_{kq})_{22}]^2\delta - (A_{kq})_{12}(A_{kq})_{22}\gamma, \end{aligned} \tag{5.31}$$

$$\begin{aligned} \gamma_{kq} &= -2(A_{kq})_{11}(A_{kq})_{12}\,\beta - 2(A_{kq})_{21}(A_{kq})_{22}\,\delta \\ &\quad + [(A_{kq})_{11}(A_{kq})_{22} + (A_{kq})_{12}(A_{kq})_{21}]\,\gamma \end{aligned} \tag{5.32}$$

for the new values. So the Gaussian term practically keeps the same form, since these parameters were stochastically variated parameters, anyway.

Even though we originally chose $\gamma = 0$ to obtain the required symmetry properties in configuration $(\tilde{k})$, in a different coordinate system, the correlation term reappears with a strength $\gamma_{kq} \neq 0$ in general. Therefore the arbitrary choice $\gamma = 0$ does not limit the universality of our basis wave functions.

For the transformation of the remaining term $(\xi_k)^{2\nu+\lambda}(\eta_k)^{2n+l}\mathcal{Y}_{\lambda l}^{LM_L}(\hat{\xi}_k, \hat{\eta}_k)$ we will make use of the identity [VMK88]

$$\left|\vec{\xi} + \vec{\eta}\right|^{2N+L} Y_{LM}(\widehat{\vec{\xi} + \vec{\eta}}) = \sum_{\substack{n_1 n_2 l_1 l_2 \\ 2n_1+2n_2+l_1+l_2=2N+L}} D_{NL}^{n_1 l_1 n_2 l_2} \xi^{2n_1+l_1} \eta^{2n_2+l_2} \mathcal{Y}_{l_1 l_2}^{LM}(\hat{\xi}, \hat{\eta}), \tag{5.33}$$

with the coefficients $D_{NL}^{n_1 l_1 n_2 l_2}$ defined by

$$\begin{aligned} D_{NL}^{n_1 l_1 n_2 l_2} &= \frac{B_{n_1 l_1} B_{n_2 l_2}}{B_{NL}} \frac{(2N+L)!}{(2n_1+l_1)!(2n_2+l_2)!} \langle l_1 l_2 | L \rangle, \\ B_{nl} &= \frac{4\pi (2n+l)!}{2^n n! (2n+2l+1)!!}, \\ \langle l_1 l_2 | L \rangle &= \sqrt{\frac{\hat{l}_1 \hat{l}_2}{4\pi \hat{L}}} \langle l_1 0 l_2 0 | L 0 \rangle, \\ \hat{l} &= 2l+1. \end{aligned} \tag{5.34}$$

The $\langle l_1 l_2 | L \rangle$ are non-zero only if $(-1)^{l_1+l_2+L} = 1$ and the three angular momenta l_1, l_2 and L "build a triangle" (i.e. fulfill $l_1 + l_2 < L$, but not equality). Using another relation for the tensor product of two bipolar spherical harmonics (see [Wag98] for the specific steps of the derivation), we arrive at

$$\begin{aligned} &(\xi_k)^{2\nu+\lambda} (\eta_k)^{2n+l} \mathcal{Y}_{\lambda l}^{LM_L}(\hat{\xi}_k, \hat{\eta}_k) = \\ &= \sum D_{\nu\lambda}^{\nu_1 \lambda_1 \nu_1' \lambda_1'} D_{nl}^{n_1 l_1 n_1' l_1'} [(A_{kq})_{11}]^{2\nu_1+\lambda_1} [(A_{kq})_{12}]^{2\nu_1'+\lambda_1'} [(A_{kq})_{21}]^{2n_1+l_1} \\ &\times [(A_{kq})_{22}]^{2n_1'+l_1'} (\xi_q)^{2\nu_1+\lambda_1+2n_1+l_1} (\eta_q)^{2\nu_1'+\lambda_1'+2n_1'+l_1'} \\ &\times \{\mathcal{Y}_{\lambda_1 \lambda_1'}^{\lambda}(\hat{\xi}_q, \hat{\eta}_q) \otimes \mathcal{Y}_{l_1 l_1'}^{l}(\hat{\xi}_q, \hat{\eta}_q)\}_{LM_L} = \\ &= \sum B_{\nu\lambda nlL}^{\nu_1 \lambda_1 \nu_1' \lambda_1' n_1 l_1 n_1' l_1' \kappa_1 \kappa_1'} (kq) (\xi_q)^{2\nu_1+\lambda_1+2n_1+l_1} \\ &\times (\eta_q)^{2\nu_1'+\lambda_1'+2n_1'+l_1'} \mathcal{Y}_{\kappa_1 \kappa_1'}^{LM_L}(\hat{\xi}_q, \hat{\eta}_q), \end{aligned} \tag{5.35}$$

which expresses the wave function of Jacobi coordinates k as a linear combination of wave functions of Jacobi coordinates q. The coefficients $B_{\nu\lambda nlL}^{\nu_1 \lambda_1 \nu_1' \lambda_1' n_1 l_1 n_1' l_1' \kappa_1 \kappa_1'}(kq)$ are a product of several constant components, including the elements of the transformation matrix (5.28), and do not have to be integer numbers. The summation indices of the last sum are further restricted by several conditions

$$\begin{aligned} 2\nu_1 + \lambda_1 + 2\nu_1' + \lambda_1' &= 2\nu + \lambda, \\ 2n_1 + l_1 + 2n_1' + l_1' &= 2n + l, \end{aligned} \tag{5.36}$$

$$\begin{aligned} (-1)^{\lambda_1+\lambda_1'+\lambda} = 1, \qquad (-1)^{l_1+l_1'+l} = 1, \\ (-1)^{\lambda_1+l_1+\kappa_1} = 1, \qquad (-1)^{\lambda_1'+l_1'+\kappa_1'} = 1, \end{aligned} \tag{5.37}$$

to guarantee the finiteness of the sum under consideration. Also, the triples $(\lambda_1, \lambda_1', \lambda)$, (l_1, l_1', l), $(\lambda_1, l_1, \kappa_1)$, and $(\lambda_1', l_1', \kappa_1')$ each have to form a triangle, which means that the

sum of two values must not be equal to the third number (cf. the triangle inequality $|\mathbf{a}| + |\mathbf{b}| \leq |\mathbf{a} + \mathbf{b}|$, where equality holds iff $\mathbf{a}$ and $\mathbf{b}$ are linearly dependent and so do not span a triangle).

5.2.2 Transformation of the spin part

The other part of the wave function that needs to be transformed is the spin term $\chi^{(\tilde{k})}_{(s,SM_S)}(k)$. We can transform it to a different partition by simply recoupling the three constituent quark spins using the transformation

$$\chi^{(\tilde{k})}_{(s,SM_S)}(k) = \sum_{s_1=0,1} P(kq)\sqrt{\hat{s}\hat{s}_1} \begin{Bmatrix} \frac{1}{2} & \frac{1}{2} & s \\ \frac{1}{2} & S & s_1 \end{Bmatrix} \chi^{(\tilde{k})}_{(s_1,SM_S)}(q) \; . \tag{5.38}$$

The phase factor $P(kq)$ depends only on the partitions and the summation indices

$$P(kq) = \begin{cases} (-1)^s, & (kq) = (12), (23), (31) \\ (-1)^{s_1}, & (kq) = (21), (32), (13) \end{cases} \tag{5.39}$$

and is the only term which depends on the Jacobi coordinates. There is no dependence at all on the specific configuration.

Looking at equation (5.38), one sees that also the spin part can be written as a linear combination of spin basis functions given in partition q, and so the whole basis function transformed from partition k to partition q is expressed as a linear combination of basis functions in partition q. This finalizes our claim that we only have to calculate matrix elements between configuration basis wave functions in potentially different configurations $(\tilde{k})$ and $(\tilde{p})$, but using the same partitions, to evaluate the full matrix element $\langle \Psi | \mathcal{O} | \Psi' \rangle$.

Chapter 6

Parametrization of the extended GBE CQM

Contents

In this chapter our parametrization of the Hamiltonian of the extended Goldstone-boson-exchange potential will be described. All force components except the spin-orbit components are included. After the description of the terms employed in the model, I will give the parameters of our best fit[1] together with the spectrum obtained with these values. Finally, each of the light and strange baryons (N, Δ, Λ, Σ, Ξ and Ω) is discussed in more detail.

[1] One has to bear in mind that these values are by far not unique, and one can always find equally good (minimal) values, depending on where one puts the emphasis of the fit. We selected some important states and tried to minimize their error as described in section 6.1.1.

6.1 Parametrization and parameter values

We employ the general form of the semi-relativistic Hamilton (3.7) with a hyperfine interaction as given in equation (3.12) and a linear confinement $V_{\text{conf}}(\vec{r}_{ij}) = V_0 + Cr_{ij}$. Both the shift V_0 and the string tension C are determined from the spectrum.

The pseudoscalar radial dependences were already described in great detail in the previous chapters, so I will only refer to the respective equations there. In our model, all three types of exchange interactions – pseudoscalar, vector and scalar meson exchange – are considered with all force types included, except the spin-orbit terms of the vector and scalar exchange. The inclusion of these missing terms are the topic of another parallel diploma thesis [Gla02].

In particular, in our model the following terms will be included:

- The pseudoscalar meson exchange (π, K, η, η') according to equation (3.15) implies both the spin-spin part as given in equation (3.16) and the tensor part from equation (3.17).
- The vector meson exchange $(\rho, K^*, \omega_8, \omega_0)$ according to equation (3.18) contains all four types of forces: spin-spin (3.20), tensor (3.21), spin-orbit (3.22) and central (3.19) forces. However, we neglect the spin-orbit terms (3.22) here, since their contribution should not be too large as already discussed in the previous chapter.
- The scalar meson exchange $(\sigma, \kappa, a_0, f_0)$ interaction according to equation (3.23) contains central and spin-orbit force components (equations (3.24) and (3.25)), where we again leave out the spin-orbit part (3.25).

All these radial dependent terms apply a Yukawa-type smearing of the δ-function in the contact term, corresponding to a form factor (3.10) involving a cut-off Λ_γ for each exchange particle $\gamma = \pi, K, \eta, \eta', \rho, K^*, \omega_0, \omega_8, \sigma, a_0, f_0, \kappa$. To keep the number of free parameters to a minimum, a linear scaling rule similar to equation (3.11) turned out to be reasonable and was already employed in earlier publications [WGPV00a]. We use the same dependence on the meson masses with a fixed and pre-determined slope of 1, but a different starting point for the pseudoscalar, vector and scalar mesons. In particular, the Λ_γ are determined as

$$\Lambda_\gamma = \Lambda_\pi + (\mu_\gamma - \mu_\pi) \quad \text{for pseudoscalar mesons } \gamma = K, \eta, \eta' \tag{6.1a}$$

$$\Lambda_\gamma = \Lambda_\rho + (\mu_\gamma - \mu_\rho) \quad \text{for vector mesons } \gamma = K^*, \omega_0, \omega_8 \tag{6.1b}$$

$$\Lambda_\gamma = \Lambda_\sigma + (\mu_\gamma - \mu_\sigma) \quad \text{for scalar mesons } \gamma = a_0, f_0, \kappa, \tag{6.1c}$$

where in the case of the scalar mesons the masses of the a_0, f_0, and κ are all taken equal as $\mu_{a_0} = \mu_{f_0} = \mu_\kappa = \mu_{\text{scalar}}$.

Such a linear scaling rule, however, can still be improved if we take the cut-off of the η' as an additional free parameter[2] in our fit. The same also holds for the K meson, which is used to treat the light and the strange spectrum in two consecutive steps instead of fitting them at the same time. Thus, in addition to the initial cut-offs Λ_π, Λ_ρ and Λ_σ we have two additional meson-specific cut-offs Λ_K and $\Lambda_{\eta'}$ resulting in 7 free parameters and 20 fixed parameters as given in table 6.1.

6.1.1 The fit function

In order to obtain an acceptable fit of the baryon spectra, we first tried to minimize the following linear combination of differences for the most important light baryon excitations:

$$\begin{aligned}\delta E =& \delta N(1440)_{\frac{1}{2}^+} + \delta N(1710)_{\frac{1}{2}^+} + \delta N(1535)_{\frac{1}{2}^-} + \frac{1}{2}\delta N(1650)_{\frac{1}{2}^-} + \\ &+ \delta N(1520)_{\frac{3}{2}^-} + \delta N(1700)_{\frac{3}{2}^-} + \frac{1}{2}\delta N(1680)_{\frac{5}{2}^+} + \\ &+ \frac{1}{2}\delta N(1675)_{\frac{5}{2}^-} + \delta\Delta(1232)_{\frac{3}{2}^+} + \delta\Delta(1600)_{\frac{3}{2}^+}\,.\end{aligned} \tag{6.2}$$

For each state the δ is taken as the relative deviation from the experimentally observed value

$$\delta State = \frac{E^{\text{GBE}}_{\text{predicted}} - E^{\text{mean}}_{\text{observed}}}{E^{\text{upper}}_{\text{observed}} - E^{\text{upper}}_{\text{observed}}}\,.$$

In this way one arrives at a first estimate for the light baryons' spectra. Then the strange baryons are included and a manual adjustment of the preliminary parameter values is made in order to arrive at a good overall fit.

6.1.2 The parameter values of the best fit

Using the fit method and the manual adjustment just described, one finds a possible optimal set of parameters with values as given in table 6.1. For the coupling constants, we use values that derive from the phenomenologically known coupling constants for the πN, ρN, and ωN couplings (see [Gla02]). The coupling constant $(g_0)^2/4\pi$ of the pseudoscalar singlet η', which was taken as a free parameter in several previous models, is set equal to the coupling constant $(g_8)^2/4\pi$ of the pseudoscalar octet; our calculations indicate this to be a reasonable choice.

The string tension of the confinement is determined as $C = 1.935$ fm^{-2} and thus is a little smaller than the values used in previous models, and also smaller than one would expect from the $\bar{q}q$ confinement. The overall shift V_0 assumes a value of -1030 MeV.

[2]The η' cannot be strictly regarded as a Goldstone boson, anyway, due to its large mass, so this specific choice just amplifies the special role of this pseudoscalar meson in the model.

Fixed parameters (phenomenological values)					
$m_u = m_d$	340 MeV	m_s	507 MeV		
μ_π	139 MeV	μ_K	494 MeV	μ_η	547 MeV
$\mu_{\eta'}$	958 MeV	μ_ρ	770 MeV	μ_{K^*}	892 MeV
μ_{ω_8}	869 MeV	μ_{ω_0}	947 MeV	μ_σ	680 MeV
μ_{scalar}	980 MeV				
$g_0^2/4\pi$	0.67	$g_8^2/4\pi$	0.67	$(g_8^V)^2/4\pi$	0.55
$(g_8^T)^2/4\pi$	0.16	$(g_0^V)^2/4\pi$	1.107	$(g_0^T)^2/4\pi$	0.0058
Free parameters (fitted to the experimental spectrum)					
Λ_π	834 MeV	Λ_K	1420 MeV	$\Lambda_{\eta'}$	1400 MeV
Λ_ρ	1145 MeV	Λ_σ	1513 MeV		
C	1.935 fm^{-2}	V_0	-1030 MeV		

Table 6.1: *Fixed and fitted parameters of the extended Goldstone-boson-exchange model constructed in this work. For the meson masses, we use the experimentally measured values, and the values for the coupling constants are derived from phenomenology [Gla02].*

6.2 The resulting spectra

In the following section we will give the full spectra of the six light and strange baryon families N, Δ, Λ, Σ, Ξ, and Ω and their lowest excitations, calculated from our parametrization of the extended GBE constituent quark model as described in the previous section. We will shortly discuss each of these baryons and give the lowest excitations for all baryonic states with $J \leq \frac{5}{2}$ up to an energy of $E \leq 2700$ MeV (at most 10 excitations) for comparison with the experimental data (as published by the Particle Data Group [H$^+$02]). For most of the predicted excited states no experimental counterparts can be found, and for some experimentally measured states the exact total angular momentum J is not known. Although we give calculated states up to an energy of 2700 MeV, this should not be interpreted as a prediction of real baryonic states of such high energies, mostly because the effective model presented in this work cannot be assumed valid up to such energies. Furthermore, for our fits we consider only very few light (and even fewer strange) states, so the good description of the lowest two or three excitations for each state is given most attention.

6.2.1 The ground states of the light and strange baryons

In the fits of the parameter values of our parametrization of the GBE constituent quark model several states (see the original fitting function (6.2) for the light baryons) are taken into account to obtain a preliminary set of good parameters. As the error of each state is considered as relative to the experimental uncertainty, this procedure leads to a high emphasis of the (best known) ground states of the baryons.

The results of our calculations are shown in figure 6.1. The theoretical levels

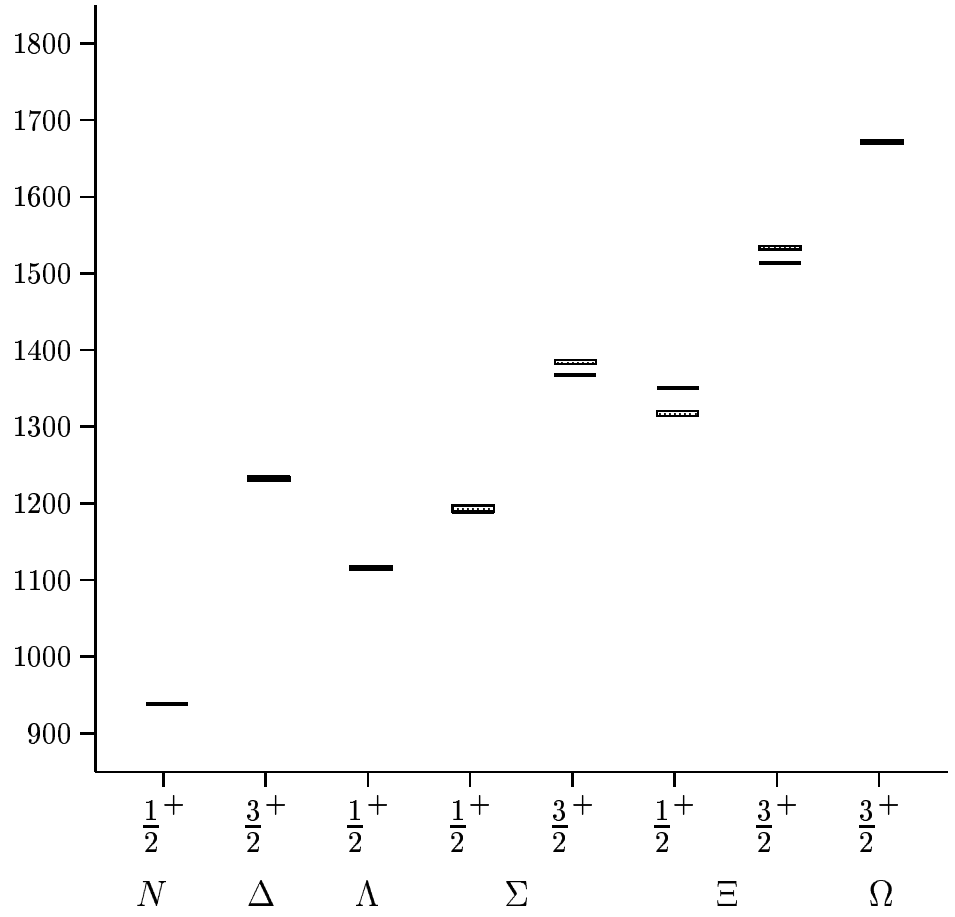

Figure 6.1: *Ground states of the light and strange baryons as predicted by our extended GBE constituent quark model. Experimental values and their uncertainties [H+02] are given as gray boxes (or practically straight lines in case of the N, Δ, Λ, and Ω ground states).*

match the experimental data rather well. The ground states of the N, the Δ, Λ, Σ, and the Ω baryons are correctly predicted within their experimental uncertainties of only few MeV. Only the $J = \frac{3}{2}^+$ triplet state $\Sigma(1385)$ from the decuplet is predicted 18 MeV too low, and the $\Xi(1314 - 1321)$ ($J = \frac{1}{2}^+$ octet) and $\Xi(1530)$ ($J = \frac{3}{2}^+$ decuplet) states are 35 above and 15 MeV below their experimental ground states respectively. The $\Delta(1235)$ can only be predicted to such a high degree, if one does not put too much weight on the degenerate $N(1675)$ and $N(1680)$ states (see the discussion in section 7.4).

The comparably large deviations of the Σ and Ξ ground states can be explained by the fact that we did not put any emphasis on the Ξ and the decuplet Σ states upon fixing our parametrization. One might be able to find a parametrization that describes these ground states better, but at the expense that the other states of the light baryons lose some quality.

We also have to mention that our parametrization is already done with a view on the inclusion of the spin-orbit terms. While these terms are neglected in our

calculations, we tried to choose our parameter set in such a way that the effects of the spin-orbit components in the vector and scalar potentials, as well as in the confinement, can be expected to improve our results. Thus some aspects of the present parametrization might not be chosen optimally for a model without spin-orbit forces, but will provide a good starting point for spin-orbit terms to be included (see the work of [Gla02]).

6.2.2 The nucleon spectrum

The complete excitation spectrum of the nucleon from our parametrization is given in figure 6.2. The nucleon ground state $N(939)$ is used to fix the over-all shift constant V_0 in the confinement, so the nucleon ground state is a priori predicted correctly. The level ordering of the $J^P = \frac{1}{2}^+$ and $J^P = \frac{1}{2}^-$ lowest positive- and negative-parity states is correctly described like it was already the case in previous versions of GBE constituent quark models. The Roper $N(1440)$ resonance falls 60 MeV below the lowest negative-parity state $N(1535)$, both of which are correctly predicted within their experimental uncertainty bounds. The remaining $J^P = \frac{3}{2}^-$ state $N(1520)$ of the first band also falls within its experimental uncertainty.

While the first band in the spectrum is very well described and falls completely inside the experimental errors, the second band is only approximately correct. Only the $J^P = \frac{2}{3}^+$ state $N(1720)$ is still predicted inside its large experimental uncertainty. The positive-parity state $N(1710)$ is predicted at an energy of $E \approx 1762$ MeV and so lies 12 MeV above the experiment. The $J^P = \frac{1}{2}^-$ state $N(1650)$ practically falls inside the experimental data (with only 5 MeV error above), and although both states are somewhat too high, the correct level ordering between the second positive- and negative-parity $J^P = \frac{1}{2}$ excitations $N(1710)$ and $N(1650)$ is obtained. Both $\frac{1}{2}^-$ excitations $N(1535)$ and $N(1650)$ are correctly described by our model in contrast to the extended model including the spin-orbit terms [Gla02], where these two states are shifted to lower energies by a considerable amount.

The $J^P = \frac{3}{2}^+$ and $J^P = \frac{3}{2}^-$ states $N(1720)$ and $N(1700)$ of the second band are not well determined from experiment and might even be degenerate (like the two $J^P = \frac{5}{2}$ states). Their experimental error is about 100 MeV, so any prediction near the experimental error box can be seen as an acceptable prediction. The $\frac{3}{2}^+$ state $N(1720)$ even falls inside the error box, while the $N(1700)$ is predicted 20 MeV below the experiment.

One of the biggest problems in obtaining a good description by our model was posed by the two degenerate $J^P = \frac{5}{2}^+$ and $J^P = \frac{5}{2}^-$ states $N(1680)$ and $N(1675)$. Experimentally they have rather sharp error bounds of 1675 to 1690 MeV and 1670 to 1685 MeV, respectively. As explained in more detail in section 7.4, it turned out that the present model is not able to explain the degeneracy of these states, while keeping at the same time a good description of the Δ baryon. Only the inclusion of the spin-orbit forces can cure this deficiency. The investigation of this problem goes

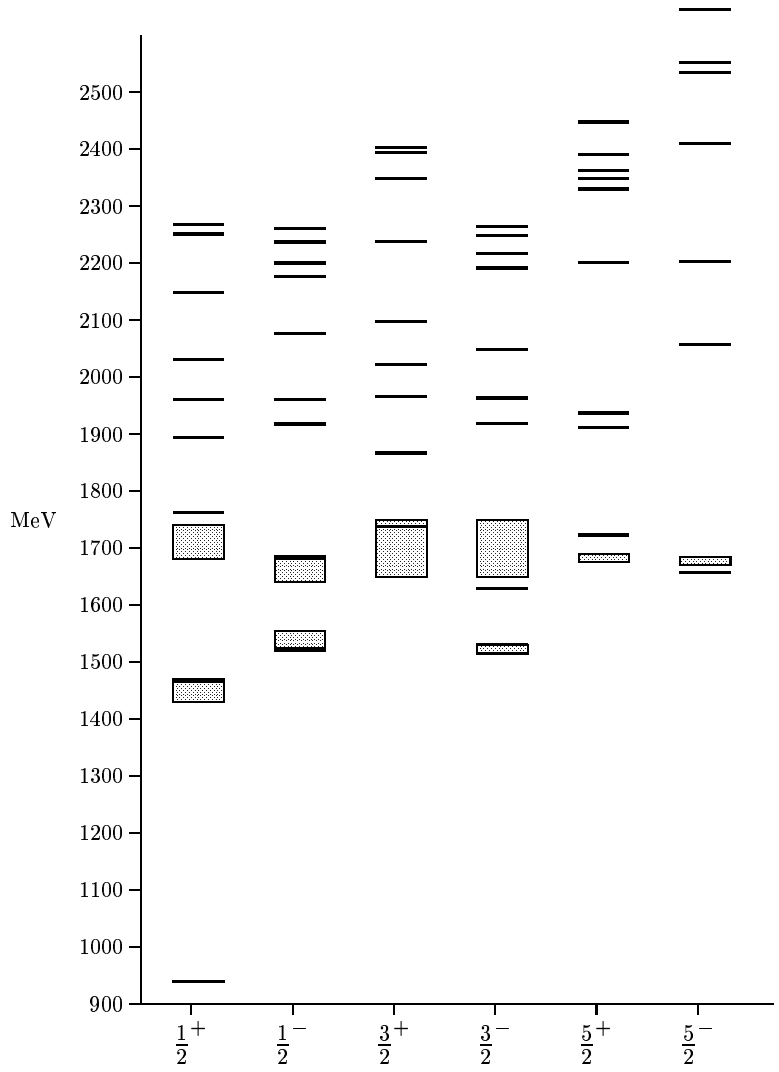

Figure 6.2: *The nucleon spectrum as predicted by our extended GBE constituent quark model. Experimental values and their uncertainties [H+02] are given as gray boxes.*

beyond our task and was the subject matter of the diploma thesis of ref. [Gla02].

Even higher excitations $J^P > \frac{5}{2}$ are not reliably observed in nature. Our calculations indicate that the energy differences in the various excitations become much smaller for these higher excitations. Thus, even if one attributes validity of the GBE model for excitations higher than about 1900 or 2000 MeV, the energy differences might simply become too small in order to discriminate between different excited states above the second band. Even more important is the fact that in this energy regime such effects like the string break-up will play an increasingly important role, and they are not incorporated in our model.

6.2.3 The Δ spectrum

The Δ baryon, which consists of the four $Y = 1$ states Δ^-, Δ^0, Δ^+, and Δ^{++} of the decuplet representation of $SU(3)_F$, has a $J^P = \frac{3}{2}^+$ ground state $\Delta(1232)$ which is exactly predicted in our calculations. The complete excitation spectrum from our model is given in figure 6.3.

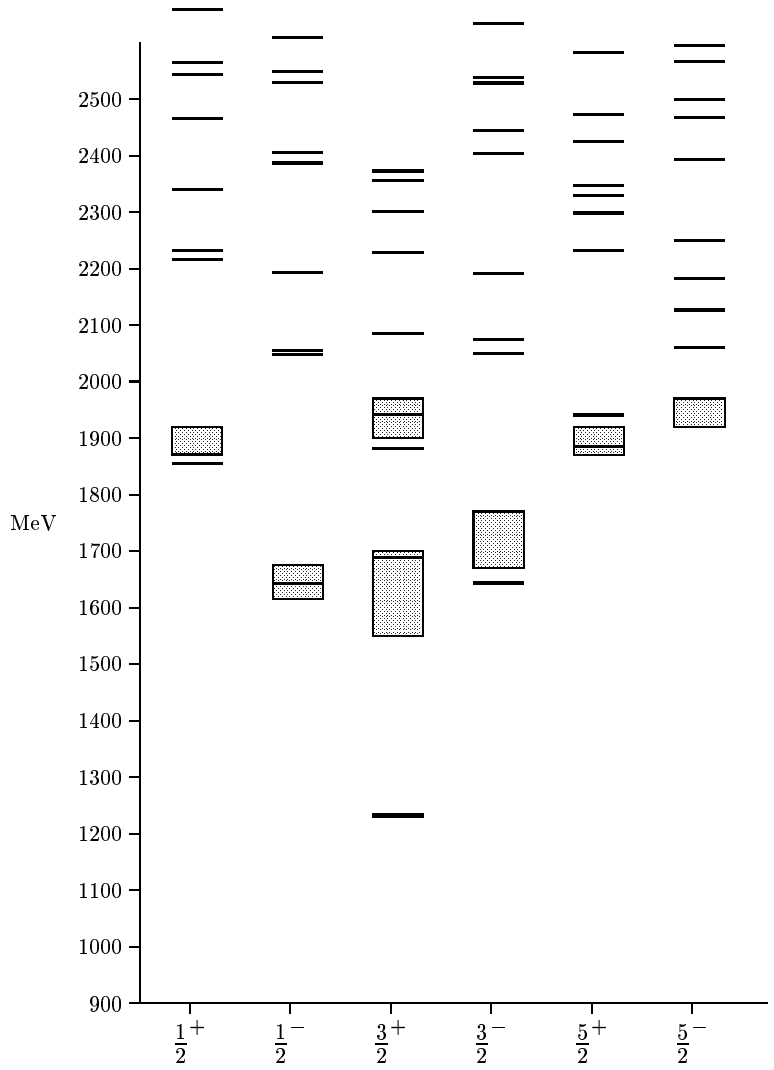

Figure 6.3: *The Δ spectrum as predicted by our extended GBE constituent quark model. Experimental values and their uncertainties [H+02] are given as gray boxes.*

The $J^P = \frac{1}{2}^-$ state $\Delta(1620)$ as well as the $J^P = \frac{3}{2}^+$ excitation $\Delta(1600)$ lie completely inside the error bounds. Only the $\Delta(1700)$ state in the first band lies about 25 MeV below the experimentally measured uncertainty. Here – like in all previous semi-relativistic GBE constituent quark models – the level ordering of the two $J^P = \frac{3}{2}$ states $\Delta(1600)$ and $\Delta(1700)$ cannot be correctly predicted, as the $\Delta(1700)$ is predicted 45 MeV below the $\Delta(1600)$ state in contrast to what the experimental data seem to indicate.

The second band in the Δ spectrum is also quite well described, however, our spectra suggest two close-lying states for each of the $\Delta(1910)$, $\Delta(1920)$, and $\Delta(1905)$ positive-parity excitations. The negative-parity $J^P = \frac{5}{2}^-$ excitation $\Delta(1930)$ cannot be reproduced by our model, where the lowest $J^P = \frac{5}{2}^-$ state lies at an energy of ≈ 2060 MeV. Higher excitations in the $J^P \leq \frac{5}{2}$ sector are not reliably observed in experiment. With regard to the similarly high-lying $J^P = \frac{7}{2}^+$ and $\frac{11}{2}^+$ states $\Delta(1950)$ and $\Delta(2420)$ we may have considerable doubts of the validity of any CQM.

6.2.4 The Λ spectrum

The Λ baryon is the first strange baryon, consisting of three quarks with different flavors u, d, and s. It also forms the flavor singlet state Λ^0 of $SU(3)$ with $Y = T_3 = 0$ and is part of the octet representation of $SU(3)_F$.

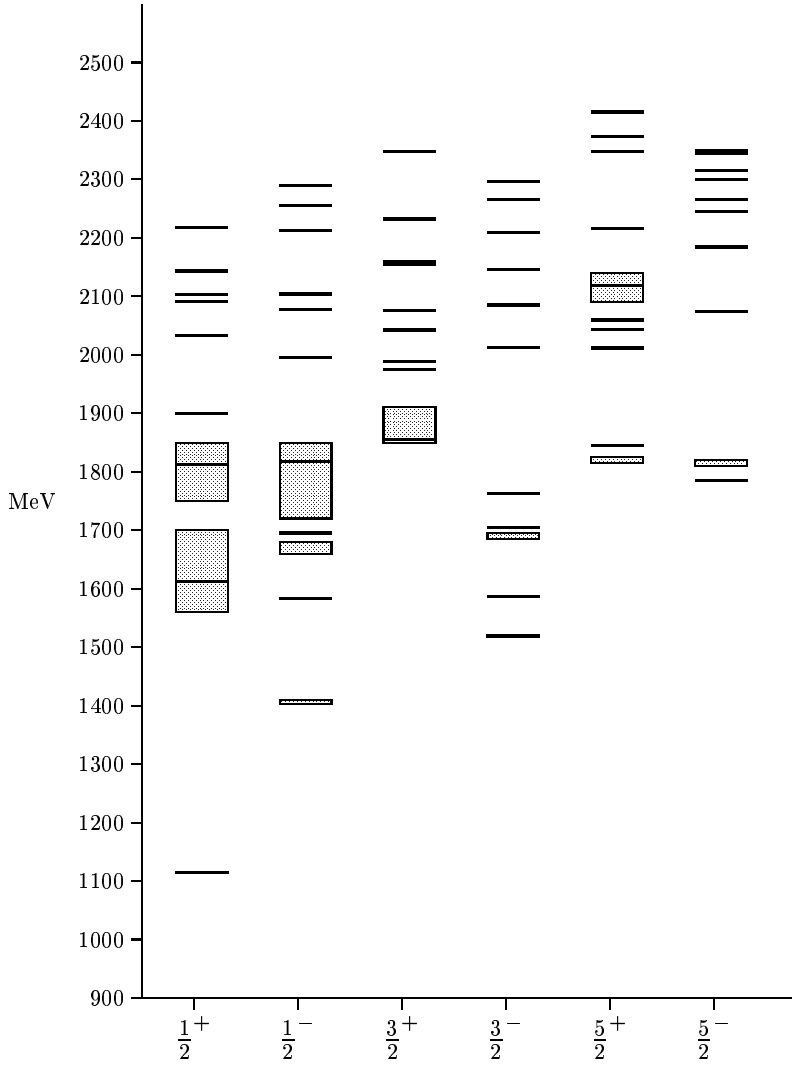

Figure 6.4: *The Λ spectrum as predicted by our extended GBE constituent quark model. Experimental values and their uncertainties [H+02] are given as gray boxes.*

Its ground state is the $\frac{1}{2}^+$ state $\Lambda(1115)$, which is exactly reproduced in our model (figure 6.4 shows the complete spectrum). However, in contrast to the nucleon spectrum, the first excitation above the ground state is the $J^P = \frac{1}{2}^-$ state $\Lambda(1405)$. This very particular state is probably not a pure QQQ state, but instead consists also of sizable contributions from $QQQq\bar{q}$ or similar states. This is because it lies close to the K - N threshold and so feels large influences from the decay channel. For these reasons, the $\Lambda(1405)$ has never been described even approximately by GBE constituent quark models. Our parametrization of the extended GBE CQM is no exception to this phenomenon, with the $\Lambda(1405)$ state assuming an energy of $E_{\Lambda(1405)} \approx 1583$ MeV and so 170 MeV above the rather accurate experimental value. Still, it remains noticeably below the $\Lambda(1600)$ positive-parity excitation and so the correct level ordering of the first positive- and negative-parity excitations is guaranteed. The next excitation, the $J^P = \frac{3}{2}^-$ state $\Lambda(1520)$, is also predicted 66 MeV above the sharp experimental value.

Of the remaining excitations, all the $J^P = \frac{1}{2}^\pm$ states practically fall inside their error boxes, and also the $J^P = \frac{3}{2}^+$ state $\Lambda(1890)$ is obtained at the lower bound of the experimental data. Like in the nucleon, the two lowest $J^P = \frac{5}{2}^+$ and $J^P = \frac{5}{2}^-$ excitations should be (almost) degenerate according to their experimental values. Again, our model is unable to yield this feature, which can only be achieved by the inclusion of the spin-orbit components of the meson-exchange and the confinement potentials [Gla02].

Experimental data also suggest a $J^P = \frac{5}{2}^+$ excitated state $\Lambda(2110)$ between 2090 and 2140 MeV. Our calculations show one energy eigenvalue in that range, however, there are three other eigenvalues below this energy, so these probably do not describe the same state. This appears as another indication that the validity of our model is restricted to an energy range of 1900 to 2000 MeV.

6.2.5 The Σ spectrum

The Σ baryon family contains both states that are members of the octet and of the decuplet representation of $SU(3)_F$. The two ground states are the $J^P = \frac{1}{2}^+$ multiplet Σ^+, Σ^0, and Σ^- at energies around 1189 to 1197 MeV and the $J^P = \frac{3}{2}^+$ multiplet $\Sigma(1385)$ with an experimentally measured energy range from 1382 to 1388 MeV. The first is predicted by our parametrization at exactly that energy, while the latter is obtained at 15 MeV below the error bars (figure 6.5).

The few known remaining excitations are predicted quite well, where the lowest $\frac{1}{2}^-$ and $\frac{3}{2}^-$ negative-parity states $\Sigma(1750)$ and $\Sigma(1670)$ seem to consist of three distinct energy eigenstates in our model, which are spread over a range of about 90 MeV. The lowest of these $J^P = \frac{1}{2}^-$ states is 30 MeV below the experimental bound, while the remaining two fall inside the error box. The $J^P = \frac{3}{2}^-$ states all lie up to 75 MeV above the experimental data. The lowest experimental $\frac{5}{2}^+$ and $\frac{5}{2}^-$ states are well described in our model, with the $\frac{5}{2}^-$ state only 14 MeV below the experiment.

According to the compilation of the Particle Data Group [H$^+$02], one should

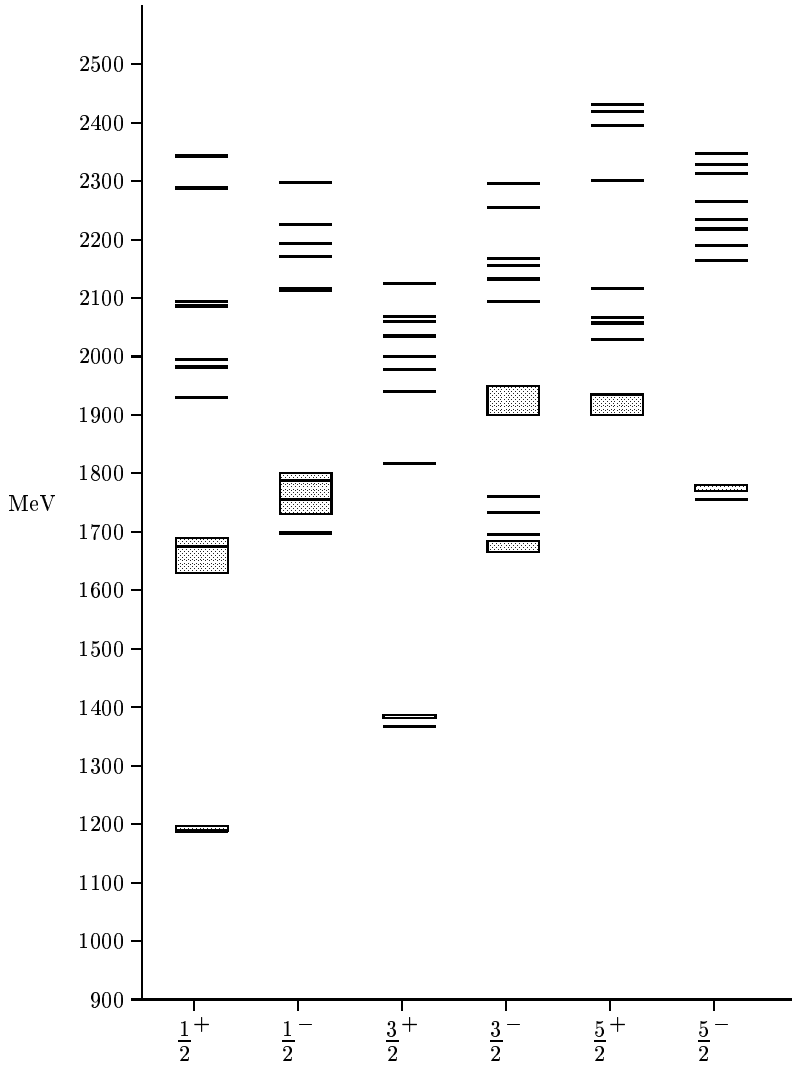

Figure 6.5: *The Σ spectrum as predicted by our extended GBE constituent quark model. Experimental values and their uncertainties [H+02] are given as gray boxes.*

expect a $J^P = \frac{3}{2}^-$ state at an energy of 1900 to 1950 MeV. However in our calculations there is a large energy gap of 330 MeV from 1760 to 2067 MeV in the spectrum, wherefore our model cannot explain this state at all.

6.2.6 The Ξ spectrum

In the Ξ spectrum, only three states are experimentally measured with a determined J^P. These are the $J^P = \frac{1}{2}^+$ Ξ^0/Ξ^- ground states at 1314 and 1321 MeV, the $J^P = \frac{3}{2}^+$ state $\Xi(1530)$ and the $J^P = \frac{3}{2}^-$ state $\Xi(1820)$. All of these are more or less well described in our calculations (figure 6.6), with the ground state lying 30 MeV too high.On the other hand the $\Xi(1530)$ is 15 MeV too low, whereas the $\Xi(1820)$ is again 11 MeV above the experimental value.

Experimentally there is another state at $E \approx 1690 \pm 10$ MeV, which is not found in

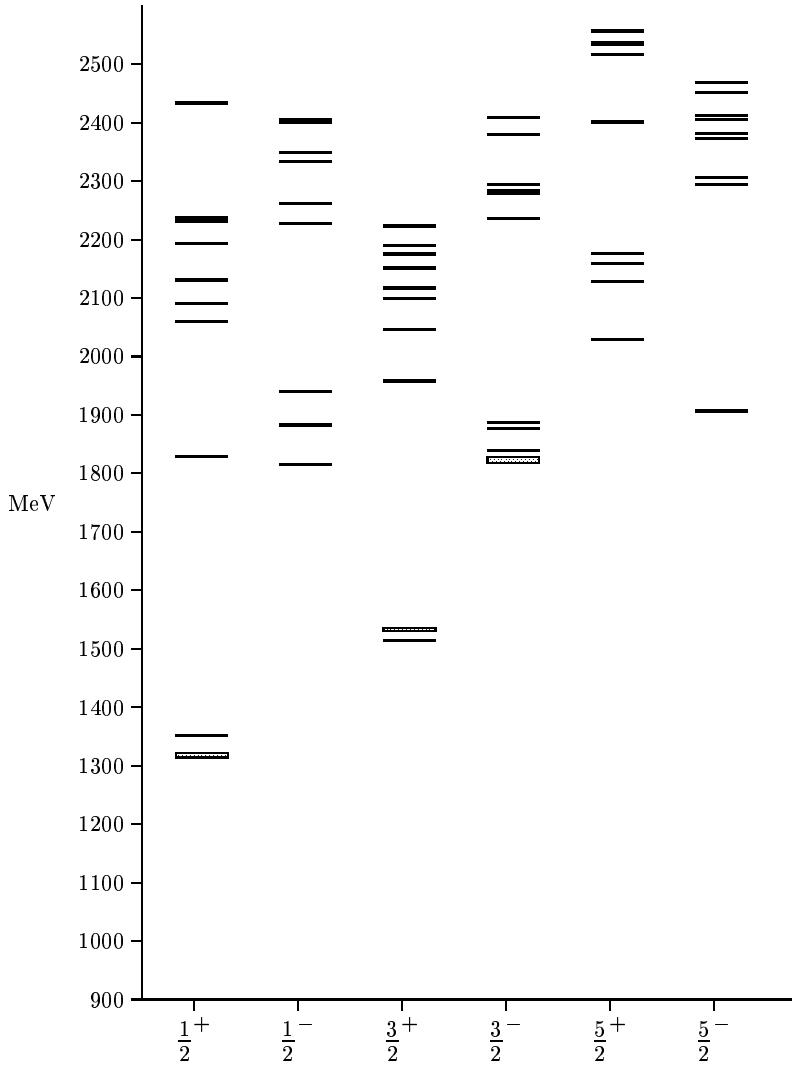

Figure 6.6: *The Ξ spectrum as predicted by our extended GBE constituent quark model. Experimental values and their uncertainties [H+02] are given as gray boxes.*

our calculations, where we only consider values of J^P up to $\frac{5}{2}$; the J^P for the Ξ(1690) is unknown and might be above $\frac{5}{2}$. Apart from this state, there are no experimental states below 1800 MeV, which is in agreement with our model.

The Particle Data Group lists two other experimental states, the Ξ(1950) with unknown J^P, and the Ξ(2030) with $J^P \geq \frac{5}{2}$. For the first of these states, our spectrum shows either a $J^P = \frac{1}{2}^-$ excitation at $E \approx 1941$ MeV or a $J^P = \frac{3}{2}^+$ resonance at $E \approx 1958$ MeV. Calculations including the spin-orbit terms indicate that the $J^P = \frac{1}{2}^-$ state actually lies below 1900 MeV, but the $J^P = \frac{3}{2}^+$ state might correspond to the Ξ(1950) experimental state. For the Ξ(2030) with $J^P \geq \frac{5}{2}$, our lowest $J^P = \frac{5}{2}^+$ state at $E \approx 2029$ MeV might be a candidate, but since we did not calculate the spectra for higher J^P, we cannot rule out a higher J^P for the Ξ(2030).

6.2.7 The Ω spectrum

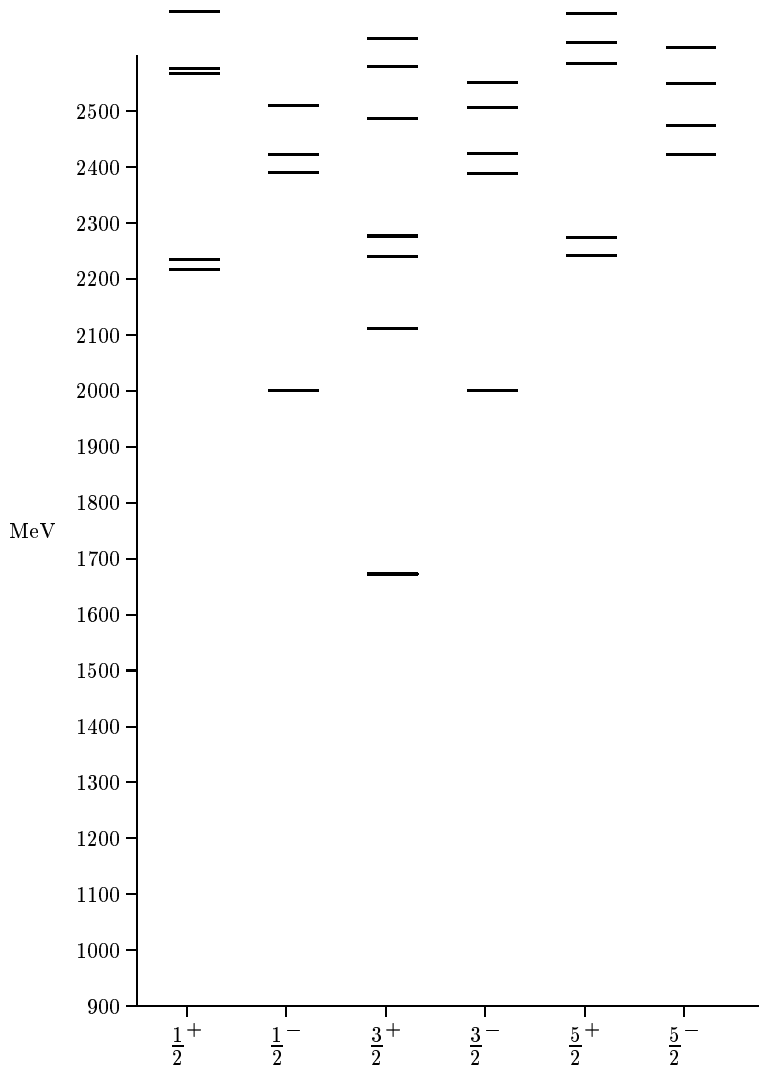

Figure 6.7: *The Ω spectrum as predicted by our extended GBE constituent quark model. Experimental values and their uncertainties [H+02] are given as gray boxes.*

Finally, the Ω is the baryon with the least experimentally known states. Only the ground state Ω^- is measured at $E \approx 1672$ MeV, however, its J^P has not been determined experimentally. The Particle Data Group still gives $J^P = \frac{3}{2}^+$ for the Ω^- as a prediction from the quark model. Our model of course supports this J^P with a calculated $\frac{3}{2}^+$ state at 1672 MeV exactly matching the experimental value. The only other known state is the $\Omega(2250)$, again with unknown J^P. In our model we find two $J^P = \frac{1}{2}^+$, two $J^P = \frac{3}{2}^+$, and two $J^P = \frac{5}{2}$ states near that energy, but we also find three lower excitations which are not measured experimentally. They lie at $E \approx 2000$ MeV and $E \approx 2110$ MeV. As already mentioned several times, our model can probably no make any reliably predictions in this energy regime.

Looking at the Ω spectrum, one has to notice the resemblance to the Δ spectrum,

which can be explained by the corresponding flavors of the constituent quarks. While the Δ^{++} consists of three u quarks, and the Δ^{-} of three d quarks, the Ω is built of three strange quarks s. Since in all of these baryonic states only force components acting between constituent quarks of the same flavors occur, one has to expect a similar spectrum, only shifted to higher energies for the Ω due to the higher mass of the strange quark.

Chapter 7

Discussion of the numerical results

Contents

In this chapter we will take a closer look at some of the problems and open questions that arose during the construction of the present extended GBE constituent quark model whose results are discussed in the previous chapter. In particular, we will first take a look at the effect of each of the free parameters, first regarding the cut-off parameters Λ_π, Λ_ρ and Λ_σ as well as the special cases of Λ_K, and $\Lambda_{\eta'}$. From the beginning our aim has been to keep the number of open parameters for a good fit to a minimum. However, in the course of our work it turned out that a simple linear dependence of the remaining cut-off parameters is simply not sufficient, and the spectrum can be improved if we treat the cut-offs for the K and the η' as separate free parameters.

After this investigation of the cut-off parameters for the smearing of the δ-function in the contact interaction, we will consider the confinement potential and discuss a possible inclusion of an additional Coulomb term of the form $\frac{\alpha}{r}$ into the confinement potential. Lattice QCD calculations [B$^+$00] suggest such a term in the $q\bar{q}$ confinement, however, our results show that in our model this term can effectively be absorbed into the V_σ and a (modified) linear confinement potential by a suitable choice of parameters.

The final problem we will address here is the near degeneracy of the $J^P = \frac{5}{2}^+$ and $J^P = \frac{5}{2}^-$ states $N(1680)$ and $N(1675)$. We will learn that this cannot be achieved to a reasonable degree in our model, where we neglect the spin-orbit forces.

7.1 The effect of the cut-off parameters

Our model relies on five cut-offs Λ_γ as free parameters. We avoid a proliferation of open parameters from the cut-offs by the linear prescription (6.1) for each of the meson families: The pseudoscalar mesons are all scaled linearly from the Λ_π according to their masses, the cut-offs for the vector mesons are derived in an similar manner from the Λ_ρ, and the scalar mesons (σ, f_0, a_0, κ) employ the Λ_σ as their initial value, from which the remaining three parameters are calculated by the relation (6.1).

Initially we even intended to derive the Λ_σ from either the Λ_π or from the Λ_ρ, however, in these cases we were unable to obtain a reasonable spectrum. Instead it turned out that using the Λ_σ as a free parameter allowed us to significantly improve the spectrum, and furthermore absorb the effect of a Coulomb term from the confinement potential (see section 7.2). Using only these three cut-off parameters Λ_π, Λ_ρ, Λ_σ already gave reasonable results. However, we found that variation of $\Lambda_{\eta'}$ separately improved the fit a lot. It also turned out that treating the Λ_K as a separate free parameter helps in adjusting the spectra of the strange baryons after the N and Δ spectra have been fixed. This is of course a consequence of the fact that the K acts as an exchange meson only between a light and a strange constituent quark and thus has no influence on the nucleon and Δ spectra[1]. Thus, when examining the effects of the cut-offs on the energy states, we will in general only look at their influences on the nucleon and delta states. The influences from the Λ_K will be checked along with several energy eigenstates of the strange baryons Λ, Σ, Ξ, and Ω.

To have greater flexibility in our experiments, in some cases we generalized the linear prescription (6.1) to include a slope parameter κ_γ:

$$\Lambda_\gamma = \Lambda_\pi + \kappa_\pi\,(\mu_\gamma - \mu_\pi) \quad \text{for pseudoscalar mesons } \gamma = K, \eta, \eta'\,, \tag{7.1a}$$

$$\Lambda_\gamma = \Lambda_\rho + \kappa_\rho\,(\mu_\gamma - \mu_\rho) \quad \text{for vector mesons } \gamma = K^*, \omega_0, \omega_8\,, \tag{7.1b}$$

$$\Lambda_\gamma = \Lambda_\sigma + \kappa_\sigma\,(\mu_\gamma - \mu_\sigma) \quad \text{for scalar mesons } \gamma = a_0, f_0, \kappa\,. \tag{7.1c}$$

Whenever we give values for either of the κ_γ in the sequel, it is meant that we used this extended scaling rule.

7.1.1 Effects of the pseudoscalar, vector, and scalar cut-offs

The (pseudoscalar) π exchange is by far the most important contribution to the light spectrum. This can be seen from the fact that already earliest models, including only the spin-spin terms of the π exchange, could predict the spectra astonishingly well. Figure 7.1 shows the effect of the Pion cut-off on the light spectra. It is important to notice that the positive-parity nucleon states $N(1440)$, $N(1710)$, and $N(1680)$ are far less affected than the negative-parity nucleon and the Δ states.

[1] The vector K^* and scalar κ mesons display a similar behavior, but their effects are considerably smaller than the one of the K. Therefore we maintained the scaling of their cut-offs due to the Λ_ρ and Λ_σ.

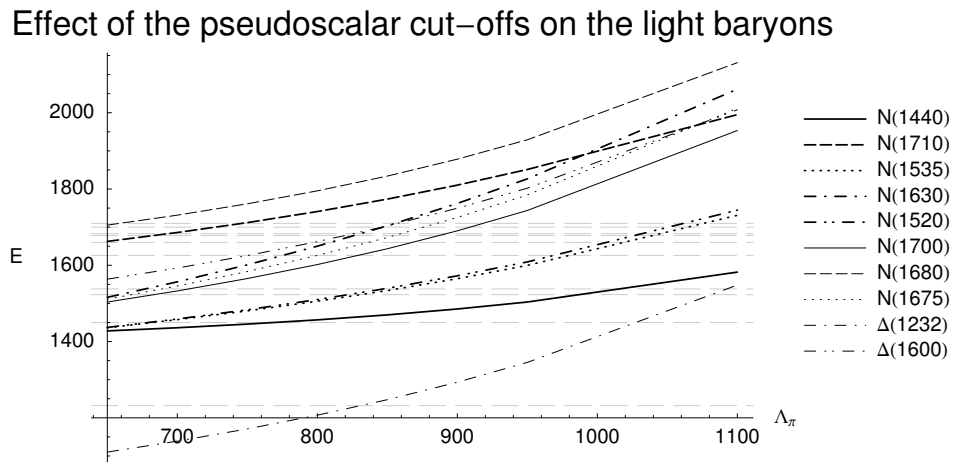

Figure 7.1: *The influence of the pseudoscalar cut-offs due to varying Λ_π on the nucleon and Δ spectra. The gray dashed lines indicate the experimental energies of the considered states.*

The multiple exchange of Goldstone bosons leads to the inclusion of the vector mesons ρ, $K*$, ω_8, and ω_0. Their cut-offs are scaled from the Λ_ρ value, which has an influence on the spectrum as shown in figure 7.2. The biggest influences are seen for the $\Delta(1232)$, $\Delta(1600)$ states, and the nucleon excitations with higher J^P.

The Λ_σ finally relates to the scalar mesons. Its effect is mostly adverse to the Λ_π and the Λ_ρ in that a higher value of Λ_σ leads to lower energies for several states. In particular, the energies of the $\Delta(1232)$ and the $\Delta(1600)$ states are shifted down considerably.

7.1.2 The separate free cut-offs Λ_K and $\Lambda_{\eta'}$

K meson exchange only acts between a light and a strange quark, and so has no influence on the light baryons (nucleon and Δ). One might thus hope to obtain a reasonable parametrization by first fitting the light baryon spectra (plus the Ω) using the remaining parameters, and afterward adjust the spectrum of all strange baryons mainly using the Λ_K (and possibly the strange constituent quark mass m_s, which was taken as predetermined at $m_s = 507$ MeV in our model). As it turned out, this is a viable approach and it was followed in our parametrization of the GBE CQM.

The effect caused by the Λ_K on the ground states of the strange baryons Λ, Σ, and Ξ is shown in figure 7.4. A larger cut-off Λ_K leads to lower energies of the positive-parity states Λ, $\Lambda(1670)$, $\Sigma(1190)$, and $\Xi(1314)$, while the remaining negative-parity states of the Λ, Σ, and Ξ baryon are affected only to a minor degree.

Finally, the η' meson plays a special role among the pseudoscalar Goldstone bosons

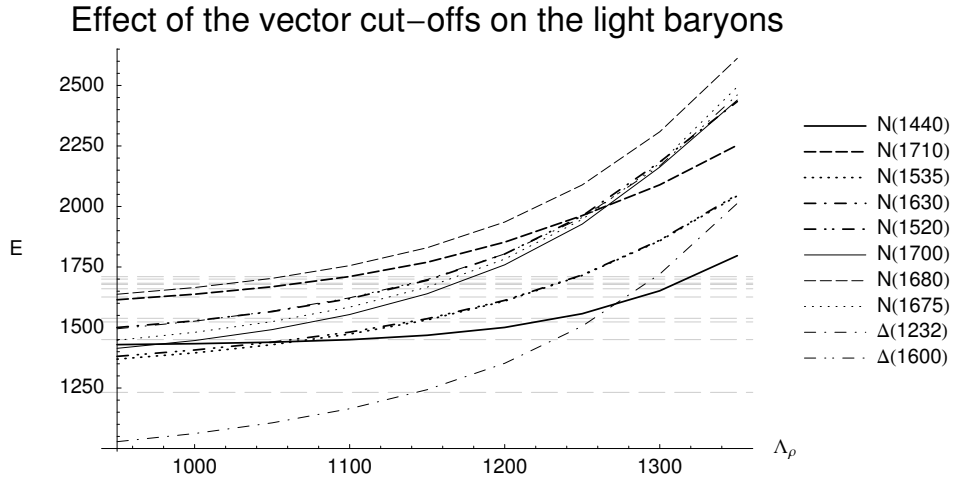

Figure 7.2: *The influence of the vector cut-offs due to varying Λ_ρ on the nucleon and Δ spectra. The gray dashed lines indicate the experimental energies of the considered states.*

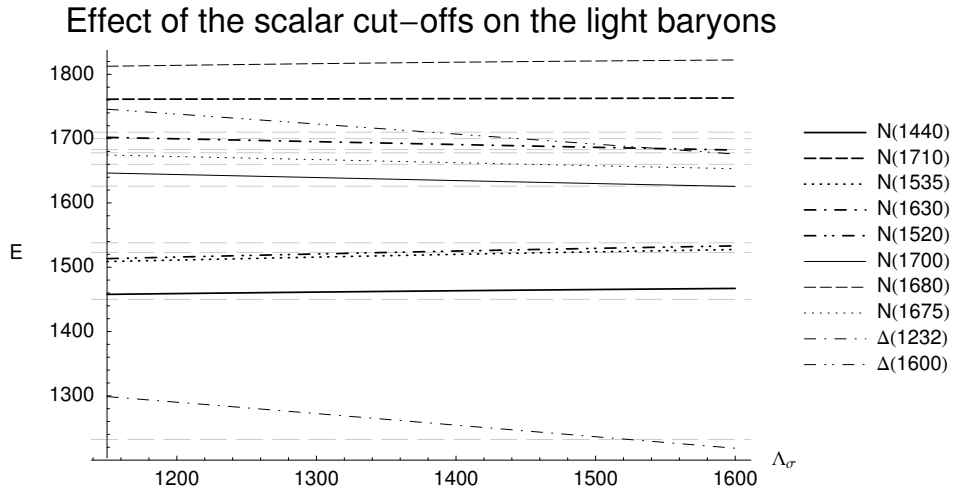

Figure 7.3: *The influence of the scalar cut-offs due to varying Λ_σ on the nucleon and Δ spectra. The gray dashed lines indicate the experimental energies of the considered states.*

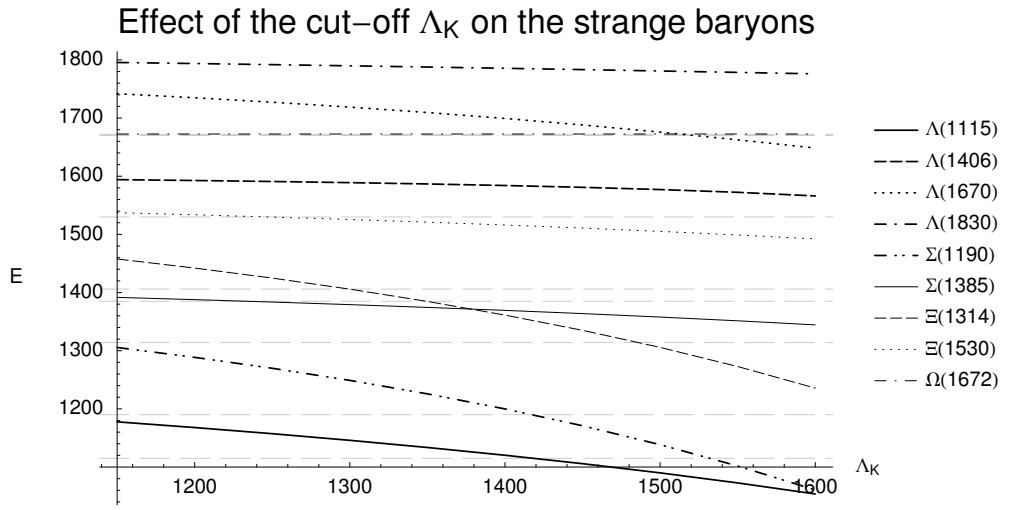

Figure 7.4: *The influence of the cut-off Λ_K on the strange baryons' spectra. The gray dashed lines indicate the experimental energies of the considered states.*

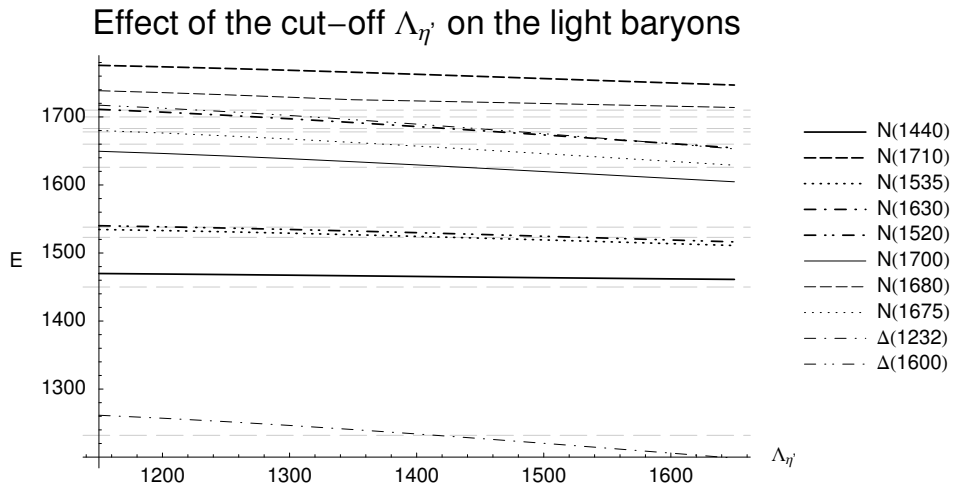

Figure 7.5: *The influence of the cut-off $\Lambda_{\eta'}$ on the nucleon and Δ spectra. The gray dashed lines indicate the experimental energies of the considered states.*

because of its large mass. It cannot even approximately be seen as a Goldstone boson, as already mentioned several times. Due to its high mass, a linear scaling rule as in equation (6.1) leads to unrealistic values for the $\Lambda_{\eta'}$, so its value has to be taken as an additional free parameter. Figure 7.5 shows its (rather minor) effect of shifting all energies down in parallel by about the same value.

7.2 Including a Coulomb term $\frac{c}{r}$ into the confinement

In the work by Bali et al. [B$^+$00] one has obtained static potentials for quark-antiquark pairs in quenched and unquenched simulations, with special emphasis on the effect of Wilson sea quarks. One fitted the ground state potentials to a Cornell-type parametrization

$$V(\vec{r}) = V_0 + \sigma r - \frac{c}{r} + g\left(\frac{1}{r} - \left[\frac{1}{r}\right]\right) . \tag{7.2}$$

Here the term $[\frac{1}{r}]$ denotes the tree level lattice propagator in position space and is included to quantify the short distance lattice artefacts. As the authors point out, this parametrization of the potential is meant to be only an effective description within a specified range "rather then being theoretically sound". Values for the coefficients V_0, σ (which corresponds to our string tension C) and c are also given in [B$^+$00]. Since in this work the calculations were done with only two quark flavors, G. Bali provided some values extrapolated to three flavors (considering that the central value is about 460 MeV) in a private communication. In particular, he gave the following values:

	2 flavors	3 flavors extrapolated
c	0.37(2)	$0.4 - 0.42$
σ	(462(58) MeV)^2	(435(30) MeV)^2

The range of validity of the fitted potential is 0.2 fm $\leq r \leq$ 1.1 fm. Below that regime, the Cornell potential underestimates the lattice values, and the lattice artefacts are considerable as Bali pointed out (however, they do not have sufficient results in that area to quantify these effects). Above that regime, the ground state potential becomes almost flat (which is in astonishing conformity with the confinement potential (3.8) chosen in previous models of the Graz group [WGPV00a, PGVW99]).

One also has to notice that this region of validity is just the range suggested by Manohar and Georgi [MG84] where the degrees of freedom can be described as constituent quarks, gluons and Goldstone bosons, with the gluons having only a small effective coupling to the constituent quarks.

We tried to use Bali's values in our confinement potential (since we are dealing with 3-quarks systems, the values need to be multiplied by a factor 3/2), neglecting the last term that includes the lattice artefacts. Within such a puristic framework

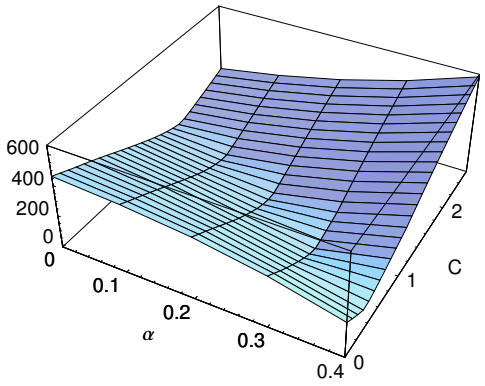

Figure 7.6: *Dependence of the fit function on variation of α and C in case of an additional Coulomb confinement potential*

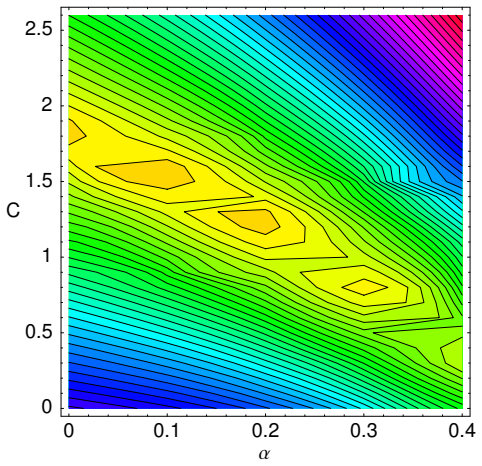

Figure 7.7: *The parameter value C for the minimal error depends linearly on α*

one cannot well reproduce the baryon spectra, as most states lie considerably above the experimental values. This cannot be cured by adjusting the other parameters of the potential and leaving the confinement untouched.

7.3 Additional Coulomb confinement potential

Although the strict lattice QCD values cannot be accommodated in the CQM, a confinement of the form (7.2) but with adjusted coefficients might still be expected to lead to an improvement over the linear confinement. To stay consistent with our previous notation, we will now call the coefficient of the Coulomb term α and the string tension C, so our confinement potential is written as $V(\vec{r}) = V_0 + Cr - \frac{\alpha}{r}$.

A first approach to get an idea of the effect of the additional Coulomb term is to vary only the two parameters C and α in the confinement and leave the other parameters fixed at their values of the best fit. Figures 7.6 and 7.7 show the deviations of the most important states upon variation of these two parameters.

The individual effects of the two confinement parameters are given in figures 7.8 and 7.9. As one can see, for moderate values of α all energy states go up simultaneously, so that by reducing the string tension one can hope to balance the effect of the Coulomb term. Consequently, one may expect good spectra also for values of $\alpha \approx 0.5$ and above. Figures 7.10 and 7.11 show two examples of acceptable spectra for the light baryons for moderate and even strong values of α. The modified parameter sets for the two versions in the figures are given in table 7.1.

As each one of these spectra seems to be reasonable, one might ask if the Coulomb term is necessary at all. It turns out that although a small $\frac{1}{r}$ term in the potential seems to be of advantage, it can be completely absorbed by other potential terms. As figures 7.8 and 7.9 suggest, the string tension can achieve this at first instance, while

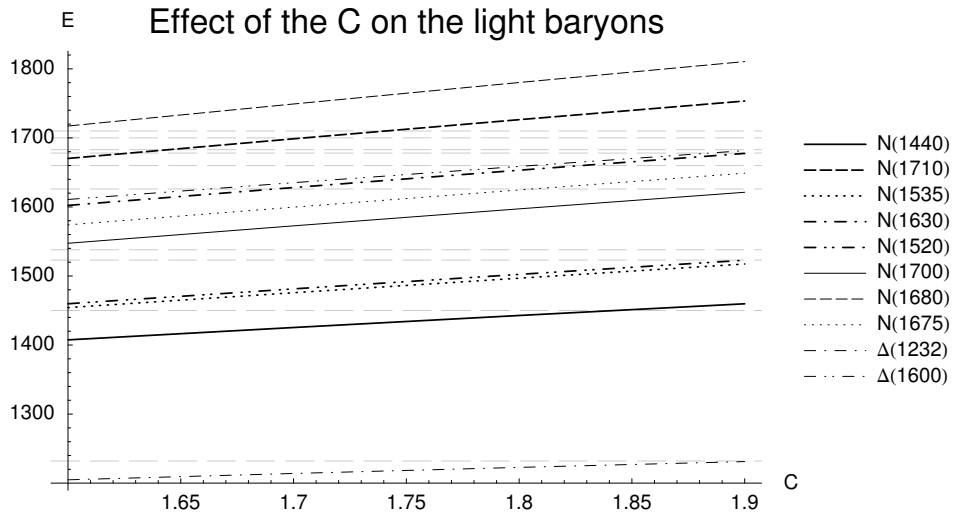

Figure 7.8: *The influence of the string tension C on the spectra.*

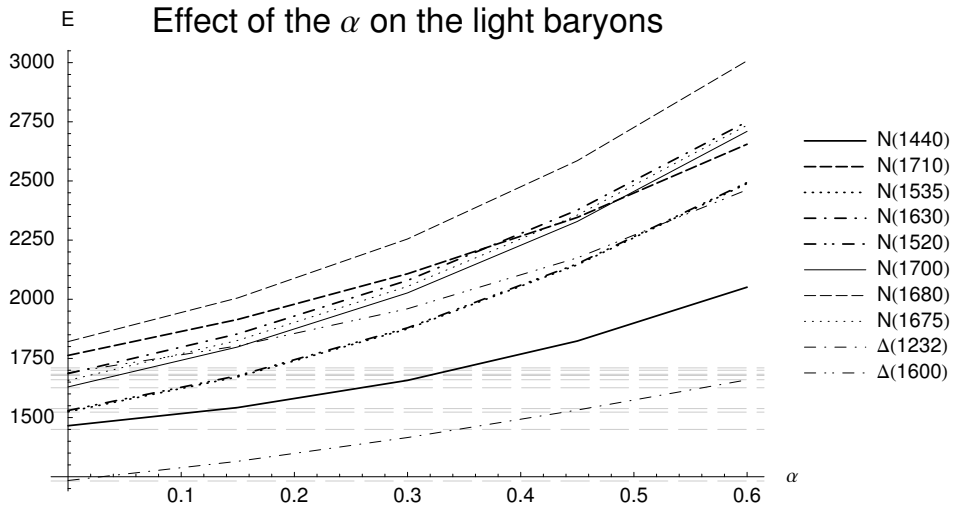

Figure 7.9: *The influence of the Coulomb term on the spectra.*

	figure 7.10	figure 7.11
Λ_π, κ_π	850 MeV, 0.9611	500 MeV, 0.7568
Λ_ρ, κ_ρ	1118 MeV, 1.0035	564 MeV, 1.3933
Λ_σ, κ_σ	1452 MeV, 1.0109	811 MeV, 1.1406
C	1.0296	0.9558
α	0.2661	0.6

Table 7.1: *Modified parameter values in case of an additional Coulomb confinement potential.*

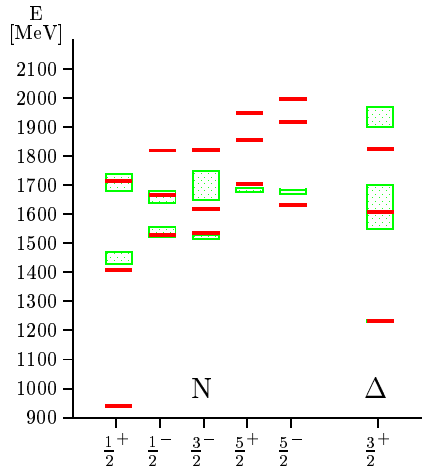

Figure 7.10: *Fit with moderate Coulomb confinement* $\alpha = 0.2661$.

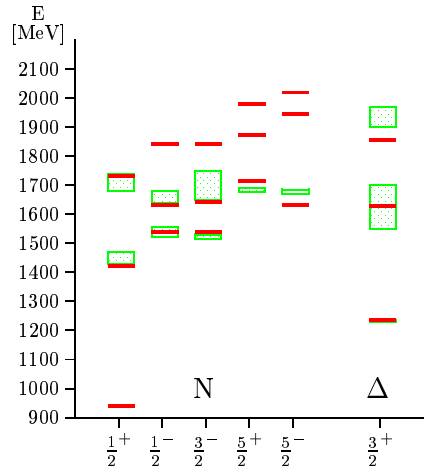

Figure 7.11: *Fit with large Coulomb confinement* $\alpha = 0.6$.

the remaining small differences can be absorbed by the scalar potential V_σ, varying especially the Λ_σ.

7.4 Near degeneracy of the $J^P = \frac{5}{2}$ states $N(1675)$ and $N(1680)$

Experimentally, the $J^P = \frac{5}{2}^+$ state $N(1680)$ and the $J^P = \frac{5}{2}^-$ state $N(1675)$ are almost degenerate, a fact which cannot be described in our model. We could not find any parameter set where these two states are even close to be degenerate without completely destroying the other states. A particular example, showing a fit where these two states are practically degenerate, is presented in figure 7.12 where the following parameter set was used:

$$\Lambda_\pi = 806 \text{ MeV}, \kappa_\pi = 0.7905, \Lambda_\rho = 1151 \text{ MeV}, \kappa_\rho = 0.9724, C = 1.9157\,.$$

The scalar cut-off parameters in this example were taken according to from the pseudoscalar cut-offs.

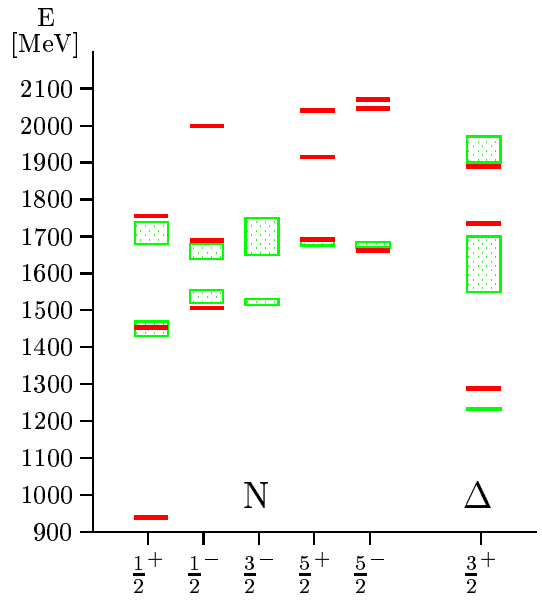

Figure 7.12: *Example of a destroyed spectrum when the* $N(1680)$ *and* $N(1675)$ *states are forced to be degenerate.*

Clearly, the $\Delta(1232)$ ground state is unacceptable. However, if one tries to shift it to lower energies (e.g. by increasing κ_π), the $N(1680)$ state will increase its energy, and simultaneously the $N(1675)$ will be shifted to lower energies.

For another case with an almost degeneracy, we found that the $J^P = \frac{1}{2}^-$ states of the nucleon were dramatically shifted to lower energies.

From our attempts it is pretty evident that a reasonable degeneracy cannot be obtained in an extended model without including the spin-orbit terms of the vector and scalar exchange potentials. The full model including these spin-orbit components in [Gla02] is finally able to produce practically degenerate $N(1680)$ - $N(1675)$ states; it also improves upon some other aspects of the GBE CQM.

Chapter 8

Conclusion

In this work we have studied several aspects with regard to the extension of the GBE CQM. In particular, we have investigated the effects of additional force components beyond the sin-spin part of the pseudoscalar exchange (which was the only piece constituting the hyperfine interaction in the originally published GBE CQM [GPP$^+$98, GPVW98]).

In addition to the pseudoscalar interaction we have examined the influences of vector and scalar boson exchanges, meant to describe effectively multiple GBE. While the coupling strengths of all force components were assumed to be fixed (as following from meson-nucleon phenomenology), we have studied the dependence on the cut-off parameters. The latter cannot directly be fixed from other sources and thus represent fit parameters in the construction of a GBE CQM. We have found that one can assume the cut-off parameters to scale linearly with the masses of the exchanged mesons, with the notable exception of the pseudoscalar η' and K mesons.

In connection with these tests of the various ingredients in a GBE hyperfine interaction we have also investigated influences form possible pieces in the confinement interaction beyond the linear term. In particular, the $\frac{1}{r}$ potential has been studied. It was found that its effect can be incorporated through a suitable parametrization of the cut-offs in the hyperfine interactions.

Based on these detailed studies we have parametrized an extended version of a GBE CQM that includes all possible force components except for the spin-orbit interaction; it provides a description of all light and strange baryon spectra of a similar or even better quality than previous versions of the GBE CQM. The spin-orbit interaction has not been included because its investigation has been the subject matter of a parallel diploma work [Gla02].

List of Figures

List of Tables

Bibliography

[A+99] S. Aoki et al. Non-perturbative determination of quark masses in quenched lattice qcd with the kogut-susskind fermion action. *Phys. Rev. Lett.*, 82:4392–4395, 1999.

[B+00] Gunnar S. Bali et al. Static potentials and glueball masses from qcd simulations with wilson sea quarks. *Phys. Rev.*, D62:054503, 2000.

[BDRW99] S. Boffi, P. Demetriou, M. Radici, and R. F. Wagenbrunn. Nucleon form factors in a chiral constituent-quark model. *Phys. Rev. C*, 60:025206, 1999.

[Ber02] Katharina Berger. Magnetic Moments and Charge Radii of Light and Strange Baryons. Diplomarbeit, Karl-Franzens-Universität Graz, April 2002.

[CKP83] J. Carlson, J. Kogut, and V. R. Pandharipande. A quark model for baryons based on quantum chromodynamics. *Phys. Rev. D*, 27:233, 1983.

[DJV80] J. W. Durso, A. D. Jackson, and B. J. Verwest. Models of pseudophysical n anti-n → pi pi amplitudes. *Nucl. Phys.*, A345:471–492, 1980.

[DM76] H. G. Dosch and V. F. Muller. On composite hadrons in nonabelian lattice gauge theories. *Nucl. Phys.*, B116:470, 1976.

[Gla02] Kathrin Glantschnig. Extended Goldstone-Boson-Exchange Constituent Quark Model for Light and Strange Baryons. Diplomarbeit, Karl-Franzens-Universität Graz, May 2002.

[Glo98] L. Y. Glozman. Baryons in a chiral constituent quark model. 1998.

[GMOR68] Murray Gell-Mann, R. J. Oakes, and B. Renner. Behavior of current divergences under su(3) x su(3). *Phys. Rev.*, 175:2195–2199, 1968.

[GPP96] L. Ya. Glozman, Z. Papp, and W. Plessas. Light baryons in a constituent quark model with chiral dynamics. *Phys. Lett.*, B381:311–316, 1996.

[GPP+97] L. Ya. Glozman, Z. Papp, W. Plessas, K. Varga, and R. F. Wagenbrunn. Light and strange baryons in a chiral constituent quark model. *Nucl. Phys.*, A623:90c, 1997.

[GPP+98] L. Ya. Glozman, Z. Papp, W. Plessas, K. Varga, and R. F. Wagenbrunn. Effective q q interactions in constituent quark models. *Phys. Rev. C*, 57:3406, 1998.

[GPVW98] L. Ya. Glozman, W. Plessas, K. Varga, and R. F. Wagenbrunn. Unified description of light- and strange-baryon spectra. *Phys. Rev. D*, 58:094030, 1998.

[GR96] L. Ya. Glozman and D. O. Riska. The spectrum of the nucleons and the strange hyperons and chiral dynamics. *Phys. Rept.*, 268:263–303, 1996.

[GV00] L. Ya. Glozman and K. Varga. Is there diquark clustering in the nucleon? *Phys. Rev.*, D61:074008, 2000.

[H$^+$02] K. Hagiwara et al. Review of particle physics. *Phys. Rev.*, D66:010001, 2002.

[KK77] V. I. Kukulin and V. M. Krasnopolsky. A stochastic variational method for few body systems. *J. Phys.*, G3:795–811, 1977.

[Mac89] R. Machleidt. The meson theory of nuclear forces and nuclear structure. *Adv. Nucl. Phys.*, 19:189–376, 1989.

[MG84] A. Manohar and H. Georgi. Chiral quarks and the nonrelativistic quark model. *Nucl. Phys.*, B234:189, 1984.

[NRZ] M. A. Nowak, Mannque Rho, and I. Zahed. Chiral nuclear dynamics. Singapore, Singapore: World Scientific (1996) 528 p.

[PGVW99] W. Plessas, L. Ya. Glozman, K. Varga, and R. F. Wagenbrunn. Effective interaction of constituent quarks in light and strange baryons. In *Proceedings of the 2nd International Conference on Perspectives in Hadronic Physics, Trieste, 1999*, pages 136–143, Singapore, 1999. World Scientific.

[RB99] D. O. Riska and G. E. Brown. Two-pion exchange interaction between constituent quarks. *Nucl. Phys.*, A653:251, 1999.

[RGG75] A. De Rujula, H. Georgi, and S. L. Glashow. Hadron masses in gauge theory. *Phys. Rev. D*, 12:147–162, 1975.

[Shu93] Edward V. Shuryak. Correlation functions in the qcd vacuum. *Rev. Mod. Phys.*, 65:1–46, 1993.

[SSRT00] P. Stassart, F. Stancu, J. M. Richard, and Lukas Theussl. Scalar meson exchange and the baryon spectra. *J. Phys.*, G26:397–403, 2000.

[SV98] Y. Suzuki and K. Varga. *Stochastic Variational Approach to Quantum-Mechanical Few-Body Problems*, volume 54 of *Lecture Notes in Physics. New Series M, Monographs*. Springer Verlag, Berlin/Heidelberg, 1998.

[tH76] Gerard 't Hooft. Computation of the quantum effects due to a four- dimensional pseudoparticle. *Phys. Rev.*, D14:3432–3450, 1976.

[Tho98] Timo Thonhauser. Meson spectra in a chiral constituent quark model. Diplomarbeit, Karl-Franzens-Universität Graz, 1998.

[VMK88] D. A. Varshalovich, A. N. Moskalev, and V. K. Khersonsky. *QUANTUM THEORY OF ANGULAR MOMENTUM.* World Scientific, Singapore-New jersey-Hong Kong, 1988.

[VS95] K. Varga and Y. Suzuki. Precise solution of few body problems with stochastic variational method on correlated gaussian basis. *Phys. Rev. C*, 52:2885–2905, 1995.

[Wag98] Robert F. Wagenbrunn. *Chiral Constituent-Quark Model for Light and Strange Baryons.* Dissertation, Karl-Franzens-Universität Graz, 1998.

[Wei75] Steven Weinberg. The u(1) problem. *Phys. Rev.*, D11:3583–3593, 1975.

[WGPV00a] R. F. Wagenbrunn, L. Ya. Glozman, W. Plessas, and K. Varga. Extended goldstone-boson-exchange constituent quark model. *Nucl. Phys.*, A663 & 664:703c, 2000.

[WGPV00b] R. F. Wagenbrunn, L. Ya. Glozman, W. Plessas, and K. Varga. Extension of the gbe constituent quark model. *Nucl. Phys.*, A666 & 667:29c – 32c, 2000.

[WPGV99a] R. F. Wagenbrunn, W. Plessas, L. Ya. Glozman, and K. Varga. Goldstone boson exchange dynamics in the constituent quark model for baryons. *Few-Body Syst. Suppl.*, 10:387, 1999.

[WPGV99b] R. F. Wagenbrunn, W. Plessas, L. Ya. Glozman, and K. Varga. Semirelativistic constituent quark model with goldstone- boson-exchange hyperfine interactions. *Few-Body Syst. Suppl.*, 11:25, 1999.

Acknowledgments

It would be impossible to name all the persons who helped me to get where I am now. However, I would like to point out a few people who were especially important in the creation of this work:

Prof. Willibald Plessas for advising this work and not giving up despite my terrible lack of time to work on this diploma thesis.

I am even more indebted to *Dr. Robert Wagenbrunn*, who took the patience (and he needed a lot) to try and explain the constituent quark model and especially the Goldstone Boson exchange in all its aspects to me. Without his invaluable stochastic variational program for the GBE CQM this work would have been impossible.

Mag. Kathrin Glantschnig for working together so well on our theses. Seeing that my results were really used in further work always helped to keep up the motivation.

I also have to thank *Dr. Thomas Melde* for various discussions about those small details that you never really think about, but which are absolutely necessary to understand the subject.

To *my parents and my whole family*, who always cared for me and supported me through my whole life.

And of course to all *my friends*, those from school who helped me getting interested in everything. Those from university, who kept up my interest in science. And of course those I just happened to meet somewhere. They all who make life really interesting.

Thank You All! Reinhold Kainhofer